University of Bath

UNIVERSITY OF BATH

PHD

Application of artificial intelligence for accurate fault location on transmission systems

Joorabian, M.

Award date:
1996

Awarding institution:
University of Bath

[Link to publication](#)

APPLICATION OF ARTIFICIAL INTELLIGENCE FOR ACCURATE FAULT LOCATION ON TRANSMISSION SYSTEMS

Submitted for Doctor of Philosophy
at the University of Bath

by

M. Joorabian Bsc Msc

1996

COPYRIGHT

Bath, October 28, 1996

UMI Number: U090524

UMI U090524

Acknowledgement

Abstract

This thesis describes a novel fault locator for extra high voltage (EHV) transmission systems based on artificial intelligence techniques. In particular, the technique developed addresses some common problems in fault location and takes into account the practical limitations in the design, extending the range of applicability of the new scheme for a whole variety of practically encountered systems and fault conditions, without sacrificing the high accuracy requirements. The method is based on utilising voltage and current waveforms at one end of the line only, and the signals employed are based on phase values.

Two fault location techniques are discussed in this thesis that are very effective in overcoming the disadvantages and improve the accuracy of the fault location over that attained with traditional techniques. The first technique is based solely on artificial neural networks (ANNs) and consists of two parts: (i) employment of an ANN for fault type classification and (ii) utilisation of separate ANNs (one for each type of fault) to accurately locate the actual fault position associated with all the commonly encountered types of fault on EHV transmission lines. In order to further improve the accuracy in fault location, an integration of fuzzy logic and ANN is adopted in the second technique.

Contents

Index to Figures

Index to Tables

List of Symbols

kV	Kilo Volts
kVA	Kilo Volt Amperes
MVA	Mega Volt Amperes
MW	Mega Watts
AC	Alternating Current
DC	Direct Current
AI	Artificial Intelligence
ANNs	Artificial Neural Networks
EMTP	Electro-Magnetic Transients Program
DFT	Discrete Fourier Transform
FNN	Fuzzy Neural Network
CAD	Computer Aided Design
FNNs	Fuzzy Neural Networks
EHV	Extra High Voltage
θ	Phase angles
x	Distance to the fault point
V_A	Voltage of A-terminal
I_A	Current of A-terminal
V_F	Voltage of fault point
I_F	Fault current
V''_A	Voltage difference between pre-fault and post-fault voltage
I''_A	Current difference between pre-fault and post-fault current
I''_{AF}	Fault current from A-terminal
Z_S	Surge impedance

Z_L	Transmission line impedance per unit length
γ	Propagation constant
$k(x)$	Current distribution factor
$Im[\cdot]$	Imaginary part
Z_A	Impedance measured at A
Z_{LA}	Line impedance between the fault and the end A
ϕ_L	Phase angle of the phase impedance
k_f	Fault current distribution factor
R_F	Fault resistance
I_{FA}	Change in the line current
D_A	Current distribution factor at station A
Z_L	Line impedance
p	Percent distance to fault
t_f	Fault inception time
HVDC	High Voltage Direct Current
EMTDC	Electro-Magnetic Transients Direct Current
GAs	Genetic Algorithms
w_0	Threshold
$\Psi[\cdot]$	Nonlinear activation function
x	Input
X	Input vector
X	Input variable
X_{min}, X_{max}	Minimum and maximum values of variable
y	Output
Y	Output vector
ART	Adaptive Resonance Training
MNN	Multilayer Neural Network
BP	Back-Propagation
w_{ij}	Weight from i to j
η	Learning factor
MFNs	Multi-layer Feed-Forward Networks
MLP	Multi-layer Perceptron

sec	Second(s)
μs	Micro-second(s)
msec	Milli-second(s)
Hz	Hertz
kHz	Kilo-Hertz
km	Kilometre
S1	Source capacity at the sending-end
S2	Source capacity at the receiving-end
Z_{S0}, Z_{S1}	Zero and positive phase sequence source impedances
X_m	Mutual impedance
Z_s	Self impedance
Z_1,	Positive phase sequence impedance
Z_2	Negative phase sequence impedance
Z_0	Zero sequence phase impedance
X_m	Mutual impedance
Z_n	Neural impedance
I_0	Zero-sequence current
SCL	Short circuit level
Z	Source impedance
V	Operating voltage
SVA	Source short circuit level in VA
R	Source resistance
X	Source reactance
NGC	National Grid Company
ACSR	Aluminium Conductor Steel Reinforced
GVA	Giga Volt Amperes
CAD	Computer Aided Design
A/D	Analogue to digital converter
CVT	Capacitor Voltage Transformer
CT	Current Transformer
DFT	Discrete Fourier Transform
V_a, V_b, V_c	Three-phase voltages

I_a, I_b, I_c	Three-phase currents
U	Universe of discourse
A	Crisp set
F	Fuzzy set
μ	Membership function
$\cup$	Union
$\cap$	Intersection
FLS	Fuzzy Logic System
S	Small
MS	Medium Small
M	Medium
ML	Medium Large
L	Large
RMS	Root Mean Square error
EI	Error Index
SCI	Single Confidence Index
ACI	Average Confidence Index
GEC	General Electric Company
E_a, E_b, E_c,	Internal voltages
rms	Root mean square value

CHAPTER 1

Introduction

Modern civilization, industrial growth and higher living standards require enormous use of energy. Electrical energy is the most convenient way of generation and delivering energy to homes and industries. Electrical power systems are designed and managed to deliver this energy to the utilization points with both reliability and economy.

1.1   Electrical Power System

The structure of an electric power system is usually very large and complex. It can be considered to consist of a generation system, a transmission system, and a distribution system. In general, the generation and transmission systems are referred to as bulk power supply, and the distribution system is considered to be the final means to transfer electric power to the individual consumers. Bulk power transmission is made up of a high-voltage network, generally 132-750 kV alternating current, designed to interconnect power plants and electric utility systems and to transmit power from the generating plants to major load centres.

I

1.1.1 Generation System

Electrical energy is generated in the generating station. The cost of electric supply is influenced by the level of investment in generation. Generation of electricity is performed by the conversion of kinetic energy into electrical energy via magnetic fields. The kinetic energy released from moving water, expanding steam, wind power, etc, is used to rotate a shaft which drives a generator.

The nature of a generator depends upon the source of energy and this in turn has some bearing on the design of the generator. There are power units based on steam, gas, water power and diesel engine drives. Generation voltage is in the range of 11 to 25 kV and the range of size of generators extend from a few hundred kVA to 500 MVA.

1.1.2 Transmission and Distribution

Bulk generating plant is connected to the consumers' loads by means of an interconnected system of transmission and distribution network. A high-voltage transmission system is required in order to connect bulk generation to the distribution systems. Which then supply the electricity on a smaller scale to the consumers [1].

The choice of transmission voltage is governed by physical factors such as electrical losses and economic factors based on the cost of line construction and maintenance. In order to transmit the necessary power over long distances, line losses become increasingly important. The use of high voltage reduces losses by reducing the current for a given amount of power. In the United Kingdom, the generating stations supply a transmission network which operates at 275 kV and 400 kV, whilst many overseas countries have transmission systems operating at 750 kV.

1.1.3 Networks

Modern power systems are highly interconnected and the power stations are synchronised together, effectively acting as a single power source for the whole system. High voltage transmission lines are used to interconnect generators and link generators to load centres. The interconnections are capable of carrying power in orders of magnitude of the effective generating capacity.

1.2 Power System Protection

Power systems and their components need to be protected when faults occur due to natural hazards as well as human error. The objective of power system protection is to detect the presence of these faults and to initiate the isolation of the affected equipment in the shortest possible time.

1.2.1 Power System Faults

Power system faults can be caused by many factors such as lightning, wind, ice, animals, and humans. These faults produce over-current and/or over-voltages at various points on the power system, and must be located and cleared before damage is caused to expensive equipments.

1.3 Transmission Line Faults

Electrical power systems are designed to ensure a reliable supply of energy with the highest possible continuity. Electrical faults can occur at any point in an electric power system and the most exposed parts are overhead transmission lines. A transmission line is also one of the most difficult parts of a power system to maintain and inspect, simply because of its dimension and the environment it is built in [2].

1.3.1 Accurate Fault Location for Transmission Lines

Fast and accurate location of faults on an electrical power transmission line is vital for the economic operation of power systems. This is more so in view of the fact that because of an increase in transmission requirements and environmental pressures, power authorities are being forced to maximize the transmission capabilities of existing transmission lines. This effectively means that in order to maintain system security and stability, there is a demand for minimizing damage by restoring the faulted line to normal as quickly as possible, hence the requirements for the development of an accurate fault locator. The degree of accuracy required is therefore increasing and is much higher than would be possible using simple conventional techniques. Even a small measurement error may require detailed local examination over several kilometres of a typical line.

1.3.2 Importance of Accurate Fault Location

Some of the important reasons for accurate fault location on transmission lines can be summarised as:

- Under normal operating conditions, assessing the condition of a system is fairly simple. However, when a fault occurs, the analysis will be much more complicated and at the same time much more important, considering the conclusions that could be inferred from the results. In this case, defining a fault allows one to subsequently simulate it to acquire complete information on the abnormal conditions under which the various devices in the system were operating at the time the disturbance occurred. Furthermore, in case of permanent faults, locating a fault will allow one to go to the exact fault point and take appropriate actions to restore power. In the case of non-permanent faults, locating a fault point allows one to identify critical points in the system (trees, pollution, defective insulators, etc.)

and take the required preventive maintenance steps.

• Accurate fault location reduces transmission line patrolling and is of particular significance in repairing long lines in rough terrain. A fault locator is also very useful for evaluating transient faults that could otherwise, cause weak spots to occur on transmission and distribution systems, resulting in future problems or more serious faults.

• The use of longer distance transmission lines coupled with demand for reduced circuit outage times is stimulating a requirement for reliable and accurate fault location techniques for transmission lines.

• Minimising outage times following a fault is paramount to the security and therefore the economical operation of a supply network. This means that it is critically important to restore a faulted line as quickly as possible.

• The need for very high accuracy is generally becoming more important since in EHV systems, there is often little visual evidence of a fault, and post-fault clearance tests performed at reduced system voltage can be inconclusive.

• The growing complexity of electric power systems demands a high performance from protection and control equipment. Fault locators have gained more importance over the years since it has become more difficult to find the fault location as the visible damage of the line has decreased due to the advent of faster circuit breakers and faster protective relays.

1.4   Current Fault Location Methods

Fault location methods currently used are based on either the theory of travelling waves or the analysis of fault and pre-fault voltage and current values at the fundamental frequency. When using algorithms based on the theory of the travelling waves, the point at which a fault occurs is determined from the delay of a reflected wave from the fault point to the point of measurement. The disadvantages of this method are the high costs of the equipment required and the significant variations in the magnitudes and frequency of travelling waves under different fault conditions. On the other hand, the algorithms based on voltage and current values at fundamental frequency allow, in general, the determination of the fault distance by finding the apparent impedance seen by the relay located at the end of the line. This impedance is supposed to be proportional to the distance between the reference point and the fault point.

1.4.1 Microprocessor Technology

The rapid progress in microprocessor technology, coupled with developments that have taken place in computer software, makes it ideally suitable for applications in electric power systems, in particular where high precision is necessary, such as in transmission line fault location. These new developments have come as a replacement for the previously outlined analog techniques which are less flexible, the accuracy attainable is not that high and they demand high maintenance.

The design of microprocessor-based fault locators includes the selection of a suitable algorithm and a hardware platform to implement the selected technique. Several approaches to the problem of a transmission line fault location have been investigated. Different principles have been applied to the problem and the techniques can be broadly classified into single-ended and multiple-ended data measurements.

Fault location techniques using fundamental frequency voltages and currents

measured at one of the line terminals generally does not provide sufficient accuracy. The majority of such techniques are based on lumped parameter line models and the objective is to evaluate the complex impedance of the line up to the fault point, from which fault distance can be deduced. Such techniques are particularly prone to inaccuracies if fault current is contributed by sources connected to both terminals of the line, and especially if fault resistance is present.

When data from multiple ends are used, it is possible to overcome some of the common problems associated with fault location based on single-ended measurements. However, a communication medium is required for transmitting fault-recorded data to the processing end in the case of the former.

1.5 Artificial Intelligence Techniques

Artificial intelligence (AI) provides powerful techniques for processing symbolic or declarative knowledge and for automated reasoning. In this respect, the advent of artificial neural networks has provided power engineers with powerful tools which are promising for solving some long-standing power system problems. Neural networks possess the ability to perform pattern recognition, prediction and optimisation in a fast and efficient manner. This is so by virtue of the fact that they have the ability to map very complex and highly non-linear input/output patterns.

With the recent advances in learning techniques for artificial neural networks (ANNs), They are being applied to many areas of power systems. ANNs show a high potential as an alternative to algorithmic and expert system methods; they have been used to preform electric load forecasting [3], detection of faults on power distribution feeders [4], autoreclosure for EHV transmission systems [5,6], real-time and off-line fault analysis [7], fault identification in an AC-DC transmission system [8] and high speed protective relaying [9].

Many intelligent system techniques have been developed over the last decade. Some

of the major ones include expert systems, fuzzy systems, neural networks and genetic algorithms. The applications of these intelligent techniques to power system problems has been a subject of interest over the past years. Because of the nature of various types of power system problems, different solutions may be required. However, the real world power system problems may not fit the assumptions of a single technique. One approach to deal with these complex real word problems has been to integrate the use of two or more AI techniques in order to combine their different strengths and overcome each other's weaknesses to effect hybrid-based solutions.

1.6   Objectives of the Project

The main objectives of this thesis are:

☐   To present an accurate fault location technique for transmission lines based on artificial intelligence (AI) techniques. The method is based on utilising voltage and current waveforms at the fault locator end of the line captured using digital fault recorders. The technique outlined also includes an accurate method for classifying all types of fault using an ANN.

☐   To establish the correct performance of the proposed fault locating technique. The approach adopted for this purpose is through modelling the fault locator on a computer and investigating the performance that might be expected when it is subjected to the simulated fault transient data attained, using the well known Electro-Magnetic Transients Program (EMTP).

The effect of transducers (CTs and CVTs) and hardware errors such as the effect of interface modules, anti-aliasing filters and quantisation are taken into account in the simulation, so that the information processed through the fault locator algorithm is very close to a real-life situation.

The extraction of the significant features from the simulation waveforms

based on spectrum analysis is presented. The approach adopted is based on frequency domain decomposition of the voltage and current waveforms using Discrete Fourier Transform (DFT) for the purposes of attaining the best training data sets for the ANNs.

The algorithm is extensively tested for a whole variety of practically encountered different systems and fault conditions. Furthermore, the effect on accuracy of parameters like fault resistance, system source capacity, different fault inception angle, etc, is ascertained.

☐   To further improve the accuracy of the fault location technique through an integrated approach comprising of fuzzy logic and an ANN, called fuzzy neural network (FNN). The technique, which utilises voltage and current fault data at one line end only, comprises of two stages: the first stage is based solely on ANN in order to classify fault types and the second stage is based on a FNN whereby fuzzy logic is employed to process the information for a second ANN for the purposes of accurately locating a fault on the line.

1.7   Scope of the Thesis

Chapter 2

A literature search of fault locator techniques for two- and three-terminal transmission lines are presented in this chapter. The techniques reviewed are divided into two groups:

i)   Algorithms using data from one end of a transmission line only.

ii)   Algorithms based on information from all ends of a transmission system.

AI based fault location techniques are also reviewed in this chapter.

Each technique is described individually and some of the advantages and disadvantages are discussed.

Chapter 3

The applications of AI and ANN in power systems are reviewed. Structure of an expert system, a fuzzy logic and neural networks are discussed with particular emphasis on multi-layer-perceptron and the back-propagation algorithm that is used to adapt the weights to achieve the desired non-linear mapping from inputs to outputs. Practical issues concerning the design, training, and testing of ANNs are also discussed.

Chapter 4

This chapter describes the simulation of power systems under faults to generate accurate and realistic fault data and this is achieved through the employment of the well proven Electro-Magnetic Transients Program (EMTP). The simulation study is based on a plain feeder EHV transmission line system. The overhead transmission line used in this work is based on a single circuit of the typical quad-conductor 400 kV vertical construction line currently used on the UK supergrid system.

Although the fault location technique is based on Computer Aided Design (CAD) studies, however, practical considerations, such as the effect of transducers, and hardware errors i.e. anti-aliasing filters and quantisation, etc, on the primary system fault data are also included in the simulation and these are also briefly discussed.

Chapter 5 .

An accurate fault location technique using ANNs is presented in this chapter. The feed-forward multi-layer ANN based on supervised learning and the widely used training rule of error back-propagation is chosen for this study. The instantaneous

three phase voltages and currents derived at the fault locator end are used to train and test the ANN. An ANN architecture to distinguish between different types of fault is proposed and ANN topology for accurate fault location under different system and fault conditions is discussed.

Chapter 6

An integrated approach comprising fuzzy logic and ANNs called fuzzy neural networks (FNNs) for accurately locating faults on a transmission line is developed in this chapter. The method is again based on utilising voltage and current waveforms at the fault locator end of the line only and the signals employed are again based on phase values.

The approach adopted here is based on separating the problem into two parts: firstly to employ and train a single ANN to indicate on which phase(s) the fault is and whether there is ground involved in a particular fault, irrespective of the actual fault position at this stage; secondly, in order to achieve a good generalisation, to use separately designed FNNs (one for each type of fault and each comprising fuzzy logic and an ANN) to accurately locate the actual fault position associated with all commonly encountered types of fault on EHV transmission lines; these are of course all driven from the single ANN designed at the first stage.

Chapter 7

Analysis of the results are presented in this chapter and the performance of ANN for fault classification and fault location is discussed. Results for accurate fault location based on FNN is presented and compared with the previously developed fault location technique based solely on ANN architectures.

Chapter 8

Conclusions are drawn and future work is discussed in this chapter.

Chapter 2

An Overview Of Fault Location Algorithms

For Transmission Lines

2.1 Introduction

Accurate fault location for extra high voltage (EHV) transmission lines has been the subject of much research over many years, and over the past decade, digital and microprocessor based systems have become the focus of attention. Numerous fault locators based on different techniques have been developed and implemented, yet there appears to be still no optimum solution. This could be due to the fundamental limitation of all techniques. Generally, they all perform well for a specific system i.e. a particular system configuration, or a particular fault condition, but accuracy is lost when applying them more generally.

Microprocessor-based devices have had a better accuracy in locating faults in power systems than analogue-based techniques. In this respect, considerable work has been done in developing digital techniques for locating faults on transmission lines both for two- and three-terminal lines.

The design of microprocessor-based fault locators includes the selection of a suitable algorithm and hardware to implement the selected technique. Several approaches to

the problem of a transmission line fault location have been developed. Different principles have been applied to the problem and techniques for two-terminal lines can be broadly classified into single - ended and multiple - ended data measurements.

2.2 Algorithms Using Data From One-End Only

The principles of the fault location techniques discussed in this chapter are outline with reference to the single-line diagram of a power system in a faulted situation shown in figure 2.1.
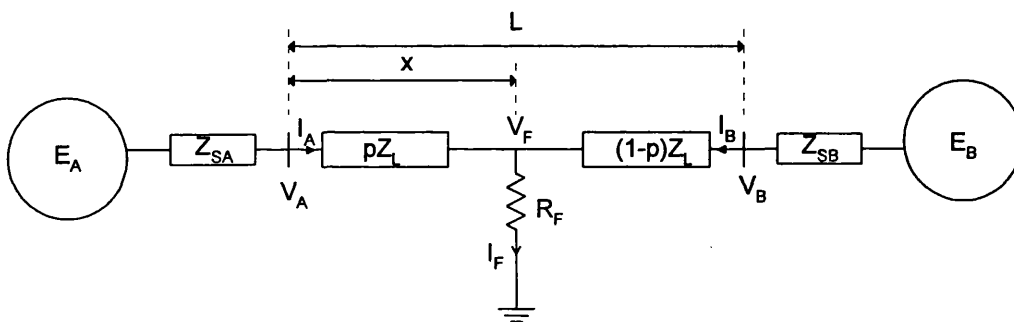
Figure 2.1 Single line diagram for a two-ended transmission system.

Algorithms using data from just one end of a transmission line are generally based on the calculation of the impedance up to the fault point, from which fault distance can be deduced. However, such techniques suffer from errors due to fault current contribution by sources connected to both terminals of the line and fault resistance, if present.

Sant and Paithankar [10] have used a fault location technique based on the measurement of the ratio of the reactance of a line from the fault locator up to the fault point to the total reactance of the line, i.e. X_f / X_n. Because X_n is a known value, the ratio X_f / X_n determines the fault position. The following expression is derived for calculating this ratio:

$$\frac{X_f}{X_n} = \frac{(\sin\theta_1)(\cos\theta_3)}{(\sin\theta_2)}$$
(2.1)

where:

$$\theta_1 = \arctan[\frac{I_A X_n}{V_A}]$$

$$\theta_2 = -\frac{V_A}{I_A X_n - V_A}$$
(2.2)

$$\theta_3 = 180° - (\theta_1 + \theta_2)$$

Equation (2.1) clearly shows that the fault position can be determined by the measurement of any two of the three phase angles θ_1, θ_2 and θ_3. The suggested technique for the new digital fault locator is based on measurements of these angles by two digital counters. The technique assumes that the line is connected to a source at one end only. The fault location estimates are, therefore, not accurate if there is remote infeed present.

Takagi et al [11] have developed a fault locator that calculates the reactance of the faulted line using a microprocessor, based on one-terminal voltage and current data. Errors caused by various factors such as load flow, fault resistance, and the unsymmetrical arrangement of the transmission line, are automatically reduced by efficient use of the software. The method to calculate the distance to a fault point is based on the following equation, which expresses a fault point voltage V_F and current I''_{AF} using the one-terminal data:

$$V_F = V_A \cosh(\gamma x) - Z_s I_A \sinh(\gamma x)$$

$$I''_{AF} = \frac{V''_A}{Z_s} \sinh(\gamma x) - I''_A \cosh(\gamma x)$$
(2.3)

Two approximations are adopted in equation (2.3), and the distance to a fault is obtained using the following equation:

$$x = \frac{Im(V_A I_A^{//}*)}{Im(Z_L I_A I_A^{//}*)}$$ (2.4)

where:

x	$\rightarrow$	distance to the fault point
V_A	$\rightarrow$	voltage of A-terminal
I_A	$\rightarrow$	current of A-terminal
V_F	$\rightarrow$	voltage of fault point
I_F	$\rightarrow$	fault current
V''_A	$\rightarrow$	voltage difference between pre-fault and post-fault voltage
I''_A	$\rightarrow$	current difference between pre-fault and post-fault (fault component current)
I''_{AF}	$\rightarrow$	fault current from A-terminal
Z_S	$\rightarrow$	surge impedance
Z_L	$\rightarrow$	transmission line impedance per unit length
γ	$\rightarrow$	propagation constant

The effect of the load flow is cancelled by using fault component current I_A'' in equation (2.4), and the effect of fault resistance is reduced by a manipulation of the previous equations. The technique initially neglects the effect of shunt capacitance, but this effect is compensated for later on.

Schweitzer [12] has proposed a fault location algorithm for transmission lines which provides an improvement to the performance of the Takagi algorithm.

Takagi et al [13] in another method have applied the law of superposition to the steady state fault analysis; the authors obtain an algebraic equation which contains an unknown variable corresponding to the fault distance, using current and voltage vectors at the local end. The following expression is derived to obtain a solution to

the fault location problem:

$$R_F [1 + k(x)] = - \frac{A(x)V_A - B(x)I_A}{C(x)V_A'' - D(x)I_A''}$$

(2.5)

where k(x), the current distribution factor, is a function of the distance x to the fault, and is defined as:

$$k(x) \equiv \frac{I_{FB}''}{I_{FA}''}$$

(2.6)

As the fault impedance is purely resistive, R_F is a real variable. The ratio k(x) also becomes real on the assumption that the transmission line is lossless and the source impedances at the two ends are purely inductive; thus, by definition, the right hand side of equation (2.5) must be real. The basic equation is obtained as follows:

$$Im \left[\frac{A(x)V_A - B(x)I_A}{C(x)V_A'' - D(x)I_A''} \right] = 0$$

(2.7)

where Im[·] denotes the imaginary part of a complex variable.

The solution x of the equation (2.7) is the distance from the local end to the fault point. As this equation is non-linear in nature, an iterative solution technique based on Newton-Raphson method is applied. First of all, the primary data of transient waveforms is smoothed out through digital filtering. Secondly by a transformation technique extracts the voltage and current vectors and finally, the Newton-Raphson technique is applied to solve the equations. With the practical consideration in mind, the application of fast algorithms such as half-cycle and truncated Fourier Transform, and Walsh transform are then examined. Finally, the digital fault locator is tested on an artificial transmission line and good performance is obtained. However, since the solution assumes lossless circuit elements, for a realistic lossy system, there are appreciable errors in the computed distance.

Takagi et al [14] in the second part of their work have presented the fundamental theory of a fault locator scheme based on the Laplace transform. The superposition principle is applied to the transient state of a faulted network. The fault current distribution factor is used again in a different manner. They have then applied the condition that the voltage across the fault resistance must have the same value if calculated for two different values of the Laplace operators. However, the authors conclude that the Fourier method is numerically superior to the one based on Laplace transform.

Wiszniewski [15] has presented a method based on the standard calculations of resistance and reactance using the fault current distribution factor, with an algorithm in which an attempt is made to compensate the error introduced by the fault resistance. The required algorithm computations are very simple and non-iterative. The first expression taking into account the current distribution factor is:

$$Z_A = Z_{LA} + (\frac{R_F}{k_f})\frac{I_A - I_L}{I_A \, e^{j\lambda}} \qquad (2.9)$$

The final expression for calculating a correct value of the reactance is obtained as:

$$X_{LA} = X_A - \frac{R_A \tan(\varphi_L) - X_A}{(a/b)\tan(\varphi_L) - 1}$$

$$a = Re \left[\frac{I_A - I_L}{I_A e^{j\lambda}} \right] \qquad (2.10)$$

$$b = Im \left[\frac{I_A - I_L}{I_A e^{j\lambda}} \right]$$

Where,

$Z_A = R_A + jX_A$	$\rightarrow$	impedance measured at A
$Z_{LA} = R_{LA} + jX_{LA}$	$\rightarrow$	line impedance between the fault and the end A
$\phi_L = \tan^{-1} (X_{LA}/R_{LA})$	$\rightarrow$	phase angle of the phase impedance
$k_f = k \, e^{j\lambda}$	$\rightarrow$	fault current distribution factor, depending on the configuration of the network

I_A $\rightarrow$ total line current at the end A during the fault

I_L $\rightarrow$ pre-fault current

R_F $\rightarrow$ fault resistance

The local signals I_A, V_A and I_L enable X_A, R_A, 'a' and 'b' to be calculated. Therefore, the reactance X_{LA}, which is proportional to the true distance between the line end A and the fault, may be determined by the means of equation (2.9). The accuracy of the error compensation depends on the assumed values for ϕ_L and λ. In fact, the fault-current distribution factor depends on the configuration of the network, but in most cases, it may be assumed that λ is equal to zero, which implies that the distribution factor k_f is real. The angle ϕ_L may also be considered as constant because the expected variations are negligible. However, in some cases, this assumption may give rise to incorrect compensation and in this case some refinements are implemented. This modified technique shows that the apparent reactance measured at one end of the line requires a certain correction to eliminate this error to give results truly proportional to the distance to the fault. Correction is based on the estimation of the phase shift between the total fault current at one end of the line and the current which flows through the fault resistance. No results or field tests are presented, and the effect of shunt capacitance is neglected.

Erikson et al [16] and Saha et al [2] have developed a microprocessor-based fault locator which uses novel compensation techniques to improve the accuracy, eliminating the errors inherent in conventional reactance-type measurements. Pre-fault and fault data extracted from the AC currents and voltages are used to compute the distance to fault. The fault locator program described utilises representative values of the source impedance to determine a correct description of the network. The following equation is the general form of fault location equation, where the values of V_A, I_A, and I_{FA} are different for each type of fault:

$$V_A = I_A \, p \, Z_L + \frac{I_{FA}}{D_A} R_F \qquad\qquad (2.11)$$

where,

I_A, V_A	$\rightarrow$	current and voltage at A
I_{FA}	$\rightarrow$	change in the line current
D_A	$\rightarrow$	current distribution factor at station A
Z_L	$\rightarrow$	line impedance
p	$\rightarrow$	percent distance to fault

The final expression is then shown as:

$$p^2 - p k_1 + k_2 - k_3 R_F = 0 \qquad\qquad (2.12)$$

where:

$$k_1 = \frac{V_A}{I_A Z_L} + 1 + \frac{Z_{SB}}{Z_L}$$

$$k_2 = \frac{V_A}{I_A Z_L}\left(\frac{Z_{SB}}{Z_L} + 1\right) \qquad\qquad (2.13)$$

$$k_3 = \frac{I_{FA}}{I_A Z_L}\left(\frac{Z_{SA} + Z_{SB}}{Z_L} + 1\right)$$

The complex expression of equation (2.11) contains the unknowns p and R_F. However, equation (2.11) is separated into two simultaneous equations, one real and one imaginary. By eliminating R_F , a single expression results with the single unknown p. This is solved by using the magnitude and phase derived from Fourier analysis routine which yields the fundamental components of the signals. For a multiphase system, the fault type has to be defined before using the method.

The proposed equipment was tested under dynamic conditions (field tests) with good results. However, the results are given only for a short line, and the effect of shunt capacitance is ignored.

The techniques developed by Takagi et al [11], Winsznieuski [15], Eriksson et al [16] and Saha et al [2] depend on a knowledge of the source impedance values to calculate the current distribution factor. However, equivalent source impedances are not readily available in all cases. Also, the system configuration changes from time to time modifying distribution factors, which must be determined for every fault.

Cook [17] has also presented an approach dealing with the current distribution factor. The technique also requires an assumed value of the remote end source impedance which is then used to determine the argument of this factor, rather than its magnitude. Much smaller errors are claimed by the author for such a technique. The effect of shunt capacitance is, however, neglected.

A fault location method by dynamic system parameter estimation is presented by Richards and Tan [18] for a double-end fed transmission line using data from one end only. The line is represented as a lumped parameter circuit. The system model includes Thevenin equivalents including resistances and inductances at both ends of the line, and an unknown fault resistance. The fault location problem is then treated as a parameter estimation problem of a dynamic system, in which the response of the physical system is compared to the lumped parameter model. The model's parameters are varied until an adequate match is obtained with the physical system response. Using instantaneous symmetrical components, the equations are simplified. The fault location algorithm does not require filtering of DC offset and high-frequency components. Using the simulated transmission line, several tests were conducted. The final estimates are within 1% accuracy in each case. However, the effect of the shunt capacitance is neglected, and the effect of some problems relating to real transmission lines, like mutual coupling of parallel lines or line transposition, are not considered.

2.3 Algorithms Using Data from Two Ends

It has been shown by some authors that, using information at both ends of the line,

can improve significantly the accuracy on fault location for transmission lines. Generally, the techniques are independent of fault impedance or changes in the power system source operating configuration. However, communication between the ends and in some cases, a method to determine the phase angle of the voltages and currents at a common reference axis are necessary. The accuracy of fault location also depends on synchronising the measurements at both ends of the line.

Transmission line fault location algorithms developed by Schweitzer [12,19] use steady state voltage and current data of both ends of the line. The author offers an improvement upon method of Takagi which uses data from one end only. In this technique, firstly the location is computed using a short line model. Where the short line approximation is unjustified, i.e. with lines longer than about 80km, the derivation may be repeated using distributed-parameter equations. Synchronization of data is implemented for maximum accuracy at the two substations. The two-ended algorithm described by the author provides an alternative which does not require any assumptions for the system outside the monitored line. The accuracy of the two-ended method is limited by the accuracy by which the parameters of the lines can be determined, and also by the accuracy of the measurement system.

Johns and Jamali [20] have presented an accurate fault location technique for transmission lines which uses post-fault voltage and current derived at both line ends. The method involves monitoring and filtering the voltages and currents measured at each end of the line so as to produce a measure of steady state power frequency of voltage and current phasors. The algorithm is based on natural modes and matrix function theory. A method similar to Schweitzer is used to derive an exact equation to obtain the distance to a fault on transmission lines. With reference to figure (2.1), the voltage at the fault point V_F, using data at end A is:

$$V_F = V_A\cosh(\gamma x) - Z_0\sinh(\gamma x)I_A \qquad (2.14)$$

and the voltage at the fault point using data at bus B is:

$$V_F = V_B \cosh(\gamma(L-x)) - Z_0 \sinh(\gamma(L-x))I_A \tag{2.15}$$

Equations (2.14) and (2.15) are equated so as to eliminate V_F, and the result obtained is x, the distance to the fault point, which is:

$$x = [\tan^{-1}(-B/A)]/\gamma \tag{2.16}$$

where;

$$A = Z_0 \cosh(\gamma L)I_B - \sinh(\gamma L)V_B + Z_0 I_A$$

$$B = \cosh(\gamma L)V_B - Z_0 \sinh(\gamma L)I_B - V_A$$

The calculated value of x has a very small imaginary part which is ignored. The real part is thus taken to represent the fault distance. In all cases, the algorithm error is less than approximately 1.5% and overcomes many problems associated with phase values, such as due to line loading, effect of source parameters, power swings, etc.

Sachdev and Agarwal [21] have presented a non-iterative technique that estimates the location of the line fault from fundamental frequency voltages and currents measured at the line terminals. These measurements would normally be available if digital impedance relay are used to protect the line. The measurements taken at the two line terminals are not required to be synchronized. Also, source impedance, current distribution factors and pre-fault currents are not used in the estimation procedure. The proposed technique uses the apparent impedances as seen from the terminals of a transmission line. To establish the basic approach, a symmetrical three phase system experiencing a balanced three phase fault is considered. The technique was tested using simulated data. The results indicate that the estimation errors are less than 5% of the line length except for a small section near the mid-point of the line. The effect of the shunt capacitance is neglected.

In another approach based on two-ended data, Sachdev and Agarwal have proposed a procedure to compensate for the effect of the shunt capacitance [22]. An estimate is first obtained from the positive sequence reactance using the series lumped line

model by measurements from both line ends. Based on the initial fault distance, the shunt capacitance on each side can be estimated. The sequence charging currents through these two capacitances can be calculated using the sequence voltages obtained from the previous estimation procedure; the sequence line currents towards the fault point are then obtained by subtracting the charging current from the previous line current and the fault distance is then estimated again. This procedure is repeated until convergence is obtained. A resistive fault path is assumed and the fault location depends on the estimated fault resistance and the phase angle difference between the zero sequence currents from both line ends.

Girgis, Hart and Peterson [23] have presented a fault location technique for two- and three-terminal lines. The method is based on digital computation of the three-phase current and voltage phasors at the line terminals. These phasors are obtained at each end of the line and communicated to another processor to calculate the fault position. The authors claim that the method is independent of the fault type and insensitive to source impedance variations or fault resistance. Furthermore, it considers the synchronisation errors in sampling the current and voltage waveforms at the different line terminals. The technique is tested using EMTP-generated transient data and high accuracy is shown. However, there is no mention of the effect of the CVTs, CTs and transducer/recording equipment interfaces. The line shunt capacitance is also ignored in the algorithm.

Kezunovic et. al. [24] have introduced a new fault location algorithm based on synchronized sampling. A time domain model of a transmission line is used as the basis for the algorithm developed. Samples of voltages and currents at both ends are taken synchronously and used to calculate fault location. The authors have discussed two different types of algorithm utilizing a short-line model and a long-line model. The performance of both these algorithms are tested using EMTP simulations of faults on transmission lines. Small percent of error is reported for all test cases under varying fault conditions. However, variation of system configurations are not considered.

Zamora et al [25] have presented a technique for fault location for two-terminal transmission lines. The method is based on measurements of the fundamental components of fault and pre-fault voltage at the two ends of a transmission line. These values are determined by filtering the signals measured by means of devices located on both ends of the faulted line. The method to locate a fault point on a transmission line is based on the calculation of the distance factor Kv. This method is suitable when the fault has been previously detected. This factor is a function only of the impedance of the line model and the distance to the fault point, which is the unknown value to be determined. The distance to fault is determined from the numerical value of Kv (defining the fault) and the mathematical function of Kv (determined for the particular transmission line under analysis). The numerical value of distance factor Kv, which defines the point at which the fault occurred, is given as:

$$Kv = \left| \frac{V_A}{V_B} \right|$$
(2.17)

The accuracy of the technique is tested using simulated data provided by a fault-analysis computer program. The estimated fault locations under different fault conditions are within 2.25% of the actual fault location.

2.4 Fault Location Techniques for Three-Terminal Lines

Three-terminal lines (teed feeders) are an extension of the two-terminal lines with an intermediate infeed. Not much work has been reported hitherto for fault location on teed feeders. Fault location on multi-terminal lines represents a problem presumably due to the infeed currents of the third source and also due to the presence of fault resistance.

Girgis et al [23] have presented a technique for locating faults on teed feeders and the method is based on utilising information from all three ends. Data from different ends are communicated to a processor at one particular end in order to calculate the

fault location. The local phasors are assumed to have a common reference, but synchronization at the different terminals is not required. The method uses the phase components and consider the line section to be untransposed. Although this technique adequately deals with some of the problems relating to teed feeders, the limited study presented is based on neglecting the line shunt capacitance, which would imply that the high accuracy attained can only be sustained on relatively short line lengths. Moreover, practical considerations such as transducer and hardware errors are not considered.

Aggarwal et al [26] have presented an alternative approach to accurately locating faults on teed feeders. The technique developed addresses the forgoing problems and takes into account the practical limitations. The method is based on utilising voltage and current waveforms at all three ends of typical EHV teed feeders, which are then filtered using Discrete Fourier (DFT) techniques so as to produce a measure of the steady-state power frequency voltage and current phasor. the technique makes use of superimposed modal components of voltages and currents rather than total phase values. The fault location algorithm is based on designating the line end closest to the fault as reference, and identifying the faulted leg before determining the distance to fault. The actual distance to fault from the nearest end is then calculated. The fault location technique is tested using simulated fault data from practical 400 kV teed feeders configurations. Errors of less than 2% are obtained.

2.5 AI-Based Fault Location Techniques

Girgis and Johns [27] have developed a hybrid expert system to identify the faulted section and interpret protective apparatus operation in a large interconnected power system. The expert system presented by the authors includes four stages. The first stage determines the faulted section of the power system and reports the correct and incorrect breaker and relay operation. The second stage interfaces the expert system with a data base to combine the real-time phasor measurement of the selected current and voltage waveforms with the relays and breaker status. In the third stage, the

expert system utilizes these phasor quantities to classify the fault. The fourth stage interfaces the expert system with fault location algorithms to select the most suitable algorithm for the specific situation detected; the main purpose of this stage is to find the fault location when the faulted section is a transmission line. Algorithms are developed in Fortran to compute the fault location based on the magnitudes and angles of the phase voltages, phase currents and the zero-sequence currents selected by the expert system at specified buses during the fault type classification stage. In determining the distance to the fault, the mutual coupling between parallel lines, fault current, and the fault resistance are sources of inaccuracy.

Two methods of fault location techniques are developed. The first method assumes that the voltage and current phasors are available at only one terminal of the line. The second method assumes that the current and voltage phasors are obtained from both terminals of the line. The former of the two methods, computes firstly the apparent impedance based on a selected voltage and current pairs. These voltage and current pairs depend on the fault type; the algorithm compensates for the unknown fault resistance by assuming that the fault current in the case of a single-line-earth fault to be proportional to the zero-sequence current and proportional to the compensated phase current in the case of interphase faults. The second algorithm eliminates the zero-sequence current component of the fault current and the associated current distribution factor to avoid inaccuracy in the zero-sequence impedance values. A current distribution factor is then developed for the positive and negative sequence networks. It requires information on source impedances at the time of the fault occurrence. This paper indicates that the application of expert systems for power system protection is promising and deserves further investigation.

Kanoh et al [28] have proposed a fault location method that uses an artificial neural network (ANN) to analyze the distribution pattern of the ground wire current along the power line. The proposed ANN comprises three sets of three-layer ANNs which follow the back-propagation learning procedure. The first and second ANNs calculate candidate-1 and candidate-2 for the fault section using current amplitude and phase

angle distribution patterns, respectively. The third ANN then defines the actual fault location using these candidates and a current amplitude distribution pattern. The technique used to determine ANN structure involves analysing the inference process of locating the fault point from the ground wire current distribution. In order to measure the current distribution patterns, current sensors are installed on the overhead ground wire. The method is tested for different fault cases and the accuracy of 98.4% is claimed by the authors.

Kandil et al [29] have discussed the possibility of using ANNs to identify faults that may have occurred in an AC-DC power system. In this paper, three different ANN architectures to distinguish between different types of faults on the AC-DC system are proposed. These can sense AC bus voltages either as rms values (with or without phase angle information) or as sampled instantaneous values of sine waves. The output layer of each ANN consists of six nodes categorising each type of fault. The HVDC system modelled is based on one pole of the two-pole 1000 MW Chateauguay (Hydro-Quebec) back-to-back tie. The model is simulated using the EMTDC package. A comparison between the three mentioned methods is made, and it is concluded that some confusion can occur in distinguishing a line-to-line fault from a remote AC fault and a delay of 1-2 cycles in detection of faults when using rms values is expected due to an algorithm required for determining the rms value.

2.6 Summary

A literature review of fault locator algorithms for two- and three-terminal transmission lines are discussed. The techniques reviewed are based on using data either from one end of the transmission line or from both ends. AI-based fault location techniques are also covered in this chapter. Each technique is described individually and some of the advantages and disadvantages are stated.

Chapter 3

Artificial Intelligence Techniques

3.1 Introduction

This project is concerned with research into an alternative fault location technique based on Artificial Intelligence (AI). It is the study of mental faculties through the use of computational models and is defined as the study of ways of making machines, especially computers, solve problems intelligently. It consists of a number of powerful tools and techniques for problem solving and recent advancement has increased the power and popularity of many AI techniques. There are a number of AI techniques in use today such as expert systems, fuzzy logic and Artificial Neural Networks (ANNs). Various AI applications have been applied to power system problems over the years.

3.2 Artificial Intelligence in Power Systems

Modern power systems are required to generate and supply high quality electric energy to consumers. In order to achieve this requirement, computers are extensively applied to power system operation, planning, monitoring and control; power system application programs for analysing system behaviour are stored in computers. For example, at the planning stage of a power system network, system analysis programs are executed repeatedly; engineers adjust and modify the input data to these programs

according to their experience and heuristic knowledge about the system until satisfactory plans have been determined. However, the programs developed hitherto are based on mathematical models and are implemented using languages suitable for numeric computation only. For sophisticated approaches to system planning, for example, development of methodologies and techniques to incorporate practical knowledge of power engineers into programs (which also include the numeric analysis programs) are needed.

Power system analysis programs and other application programs are employed in energy control centres for the purposes of investigating and predicting the behaviour of power systems under steady-state operations. Whilst these programs are powerful tools, their ability to assist operation engineers to make efficient decisions is very limited when unplanned or unexpected modes of system operation occur. The abnormal modes of system operation may be caused by network faults, active and reactive power imbalances, or frequency deviations. An unplanned operation may lead to a partial or a complete system blackout. Under these emergency situations, power systems are restored back to the normal state according to decisions made by experienced operation engineers.

Power system decision problems have been predominately studied and solved through numerical analytical programs because of the mathematical inheritance. Because of the laborious work involved in data preparation and time required for the detailed analysis of the results, the time available for comprehensive assessment and decision making has been sacrificed. Such tasks are made very difficult for humans to provide effective and efficient solution to the problems without some decision aides. Moreover, subjective problem solving approaches can very heavily depend on the persons (operator/engineer) own judgment and preferences in performing the task. In order to improve the situation, the establishment of an overall method for the assessment and enhancement of a power system is urgently required by power engineers. Hence, the search for better tools for aiding and guiding decision making is inevitable which can primarily improve the man-computer interaction as well as

break away from the obscureness which traditional computer methods inherit.

AI has provided techniques for encoding and reasoning with declarative knowledge. In particular, the advent of ANNs, an intelligent machine learning technique, provides neural network modules which can be executed in an online environment. These new techniques supplement conventional computing techniques and methods for solving power system problems.

3.3   Expert System

An expert system is a rule-based AI application program for doing a task which requires expertise. The expert program is built from explicit pieces of knowledge extracted from human experts using AI programming techniques such as symbolic representation, inference, and heuristic search. Knowledge-based systems can be distinguished from other branches of artificial intelligence by their emphasis on domain-specific knowledge, rather than the more general problem-solving strategies. Since their strength derives from such domain-specific knowledge rather than more general problem-solving strategies, expert systems are often call "knowledge-based". More recently, expert systems have been developed in many areas such as oil exploration, computer-chip design, disease diagnosis and engineering. The application of expert systems to power systems field is relatively new. However, there are some applications related to power system planning, fault section analysis, fault type classification and fault location [30,31].

3.3.1   Structure of an Expert System

Most production expert systems include the basic components related to each other as shown in figure 3.1.
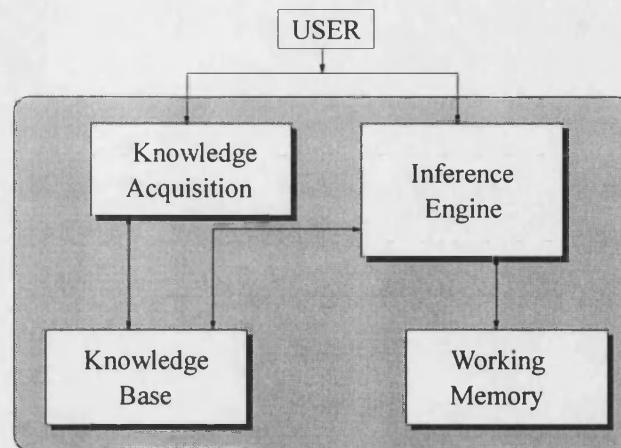
Figure 3.1 Structure of an expert system.

Expert systems typically have four components:

1) A *knowledge base*. This source of knowledge includes domain specific facts and heuristics useful for solving problems in the domain, generally structured in the form of production rules.

2) An *inference engine*. This is the knowledge processor which is modelled after the expert's reasoning. The engine works with available information on a given problem, coupled with the knowledge base, to draw conclusions or recommendations.

3) A *knowledge-acquisition*. The knowledge-acquisition interface assists experts in expressing knowledge in a form suitable for incorporation into a knowledge base.

4) A *working memory*. The working memory or global data base registers the current problem status and history of solution to date.

The user interface assists users in consulting the expert system, prompting them for information required to solve their problems, displaying the program's conclusions,

and explaining its reasoning. Generally, these interfaces attempt to provide the user with most of the capabilities they would have if they were interacting with a human expert.

3.3.2 Characteristics of Expert Systems

Some of characteristics shared by almost all expert systems can be summarised as:

- The system performs at a level generally recognized as equivalent to that of a human expert or specialist in the field.

- The system is highly domain specific, that is, it knows a great deal about a narrow range of knowledge rather than something about everything.

- The system can explain its reasoning, that is, to provide a useful tool it must be able to justify its advice, or conclusion.

- If the information with which it is working is probabilistic or fuzzy, the system can correctly propagate uncertainties and provide a range of alternate solutions with associated likelihoods.

3.4　Fuzzy Logic

Fuzzy logic models the vagueness of human reasoning by reflecting uncertainty about a variable's value through the assignment of a set of values to the variable; each variable has a degree of membership of the set which reflects the likelihood of the variable having that value. A membership function defines the degree of membership over the range of possible values or universe of discourse. Such a function can be assigned for a linguistic value or a fuzzy set that describes the set of values. It is this property that gives fuzzy logic its power to model qualitative reasoning and to be

used in knowledge representation.

The concepts of fuzzy logic and other AI techniques integrate very well to provide a hybrid system. The hybrid system techniques can be developed in a variety of ways. One of the most successful areas of AI techniques has been the integration of neural networks and fuzzy logic to give birth to an emerging area of research call "fuzzy neural networks" or "fuzzy neural system". Paradigms based upon this integration are believed to have considerable potential in the area of expert system, medical diagnosis, control systems, pattern recognition, and system modelling. Fuzzy logic and fuzzy neural networks are discussed in more depth in chapter 5.

3.5 Genetic Algorithms

The theory behind genetic algorithms (GAs) was proposed by John Holland in his landmark book *Adaptation in Natural and Artificial Systems* published in 1975 [32], and advanced by many other researchers. Genetic algorithm simulates a heuristic probabilistic search technique that is analogous to the biological evolutionary process. The difference between GAs and other optimisation techniques is that they work with a population of individuals represented by bit strings and need only fitness information of objective functions, thus avoiding some stiff mathematical difficulties with practical problems. Since GAs search for a group of candidates, they are likely to escape from local minimum to arrive at the global minimum. Thus, simple but powerful search strategies attract world-wide attention. The main demerits of GAs is the time consuming process of search and the combination explosion of off springs and its evolutionary process heavily depends on factors such as crossover, mutation rate, and chromosome length etc. In order to overcome the deficiencies of conventional GAs, many improved genetic algorithms have been presented, such as Steady-State Genetic Algorithms, Ranking Genetic Algorithms, Genetic Algorithms with Varying Genetic Parameters, and Genetic ALgorithms with Immigration. They have improved conventional genetic algorithms to some extent. It is visualised that hybrid systems are the way forward in the next generation of intelligent systems.

Experience with fuzzy logic and genetic algorithms has proven that the combination of them can efficiently make up for their own deficiency. Generally speaking, the combination strategies of fuzzy logic and genetic algorithms has two modes: (i) employ GAs to optimise the parameters of fuzzy logic and (ii) employ fuzzy logic to automatically modify the genetic parameters (such as crossover and mutation rate) during its optimisation process.

3.5.1 Application of Genetic Algorithms in Power Systems

GAs have emerged as an attractive alternative or complement to conventional optimization techniques. GAs with an inherent global optimization property, offer a fast, robust and efficient algorithm. Since it was first introduced to solve reactive power scheduling in 1991, many papers have appeared which study the feasibility and capability of GAs over a broad range of power system problems. The main areas include: economic dispatch, unit commitment, reactive optimization, planning and power system control.

3.6 Artificial Neural Networks

Artificial neural networks constitute a new approach to computation based on modern neurophysiology; a simplified model of the human neuron is organized into networks similar to those found in the brain. The human brain is the most complex computing device known to man, and its powerful thinking and remembering and problem-solving capabilities have inspired scientists to make machines in its image. To build intelligent machines, scientists needed to understand the structure and computations of the brain first. Initially, psychologists and latterly, neurophysiologists studied the structure of the nervous system with a view to simulating its functions.

The work of McCulloch and Pitts in 1943 had shown that a network of neurons with binary response function was capable of computation. Dean Edmonds and Marvin Minsky built an electromechanical learning machine in 1951. In the late 1950s and

early 1960s, Frank Rosenblatt developed the first successful neuro-computer which he call perceptron. During 1960s and 1970s, which is call the dark age of neuro-computing, little explicit research was carried out. However, in the 1980s, several events occurred which reestablished neural network research as a credible endeavour and culminated in the IEEE First Annual International Conference on Neural Networks (ICNN) in 1987. Since then, researchers focusing their efforts in the field of neural networks have produced impressive results.

The field is also known as neuro-computation, collective computation, connectionism, etc. The term neural network implies that it was originally aimed more towards modelling networks of real neurons in the brain. However, the models are extremely simplified compared to the latter, though they are very valuable for gaining an insight into the principles of biological computation.

3.6.1   Biological Basis for Artificial Neural Networks

The human brain, the most amazing carbon-based computer in existence, weighing a little over three pounds, consists of approximately 10 billion individual nerve cells called neurons. All human activities and behaviour can ultimately be traced to the activity of these tiny cells. Each neuron is interconnected to many other neurons, forming a densely connected network call a neural network. These massive interconnections provide an exceptionally large computing power and memory. From an information-processing point of view, the signal flow goes from dendrites through the cell body and out through the axon. The junction point of an axon with a dendrite of another neuron is call synapse. Synapses provide memory to the past accumulated experience or knowledge.

The basic building block of the nervous system is the neuron. A schematic diagram of the biological neuron is shown in figure 3.2 which comprises of a cell body, dendrites and an axon.
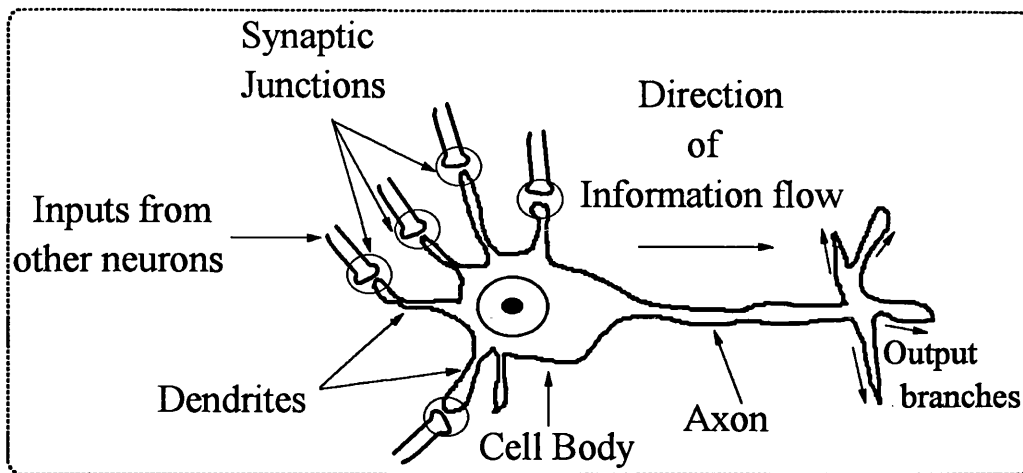
Figure 3.2 A schematic view of the biological neuron.

Each neuron is activated by the flow of biochemicals across the synapses. The transmission of these biochemicals across the synaptic junction causes a change in the ionic concentration within the neuron, which, in turn, produces a change in its electrochemical potential. These inputs may be excitatory (positive) and increasing the electrochemical potential of the post-synaptic neuron, or conversely, they may be inhibitory (negative) and reduce the electrochemical potential. If the net potential is above a certain threshold level then the neuron will "fire" a sequence of pulses along an axon leading the synaptic junction of another neuron. The electrochemical activities at these synaptic junctions exhibit complex behaviour because each neuron makes several hundred interconnections with outer neurons. Each neuron acts as a parallel processor because it receives pulses in parallel from neighbouring neurons and then transmits pulses in parallel to all neighbouring synapses.

The explanation of biological operation is greatly simplified, when seen from a neuro-biological point of view, although, it explains the basic principles involved. ANNs are much more simplified than their biological counterparts. They are described in the following section.

3.6.2 Artificial Neural Network Models

Due to the complexity and diversity of the properties of biological neurons, it is extremely difficult to compress their characteristics into a model. Towards this goal, a model of the biological neuron, also called a neural unit, or simply a neuron has been developed in the neural network paradigm. The neuron receives inputs from a number of other neurons or from the external world. A weighted sum of these inputs constitutes the argument of nonlinear activation function, as illustrated in figure 3.3. The neuron is said to have been fired if the weighted sum of its inputs exceeds a certain threshold, w_0.
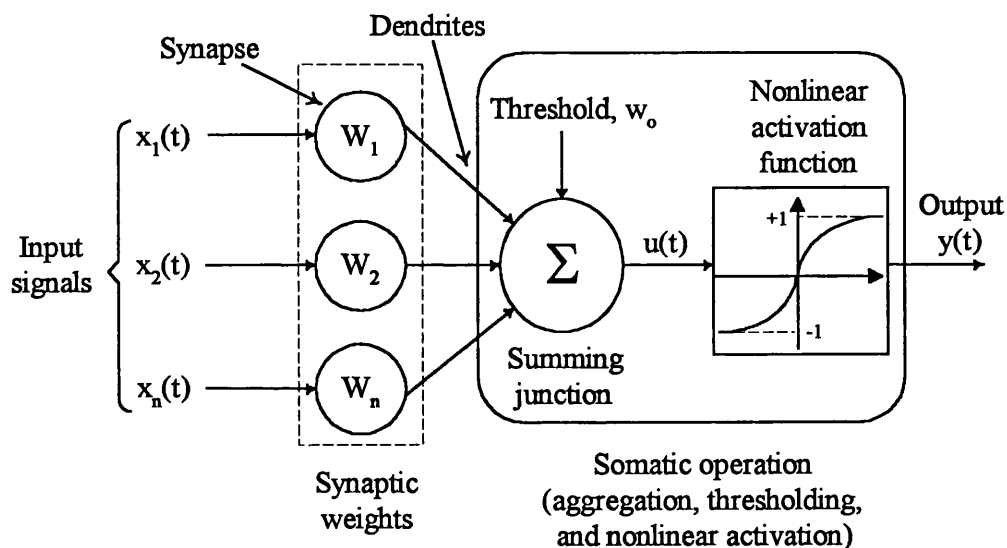
Figure 3.3 Model of an artificial neuron (unit).

Mathematically, the function of a neuron can be modelled as:

$$y(t) = \psi \left[\sum_{i=1}^{n} w_i x_i - w_0 \right] \tag{3.1}$$

where $[x_1, \ldots, x_n]$ represent input signals, $[w_1, \ldots, w_n]$ are the synaptic weights, $y(t)$ is the neural output, and $\Psi[\cdot]$ is some nonlinear activation function with threshold w_0.

Model of the artificial neuron is usually referred to as feed-forward neural network. These feed-forward networks respond instantaneously to inputs because they possess no dynamic elements in their structure. A schematic representation of a feed-forward neural network is shown in figure 3.4.
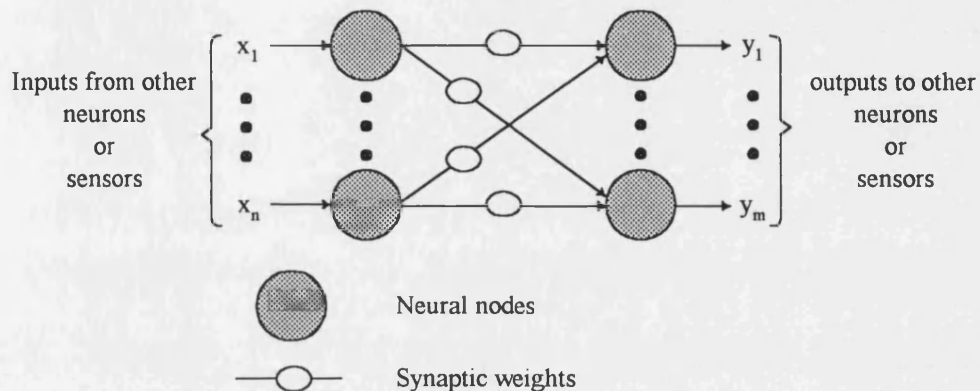
Figure 3.4 A feed-forward neural network with n-inputs and m-outputs.

A neural extension of feed-forward network is the feedback (dynamic) neural network that incorporates feedback and dynamical elements in its structure. There are several dynamic neural structures based on different neural paradigms. As mentioned in section 3.4, with the parallel growth in the field of fuzzy logic, many neural models encompassing the principles of the neural networks and fuzzy logic are also being developed.

3.6.3 Nonlinear Activation Function

The nonlinear activation function $\Psi[\cdot]$ maps the net input value $u(t) \in [-\infty, \infty]$ to a neural output, where:

$$u(t) = \sum_{i=1}^{n} w_i x_i \tag{3.2}$$

In general, the neural output is in the range of $[0, 1]$ for unipolar signals and $[-1, 1]$ for bipolar signals. The nonlinear activation operator transforms the aggregate $u(t)$ into a bounded neural output $y(t)$; that is:

$$y(t) = \psi[u(t)] = \psi \left[\sum_{i=1}^{n} w_i x_i \right] \tag{3.3}$$

Many different forms of mathematical functions can be used to model the nonlinear activation function. The most frequently used ones are the identity, the linear threshold function, the sigmoid function and the hyperbolic tangent function. The hyperbolic tangent function is just a bipolar version of the sigmoid function: the sigmoid is a smooth version of a {0,1} step function whereas the hyperbolic tangent is a smooth version of a {-1,1} step function. The sigmoid and the hyperbolic tangent transfer functions are shown in figure 3.5. The hyperbolic tangent function was used in this research because it trained faster and more effectively than the logistic transfer function.
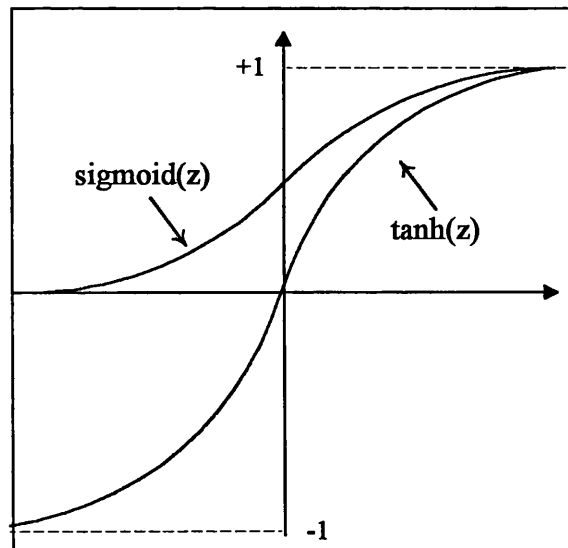
Figure 3.5 Sigmoid and hyperbolic tangent functions.

The sigmoid function is defined by:

$$f(z) = \frac{1}{1 + e^{-z}}$$
(3.4)

The hyperbolic tangent function is defined by:

$$f(z) = \frac{e^z - e^{-z}}{e^z + e^{-z}}$$
(3.5)

3.6.4 Neural Network Architecture

The neurons are normally connected to each other in a specified fashion to form the neural network. These arrangements of interconnections could form a single layer or several layers. In a large number of neural network models, such as the Perceptron, Linear Association, Multi-layer feed-forward network and the adaptive resonance training (ART) model, the output from the units from one layer is only allowed to activate neurons in the next adjacent layer. However, in some models such as Kohonen nets, the signal is allowed to activate neurons in the same layer [33,34].

The single-layered feed-forward network illustrated in figure 3.4, can only perform certain simple pattern-detection functions. The power of neural computation comes from the number of neurons connected in a network structure. Larger networks generally offer greater computational capabilities. Arranging neurons in layers or stages is supposed to mimic the layered structure of a certain portion of the brain. These multilayer networks have been proven to have capabilities beyond those of a single layer. The most commonly used neural network architecture is the multilayer neural network (MNN) based on error back-propagation (BP) learning algorithm.

3.6.4.1   Multilayer Feed-Forward Networks

The second class of a feed-forward neural network distinguishes itself by the presence of one or more hidden layers, whose competition nodes are correspondingly called hidden neurons. The function of the hidden neuron is to intervene between the

internal input and the network output. By adding one or more hidden layers, the network is enable to extract higher order statistics i.e. non-linear relationships. A schematic representation of a multilayer feed-forward neural network is shown in figure 3.6.
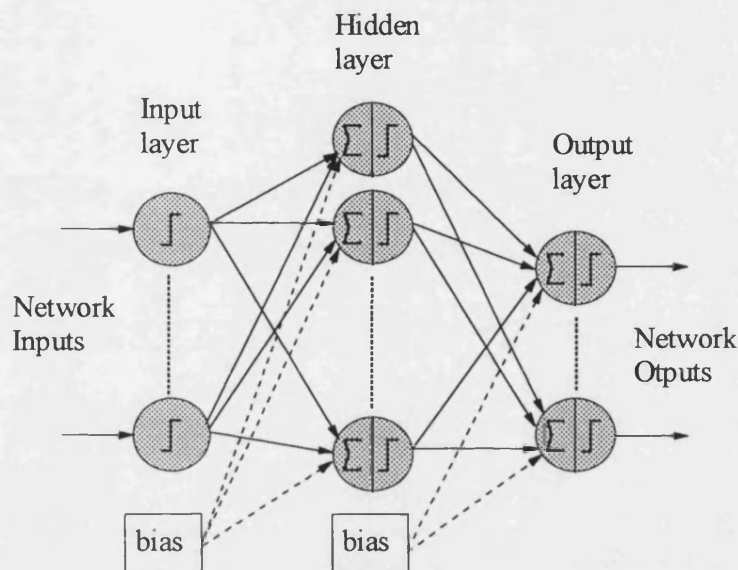
Figure 3.6 A multilayer feed-forward neural network with one hidden layer.

The neural network must have a mechanism for learning. Learning (also called training) is done for a subset of the input vectors, called the training set, whose properties are known or representative. Learning alters the weights associated with the various interconnections and thus leads to a modification in the strength of interconnections.

A neural network is characterized by its architecture, its processing algorithm and its learning algorithm. The architecture specifies the way the neurons are connected. The processing algorithm specifies how the neural network with a given set of weights calculates the output vector y for any input vector x. The learning algorithm specifies how the neural network adapts its weights for all given training vectors x. The form of learning, where the output is changed towards a desired value is known as

supervised learning, and is usually performed by a variant of back-propagation algorithm.

3.6.4.2   The Back-Propagation Learning Algorithm

The learning rule of multilayer perceptrons is called the "generalised data rule", or the "back-propagation rule". The main idea is to minimize the error between the desired and actual outputs through adjusting the weights by back-propagating the error from output layer to hidden layer. It is based on an iterative gradient algorithm and is outlined below.

Step 1   **Initialize Weights and Thresholds**

set all weights and modes thresholds to small random values.

Step 2   **Present Input and Desired Outputs**

Present a continuously valued input vector space to the input neurons,

$\vec{I}$, and get the desired output, $\vec{d}$.

Step 3   **Calculate actual output**

Use the neuron transfer functions to propagate the network input vectors through to the output layer neurons.

Step 4   **Adapt weights**

Use a recursive algorithm starting at the output neurons and work back to the first hidden layer to adjust the weights by:

$$w_{ij}(t+1) = w_{ij}(t) + \eta \delta_j I_j + \alpha(w_{ij}(t) - w_{ij}(t-1)) \tag{3.6}$$

where $w_{ij}(t)$ represent the weights from neuron i, in layer n - 1, to neuron j in layer n at iteration t. η is the learning factor, which controls how much of error is used to adapt the weights, α is the momentum factor which controls how much of the previous weight

change is used for the current weight change, and δ_j is the error on the output node j. If all neuron transfer functions are assumed to be Sigmoid, then:

$$\delta_j = y_j(1 - y_j)(d_j - y_j) \tag{3.7}$$

where d_j is the desired output of neuron j, and y_j is the actual output. For node j in the hidden layer:

$$\delta_j = I_j(1 - I_j)\alpha_k\delta_k w_{jk} \tag{3.8}$$

where k goes from 1 to the number of nodes in the layers above node j.

Step 5   **Iteration**

Iterate the computation by presenting new epochs of training examples to the network until the free parameters of the network stabilize their value and the average squared error computed over the entire training set is at a minimum or acceptably small value.

3.6.5 Practical Considerations of ANN

The successful development of ANN approaches for power system problems depends on the successful learning of the correct relationship or mapping between the input and output patterns by the ANN. In order to achieve this, practical issues surrounding the design, training, and testing of a ANN need to be addressed and examined.

3.6.5.1 Learning Process

Amongst the many interesting properties of a neural network, the one that is of primary significance is the ability of the network to learn from it environment, and to improve its performance through learning; the improvement in performance takes place over time in accordance with some prescribed measurement. A neural network

learns about its environment through an iterative process of adjustments. Ideally, the network gains more knowledge about its environment after each iteration of the learning process.

An ANN is trained using either supervised or unsupervised learning. If the desired output of the ANN is known for each of the training patterns then supervised learning is likely to be the most suitable form of training algorithm. Multi-layer feed-forward networks (MFNs) are usually trained off-line using supervised learning and then used to perform pattern recognition, prediction and classification in an on-line environment. For problems in which relationships amongst input patterns are to be established, unsupervised learning is more appropriate. In this case, the self-organising model, often referred to as the Kohonen model [35], is used.

3.6.5.2   Determining the Best Network Size

The degree of freedom of an ANN equal to the number of inter connection/size, and therefore proportional to the number of hidden neurones, must be matched, in some sense, to the complexity of the classification boundary. Currently, in the absence of parameter/theoretical guidance, the only proposed method of determining the best number of hidden neurons is by comparative cross validation among performance of several ANNs. Moving from a small number of hidden neurons to a large number should decrease the overall probability of error while maintaining an equivalent error performance for the test and training data. For a small number of hidden layer neurons, the ANN will be unable to learn the training data. As this number is increased the training error will reduce until a very large number of neurons are used, when the error will start to increase again.

3.6.5.3   Generalization Versus Memorisation

One of the major features of neural networks is their ability to generalise. There is a difference between training and memorization. The generalisation is the ability to successfully classify patterns that have not been previously presented. Memorization, on the other hand, guarantees that when the ANN is presented with a specific element in the training data set, the classifier will respond in exactly the same manner that it was trained. In the case of memorization, the response to data other than training data is not satisfactory.

The ability to interpolate among the training data does not necessarily imply good generalization. A properly trained classier should respond with the same error to the training data as to test data. This is a necessary but not sufficient condition. If the error from the test data is much higher than that from the training data, then the neural system is over determined; in other words, the degrees of freedom in the classifier is too high.

3.6.5.4   Feature Extraction

One of the classical problems in pattern recognition is how to extract the discriminatory features from a given set of measurements. The mathematical approach to feature selection is to identify certain invariant properties of the pattern classes. These properties are then used to reduce the dimensionality of the pattern vectors either through a linear transformation or through the preferential choice of subset of attributes. However, it is important to recognize that the superiority of any one procedure is ultimately determined by the problem at hand.

3.6.5.5   Convergence of Training Process

To ensure convergence of the training process is achievable, methods for adjusting the learning rate and the momentum, which are parameters in the error back-

propagation learning algorithm, are required.

3.6.5.6   Scaling of Input Features

The features must be scaled such that the weights of the links of MLP can be updated. They should also be scaled in a manner such that the relative importance of the features is retained. Scaling methods to achieve these aspects should be developed.

3.6.6 ANN Applications in Power Systems

The abilities of ANNs have attracted power system researchers to investigate the applications of ANNs in power systems. Since 1989, a great deal of work performed in this new area by the researchers have been reported in the literature and in some international conferences. About 70% of the reported work on application of ANN in power systems is based on the MFN, while other types of networks are used in the remaining 30%. The areas to which ANNs have been applied in the last few years are summarised below.

Prediction and control

> transient stability [36-38]
>
> steady-state stability [39,40]
>
> load forecasting [41-43]
>
> dynamic load modelling [44]
>
> reactive power control [45]

Identification

> protection [46,47]
>
> fault diagnosis [38,48]

harmonic source and load [49,50]

Classification

alarm processing [51]

contingency analysis [52]

Optimisation

optimal power flow [53]

unit commitment [54]

generation expansion [55]

economic dispatch [56]

3.7   Summary

The applications of artificial intelligence and neural network in power system are reviewed. Structures of an expert system, a fuzzy logic and neural networks are discussed with practical emphasis on multi-layer-perceptron and the back-propagation algorithm that is used to adopt the weights to achieve the desired non-linear mapping from inputs to outputs. Practical issues surrounding the design, training, and testing of ANNs have also been covered in this chapter.

CHAPTER 4

Power System Simulation And
Practical Considerations

4.1 Introduction

This chapter describes the simulations used to generate accurate and realistic fault data. The simulation of the power system has been done using the well proven Electro-Magnetic Transients Program (EMTP) [57]. This contains mathematical models of the power system components. It can predict variables of interest within electric power systems as a function of time, typically following a disturbance such as the switching of a circuit breaker, or the occurrence of a fault. The data was calculated at 2 µs (ie simulated at 500 kHz) to give improved accuracy. Every 125th data value was recorded so that the output data was produced at the desired sampling rate of 4 kHz for subsequent frequency.

4.2 Power System Configuration

The simulation study is based on a plain feeder EHV line system. Figure 4.1 shows the power system configuration, in which symbol S1 represents source capacity at fault locator end (or local end) and S2 represents the receiving end source capacity. An X:R ratio of 30 and Z_{s0}:Z_{s1} ratio of 1.0 were used for each source terminating a busbar. The overhead transmission line used in this work is based on a single circuit

of the typical quad-conductor 400 kV vertical construction line currently used on the UK super-grid system [58]. The earth resistivity is taken to be 100 Ωm and the power system frequency as 50 Hz.

```
                    |←———— 128km ————→|
          End S                        End R
        ⎛     ⎞                       ⎛     ⎞
        ⎜ s1  ⎟——|————————————————|——⎜ s2  ⎟
        ⎝     ⎠   |                |   ⎝     ⎠
          fault locator end          receiving end
```
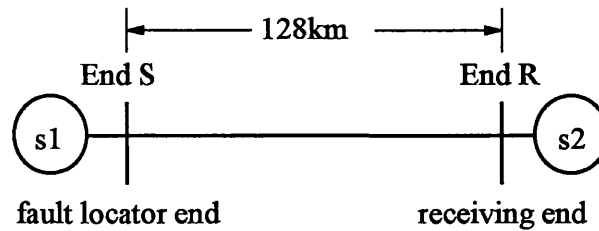
Figure 4.1 Power system configuration.

4.3   Source Configuration

In general, the source network can be represented by the Thevenin equivalent circuit of a voltage source in series with a source impedance. The source will have mutual impedance, X_m and self impedance, Z_s and also have positive phase sequence impedance, Z_1, negative phase sequence impedance, Z_2 and zero sequence phase impedance, Z_0.

In a practical EHV transmission line system, sources with a wye connection generally have a return path, either through the ground or a neutral conductor. Figure 4.2 shows an equivalent circuit of a three phase wye-connected source.
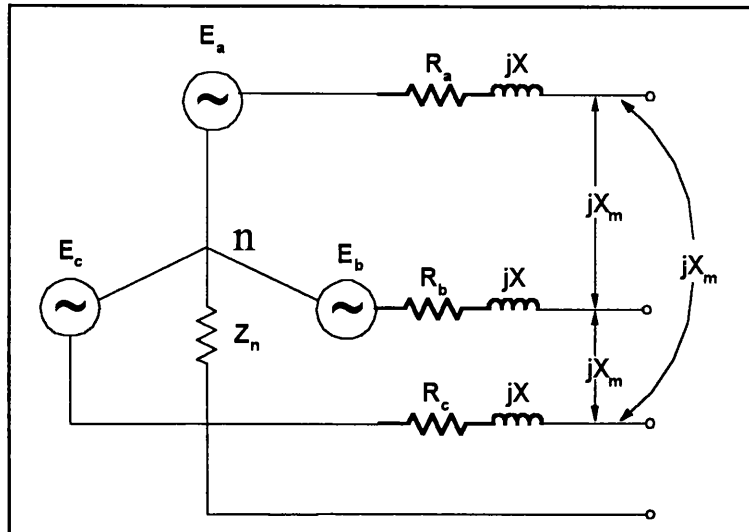
Figure 4.2 Equivalent three phase source circuit.

Where:

$R_a+jX=R_b+jX=R_c+jX=R+jX$ are source impedance, jX_m is mutual impedance and Z_n is neural impedance.

It is important to note the zero-sequence system, since a wye-connected load with a neutral path provides a return path for zero-sequence currents (I_0) flowing through the three phases. The total three phase current ($3I_0$) flows through the ground. If the neutral is grounded through neutral impedance, Z_n, an impedance of $3Z_n$ should be inserted between the neutral point n and the ground. The reason for this is that the neutral current produces a zero sequence voltage drop of $3I_0Z_n$, between the neutral point n and the ground.

The zero, positive and negative sequence impedance calculations can be obtained from reference [59], which also gives the following two equations:

$$Z_0 = R + j(X + 2X_m) + 3Z_n$$

$$Z_1 = Z_2 = R + j(X - X_m)$$

(4.1)

If the mutual impedance, X_m , is very small, and the source capacity of short circuit level (SCL), transmission line voltage (400 kV), source X:R ratio and Z_0:Z_1 ratio are given, then the neutral impedance Z_n can be obtained from equation 4.1.

4.3.1 Specifying Source Quantities

In practice, the information about the source in given in terms of short circuit level (SCL), X:R ratio and Z_{s0}:Z_{s1} ratio. Generally, source impedance are predominantly reactive with angle in the region 75° to 90°.

The power sources are modelled in the EMTP using three single phase voltage sources with a 120° phase shift between each one. At each line end, the shunt capacitance of the busbars was assumed to be 0.1 μF which is typical for a 400 kV system. The source capacity at each line end was modelled using a series impedance whose value was calculated as follows:

$$Z = \frac{V^2}{SVA}$$

(4.2)

Z   -   source impedance (Ω)

V   -   operating voltage (V)

SVA   -   source short circuit level in VA

$$Z = R + jX$$

(4.3)

$$X = Z\sin(\tan^{-1}(X{:}R \ ratio))$$

(4.4)

$$R = \frac{X}{X:R \ ratio}$$ (4.5)

where,

R   -   source resistance (Ω)

X   -   source reactance (Ω)

4.4   Transmission Lines Configuration and Parameters

An overhead transmission line consists of resistive and reactive parameters that are distributed along the length of the line. They can be represented by an equivalent circuit with lumped components as T or π network. However, it is required for an exact representation of a transmission line in that the parameters of the lines be uniformly distributed along the whole length of the line. In the three-phase system, the characteristic of each phase is influenced by its two neighbours, as well as reflection in earth planes and lines.

4.4.1   Transmission Line Design

The function of an overhead three-phase electric power transmission line is to transmit bulk power to load centres and large industrial users beyond the primary distribution lines. A given transmission system comprises conversion structures and equipment at a primary source of supply, including lines, switching, and conversion stations, between a generating or receiving point. In this respect, it is very important to select the best line configuration to meet the system requirements. The important factors affecting choice of line configuration and conductor spacing are:

   □   Transmission line voltage.

   □   Conductor type and size.

   □   Insulator type.

□   System protection.

□   Grounding.

□   Climatic conditions.

□   Mechanical design.

   (a)   Span length.

   (b)   Conductor sag.

   (c)   Conductor spacing.

   (d)   Conductor hardware selection.

4.4.2   Electrical Factors

Electrical design dictates the type, size, and number of bundle conductors per phase. Phase conductors are selected to have sufficient thermal capacity to meet continuous emergency overload and short-circuit current ratings. For EHV transmission lines, the number of bundle conductors per phase is selected to control the voltage gradient at conductor surfaces, thereby reducing or eliminating corona.

The number of insulator discs, vertical or V-shaped string arrangement, phase-to-phase clearance, and phase-to-tower clearance, must be selected to provide adequate line insulation. Line insulators isolate the towers from the conductors; therefore they must withstand transient over-voltages due to lightning and switching surges.

To protect the phase conductors from lighting strokes, earth wires are located on the towers. The towers are well earthed and counterpoise is used parallel to the line to reduce the tower footing resistance.

4.4.3   Mechanical Factors

The strength of the conductors, insulator strings, and support structures are considered in the mechanical design of the transmission lines. Conductors and suspension insulator strings must be strong enough to support the phase conductors with ice and

specified wind in addition to their own weight.Towers are designed to support the phase conductors and earth wires with ice and wind loading.

4.4.4 Environmental Factors

In order to select a line route for a transmission line, the land usage and visual impact must be included in the tower design. The effect on local communities and population centres, land values, access to property, wildlife, and use of public parks and facilities must all be considered. Also, the biological effect of prolonged exposure to electric fields near transmission lines must be considered.

4.4.5 Economic Factors

The total installed cost of the line and the cost of line losses over the operating life of the line, must be kept at lowest overall level. Power utilities use digital computer programs and physical experience to achieve optimum line design.

4.4.6 Transmission Line Transposition

In long transmission lines, if the spacing between phases are unequal, unbalanced flux linkages occur, and the phase inductances are unequal. Therefore, to restore balance, the conductor positions along the line are exchanged (transposed) at two locations such that each phase occupies each position for one-third of the line length.

In practice, it is not common to built overhead lines with transposition towers for economic reasons. However, an interchange of conductor positions can be done at switching stations in order to balance the voltage drops in the three phases.

4.4.7 Transmission Line Studied

The overhead transmission line used in this work is based on a single circuit of the typical quad-conductor 400 kV vertical construction line currently used on the UK super-grid system [58], where a, b and c represent three phase conductors and e represents the earth wire. Figure 4.3 shows the construction of transmission line used in the simulation of the system.
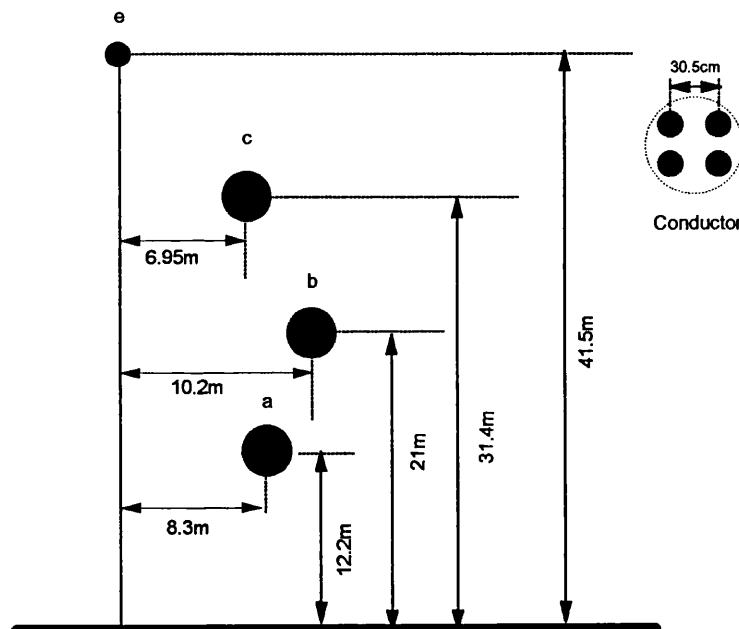
Figure 4.3 400 kV single circuit transmission line construction.

4.4.8 Phase Conductors

Each phase conductor is composed of an aluminium tubular conductor and steel reinforced core. Table 4.1 gives the conductor parameters which are taken from the GEC Protection Relay Application Guide [60].

Nominal Aluminium area (mm²)	Stranding and wire diameter		Approximate overall diameter (mm)	Resistance at 20°C (Ω / km)	Sectional area of Aluminium (mm²)	Total section area (mm²)
	Aluminium (mm)	Steel (mm)				
400	54/3.53	7/3.18	28.62	0.06740	428.9	484.55

Table 4.1 Aluminium Conductor Steel Reinforced (ACSR) overhead conductor data.

In the line system simulation model, line parameters are selected as below:

1) Phase conductors are 4×54/7/0.33cm a.c.s.r. with 30.5cm bundle spacing.

2) Earth wire is 54/7/0.33cm a.c.s.r.

3) Earth resistivity is 100 Ωm.

4) Conductor resistance is 0.06740 / 4 = 0.0168 Ω/km.

5) Earth wire resistance is 0.06740 Ω/km.

6) Conductor overall diameter = 28.62 mm.

Using EMTP line constants program [57], parameters of the line are calculated for each section of the line.

4.5   Fault Analysis

A fault may occur on a transmission system for a number of reasons, some of the common ones being:

☐   Lightning, high winds, snow, ice and frost,

☐   Switching,

☐   Falling debris,

☐   Broken conductor(s),

☐   Long term ionisation of the air.

Some of these factors can cause transient faults and some can cause permanent faults on the transmission system. Faults give rise to abnormal operating conditions, usually excessive currents and voltages at certain points on the system. Protective equipment is used on the system to guard against abnormal conditions. Various types of faults that occur on transmission lines are simulated herein using EMTP.

4.6   Fault Transient Simulation

To consider all practically encountered different system and fault conditions on transmission lines, a range of different faults were simulated. Some of the factors that were varied in the simulation are:

- The source capacity
- Fault position
- The fault type
- The line length
- The line configuration
- The fault inception time
- The fault resistance

4.6.1   The Source Capacity

Fault-transient waveforms are significantly affected by the source parameters. Source capacities based on SCL ranging from 2.5GVA to 20GVA are used in the simulation study at both ends of the line. Figure 4.4 shows a comparison between the response for a solid midpoint fault when the sending source capacity takes both large and small values. The voltages, in particular, are much smoother when the source near the point of observation is large. Such a response is obtained because the travelling wave components of current propagating into the source do not cause significant voltage transients if the source impedance is small; i.e. the busbar voltage is held nearly constant and is not easily distorted. However, in the case of a small sending-

source capacity i.e. large source impedance, very considerable waveform distortion occurs. This is due to the low capacity of the source adjacent to the point of observation, which therefore constitutes a major point of electrical discontinuity from which high-frequency components are easily reflected.
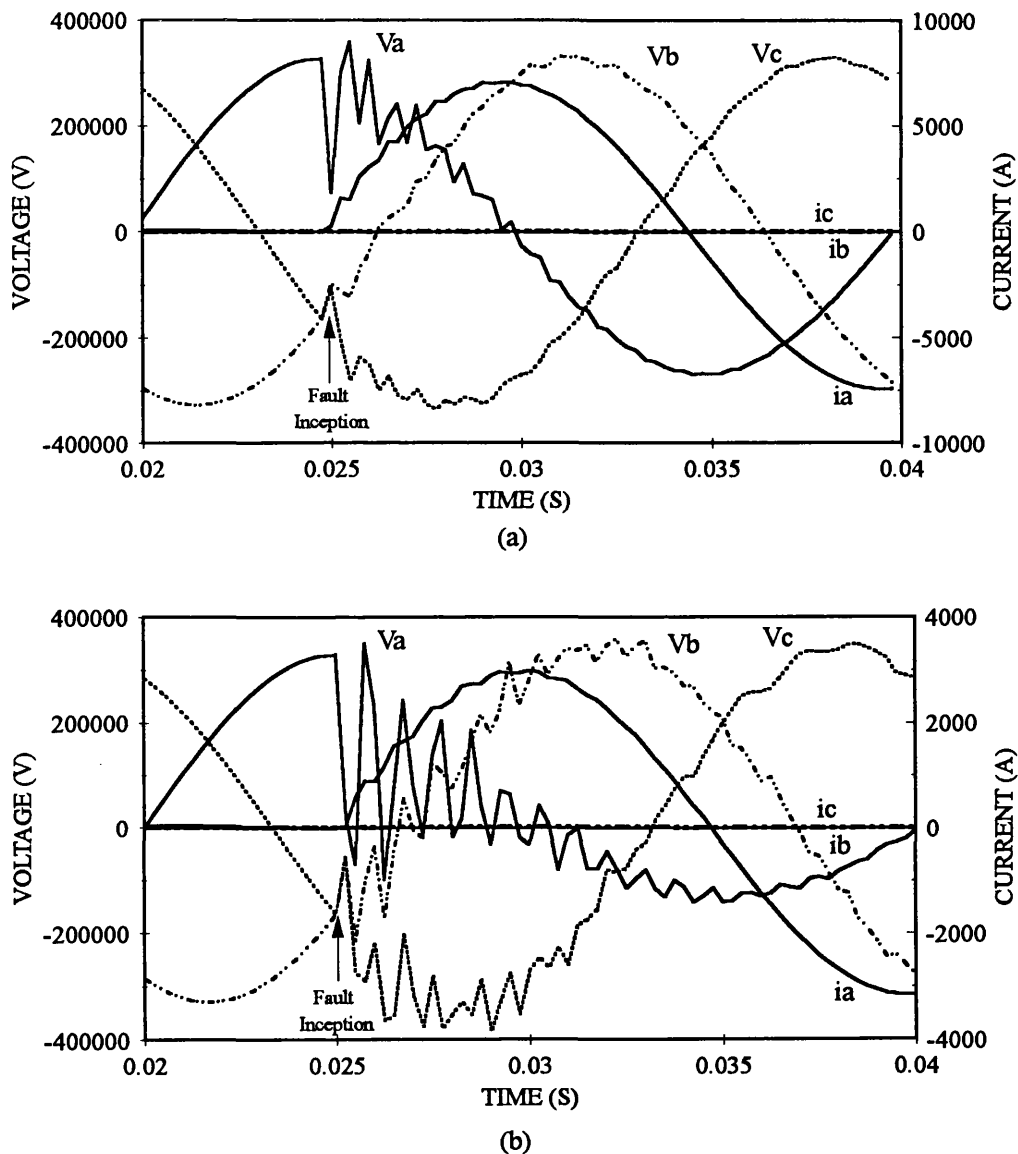
Figure 4.4 Effect of source capacities on voltage and current waveforms.
'a'-earth solid fault at midpoint.
(a) sending end s.c.l. = 20 GVA, receiving s.c.l. = 20 GVA
(b) sending end s.c.l. = 2.5 GVA, receiving s.c.l. = 20 GVA

4.6.2 Fault Position

The transit time between the fault and source discontinuities varies with fault position, and it follows that the apparent frequency of the superimposed travelling-wave components decreases as the fault position becomes more distant from the point of observation. In this simulation study, fault position was varied from 0 to 100% of the line length. The fault-transient waveforms for a solid 'a'-earth fault are shown in figure 4.5.
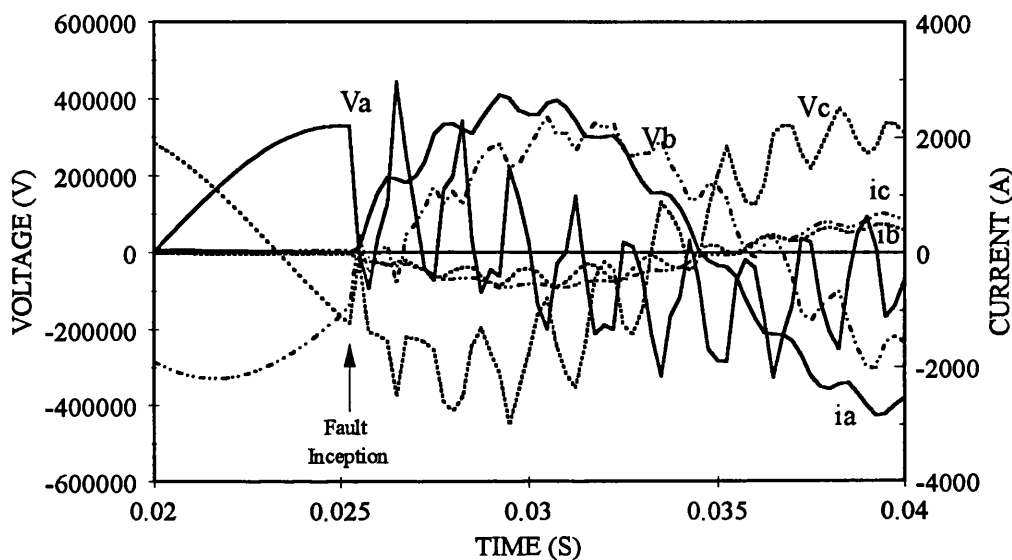
Figure 4.5 Voltage and current waveforms for receiving end fault.
'a'-earth solid fault at receiving end.
sending s.c.l. = 2.5 GVA, receiving s.c.l. = 20 GVA

4.6.3 The Fault Type

Various types of faults that occur on transmission lines are considered in the simulation study. Generally, the fault type on EHV transmission lines can be classified as:

- □ Single line-to-ground fault
- □ Double line-to-ground fault
- □ Line-to-line fault

    ☐   Three phase fault

    ☐   Three-phase-to-ground fault

Faults not involving earth give rise to waveforms which are generally very distorted. Figure 4.6 shows the waveforms obtained for an 'a'-'b' fault, and by comparing this with an 'a'-earth for corresponding source conditions, shown in figure 4.4(a), it is clearly evident that the travelling waves persist for considerably longer in the former case.
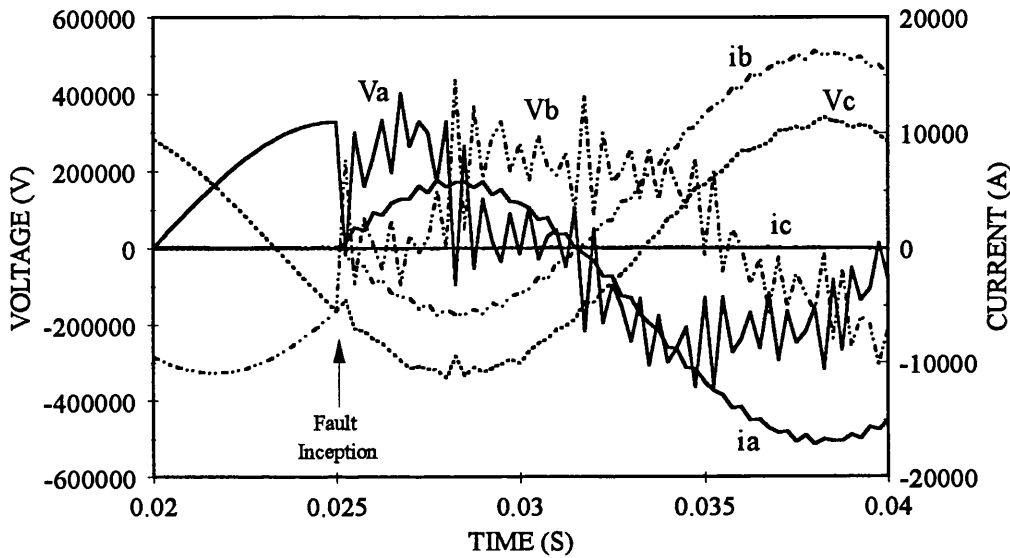
Figure 4.6 Voltage and current waveforms for line-to-line fault.
'a'-'b' fault at midpoint.
sending end s.c.l. = 20 GVA, receiving end s.c.l. = 20 GVA.

4.6.4 The Line Length

The EHV transmission lines can vary considerably in length. In this thesis, the core of the simulation study is based on a line length of 128km for the 400kV transmission line. However, Transmission lines with different length are also included in the simulation.

4.6.5 The Line Configuration

Typical configuration of overhead line circuits operating at UK transmission voltages is given on reference [60]. Training data is based on the line configuration shown in figure 4.3. However, other configurations were also used in the simulation as test data.

4.6.6 The Fault Inception Time

In practice, faults can occur at any point on wave i.e. the fault inception angle cannot be defined in advance. In this study, the faults have been applied at instances corresponding to voltage maximum, at 45° angle , and at zero voltage on the faulty phase or phases. In the latter case, the travelling waves are reduced because there is not a large and sudden voltage change at the point of fault. Figure 4.7 typifies the waveforms for fault at voltage zero at the receiving end. Distortion is extremely small, and the offset nature of the current waveform is clearly observed.
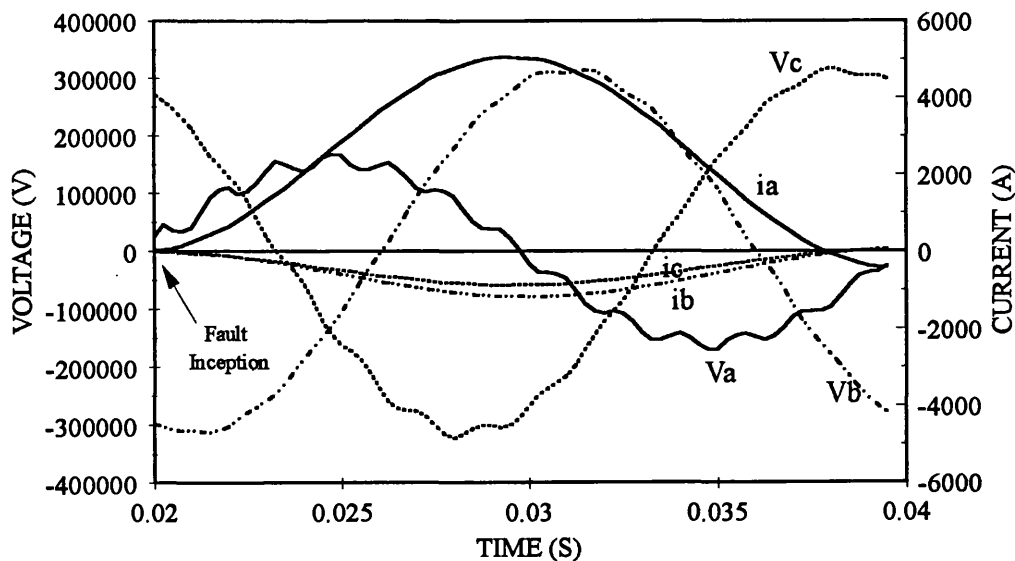
Figure 4.7 Voltage and current waveforms for fault applied at voltage zero.
'a'-earth solid fault at receiving end.
sending end s.c.l. =2.5 GVA, receiving end s.c.l. = 20 GVA.

4.6.7 The Fault Resistance

The effect of fault resistance for all types of fault involving a fault resistance was examined. The simulations were carried out varying the fault resistance from 0 to 200 Ω and it was found that values of fault resistance up to 10 Ω made little difference to the fault-transient waveforms. Beyond this value, the travelling wave components become progressively more damped, and there is a marked reduction in the initial voltage change which occurs for faults near voltage maximum. Figure 4.8 shows the waveforms obtained for an 'a'-earth fault with fault resistance of 100 Ω.
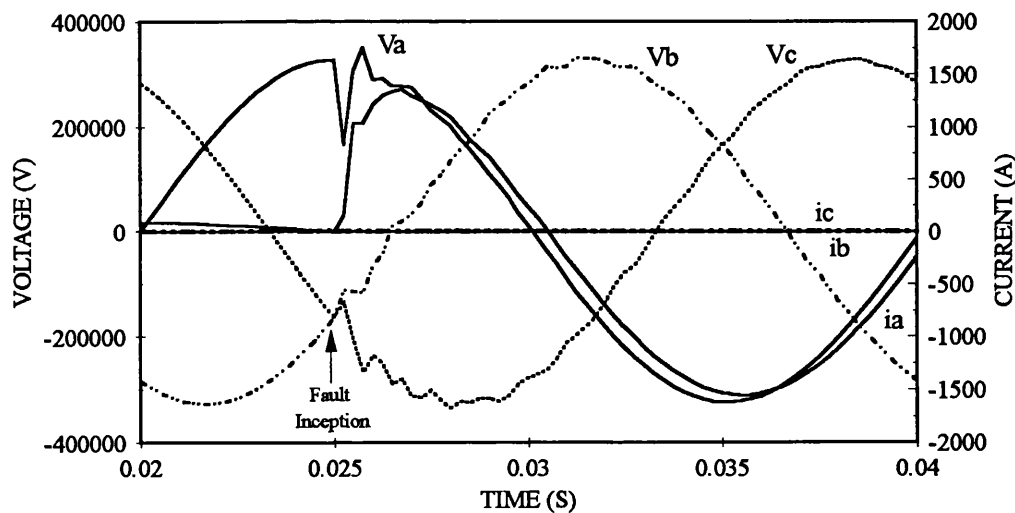
Figure 4.8 Effect of fault resistance on voltage and current waveforms.
'a'-earth fault at midpoint.
sending end s.c.l. = receiving end s.c.l. = 20 GVA, fault resistance = 100 Ω.

4.7   Practical Considerations in the Design of the Fault Locator

It is vitally important that during the performance evaluation of the fault location techniques, the voltage and current waveforms presented to the algorithm are as close as possible to those experienced in practice. In this respect, off line digital simulation of such fault transient waveforms is considered as the most appropriate and economic method. Although the fault location technique is based on Computer Aided Design

(CAD) studies, however, practical consideration, such as the effect of transducers, and hardware errors i.e. anti-aliasing filters and quantisation, etc, on the primary system fault data are also included in the simulation so that the data processed through the fault locator algorithm is very close to the real-life situation.

4.7.1 Fault Locator Scheme

The complete fault locator scheme is shown in figure 4.9. It represents the various practical stages before the processing of the fault locator algorithm. In practical fault locators, the actual data goes through analogue channels. Therefore it is necessary to take into account the effect of an analogue channel during the neural network training process. In this respect, a channel emulator is developed which includes a CVT, a low-pass analogue filter and an analogue to digital (A/D) converter.
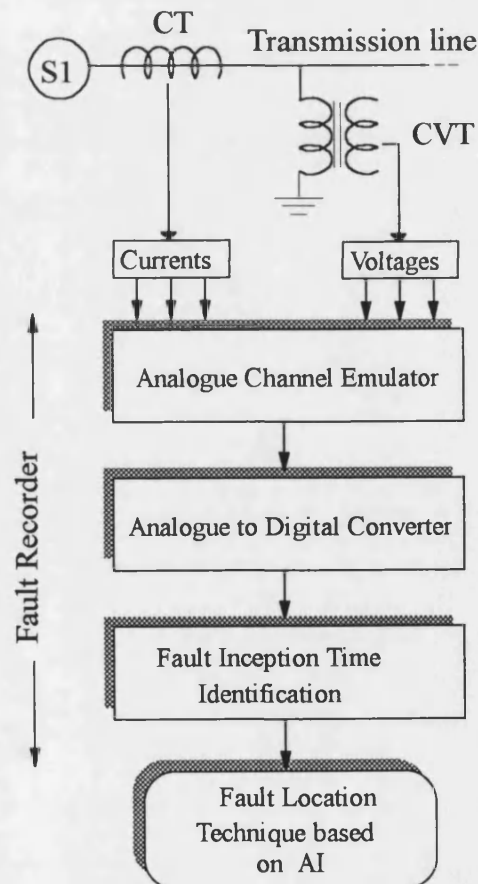
Figure 4.9 Fault locator scheme.

4.7.2 Digital Fault Recorder

Digital fault recorders have been used by the power supply authorities to continuously monitor sections of power systems to provide a record of fault conditions. These recordings provide data prior to and following the fault incident, referred to as pre-fault and post-fault information. This enables power engineers to look at conditions leading up to the fault, protection operation and how the control systems on the circuit responded, e.g. breaker operating times, protection carrier channels, etc.

The advent of microprocessor-based recording devices and the analytical capabilities provided by such devices, offer significant benefit to the user such as better performance and data recording. They provide a more convenient form of presenting the information and data processing of the primary system waveforms. In this respect, utilities have shown increased interest in implementing accurate fault location techniques.

4.7.3 Primary System Waveforms

Transient behaviour of the overhead line has been accurately predicted using the EMPT software for simulation of the power system. The precise current and voltage information for different EHV power system network configurations are derived before and after the fault. The physical arrangement of conductors, the characteristics of conductors, the effect of earth return path and effect of frequency dependent parameters are considered in the line constant program.

The various factors such as effect of fault type, differing source capacities at both ends of the line, fault resistance, etc, which influence the transient phenomena, are considered.

Figure 4.10 typifies the primary voltage and current waveforms generated for the 400kV system considered, when a single-line-to-ground fault is applied at the middle of the line.

(a)

(b)
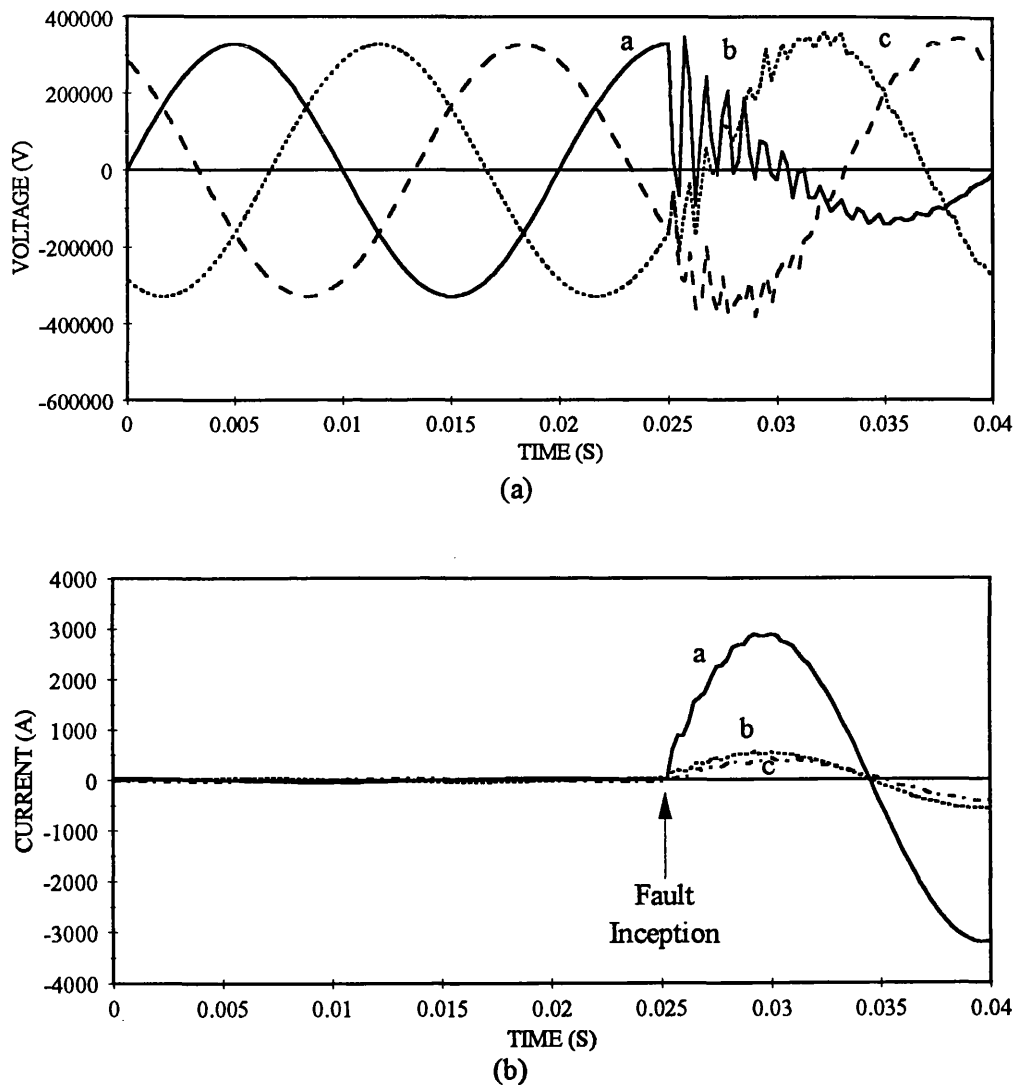
Figure 4.10   **Typical voltage and current waveforms, a-phase to ground fault at the middle of the line: S1=2.5GVA, S2=20GVA, fault resistance(R_f=1Ω).**
(a) Fault locator-end three phase voltages.
(b) Fault locator-end three phase currents.

4.7.4 CVT & CT Transducers

In any fault locator design based on CAD technique, it is extremely important to take into account the effect of CTs and CVTs on primary system waveforms as they can

have a significant bearing on the accuracies attained and therefore on any inferences drawn concerning a particular fault locator technique. These effects are incorporated into the simulation via the impulse responses of the elements. Time Domain Convolution techniques based on impulse responses of the transducers are then applied to the waveforms to produce the expected outputs.

The primary system waveforms are fed to CTs and CVTs to permit proper insulation level and current carrying capacity in relays, fault recorders and other instruments. Conventional CVTs have a very low cut-off frequency typically of 1 kHz whereas the CTs have a much wider bandwidth of typically 10 kHz.

4.7.5 Capacitor Voltage Transformer (CVT) Model

A typical CVT model is shown in figure 4.11 This device is basically a capacitance potential divider (which uses capacitors C1 and C2) coupled with a conventional electromagnetic voltage transformer. The divider reduces the system voltage (400 kV line voltage) to 63.5 volts rms (phase to neutral). L1 is an adjustable tuning inductance and T is the voltage transformer. By analysing the CVT model, its frequency response can be obtained as shown in figure 4.12 which clearly show that there is a sharp attenuation at around 700 Hz. Also there is some alternative of the frequency components of the lower end of the spectrum. Therefore, when a fault occurs, some high and low frequency signals of line voltage may be damped or reduced through the CVT.

Line terminal 400 kV
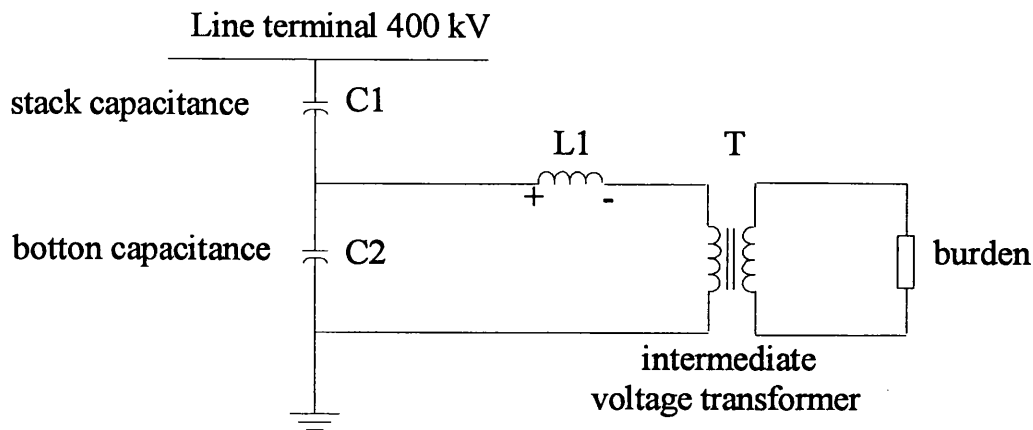
Figure 4.11 Typical Capacitor Voltage Transformer (CVT) model.
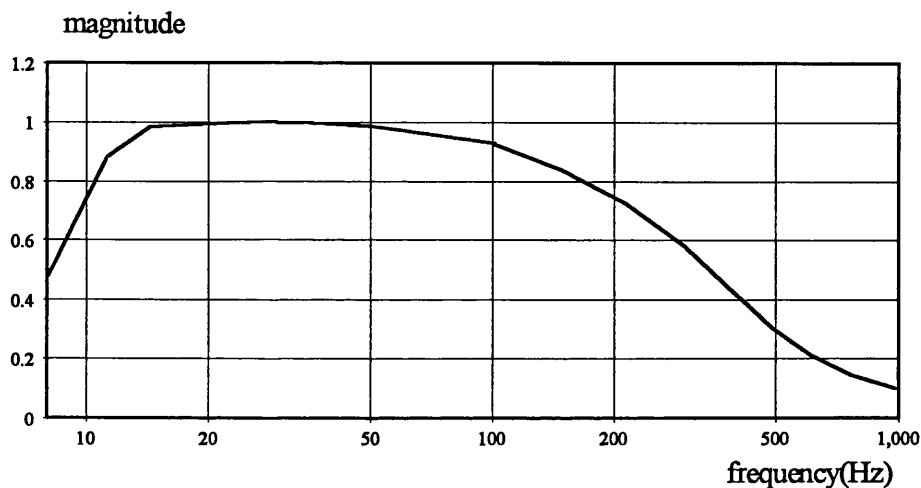
Figure 4.12 The frequency response of the CVT.

4.7.6 Current Transformer (CT) Characteristics

The function of a current transformer (CT) is to produce a current which equals the primary current divided by the turn's ratio. Under normal conditions, the CT operates well below the saturation flux and the exciting current drawn by the CT is small. However, under heavy fault conditions (particularly under DC offsets), saturation may be reached, and the measured fault current which may consist of many frequency components could be affected through the CT. To avoid large CT errors while measuring fault currents, a CT with turns ratio 2000 : 1 was selected [61].

4.7.7 Channel Emulator and Analogue to Digital (A/D) Converter

Firstly, the CVT and the anti-aliasing analogue filter frequency responses are converted into a CVT impulse response and a filter impulse response respectively. Then by using C program, an emulation of the analogue and A/D channel is developed. The emulator does two convolution calculations and one A/D conversion. In the emulator, an input fault waveform simulation data convolves with the CVT impulse response to obtain a CVT output data (63.5 volts rms). The CVT output data then convolves with the low-pass filter impulse response to obtain a filter output data which has an output of ±8.5 volts range. By selecting ±10 volts as the 12 bit A/D converter reference voltage, the A/D converter can give ±2048 quantum levels with 4.88 mV quantum level accuracy. The low pass filter is employed to avoid aliasing in voltage and current measurements during the A/D conversion and this comprises of a second order Butterworth low-pass filter.

4.7.8 Emulator Tests

Figure 4.13(a) shows the transient fault waveform for a-phase to ground fault at the middle of the 400kV transmission line with the system parameters: line length of 128 km, source capacity of 2.5GVA at S1 and 20GVA at S2. By inputting this waveform into the emulator, the CVT output, the filter output and the digital output are plotted in figures 4.13(b), 4.13(c) and 4.13(d) respectively. Figure 4.13(b) clearly shows a ±63.5 volts rms transient fault waveform. It also shows that the frequency limitation imposed by the CVT significantly reduces the input waveform high-frequency components above 700Hz. The analogue output is shown in figure 4.13(c); this waveform is the same shape as CVT output waveform in figure 4.13(b), except that the magnitude of the voltage is scaled down to ±8.5 volts. The 12 bit digital output fault waveform is shown in figure 4.13(d), the digital output range is ±2048.
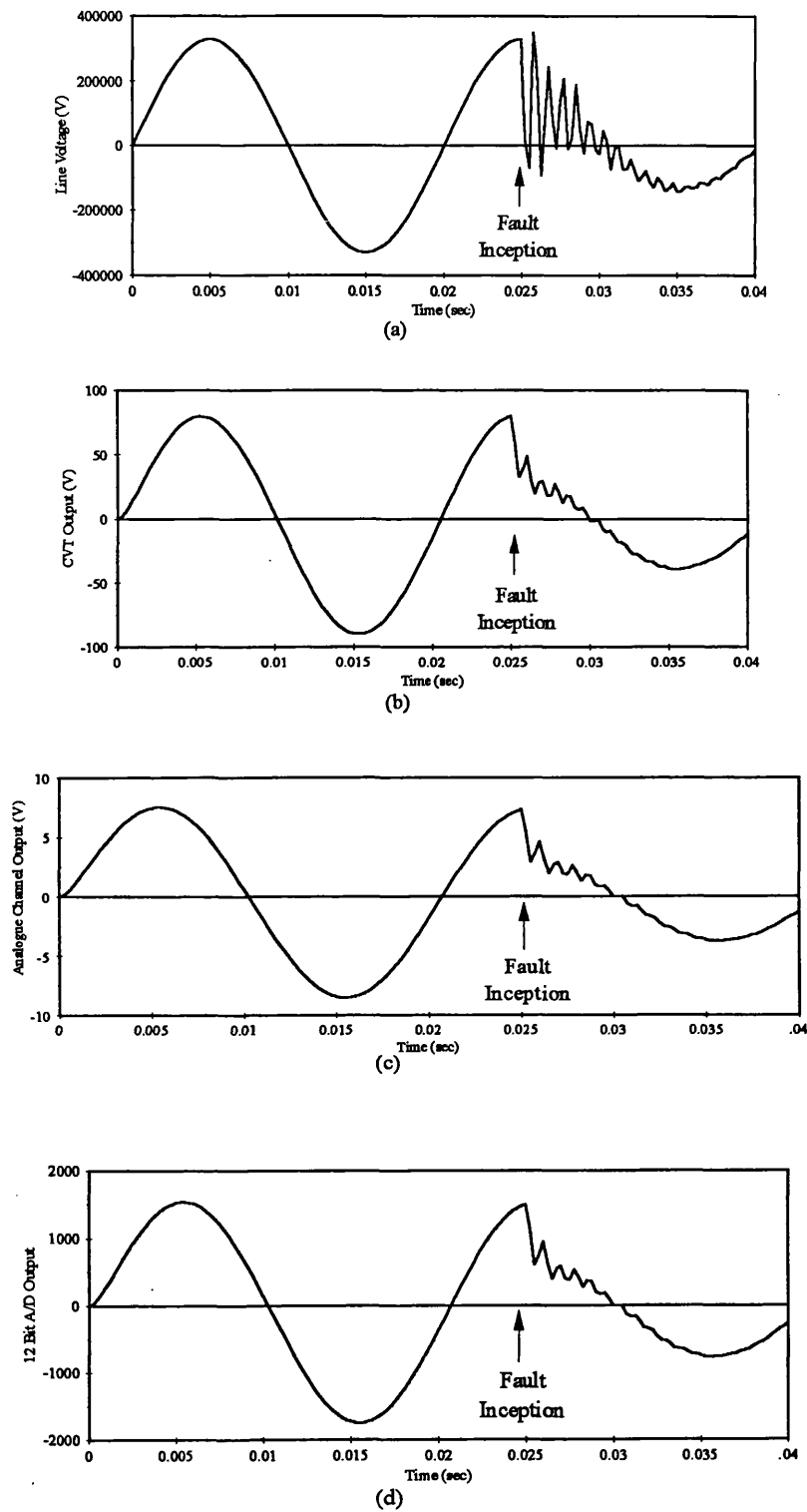
Figure 4.13 Emulator test.
(a) The study of a-phase voltage transient fault waveform.
(b) The a-phase voltage transient fault waveform output of CVT.
(c) The a-phase voltage transient fault waveform output of the analogue filter.
(d) The a-phase voltage transient fault waveform output of the 12 bit A/D converter.

4.7.9 Fault Inception Time Identification

From figure 4.10 can be seen that the voltage and current samples include both pre-fault and post-fault data; therefore it is necessary to determine the point within the recorded data of voltages and currents at which the fault has occurred.

Faults cause distortions in the current and voltage waveforms. Current and voltage peaks can change in magnitude and phase with respect to pre-fault conditions. Quantized data output of A/D converter is used for fault inception time identification. A fortran program was designed to identify fault inception time before the application of digital signal processing. This process hinges upon comparing the first three present samples from the current waveforms with the samples from the previous cycle, and any significant change, exceeding a predefined threshold level, indicates the fault inception time.

If the required threshold level is not satisfied for current samples, then the same procedure is applied to voltage samples. Different threshold levels are used for voltage samples. Figure 4.14(a) and 4.14(b) show that the decrease in the magnitude of the voltage samples is relatively less in comparison with the rise in magnitude of the current samples driving the fault. It should be mentioned that the fault inception identification program is independent of the fault type.
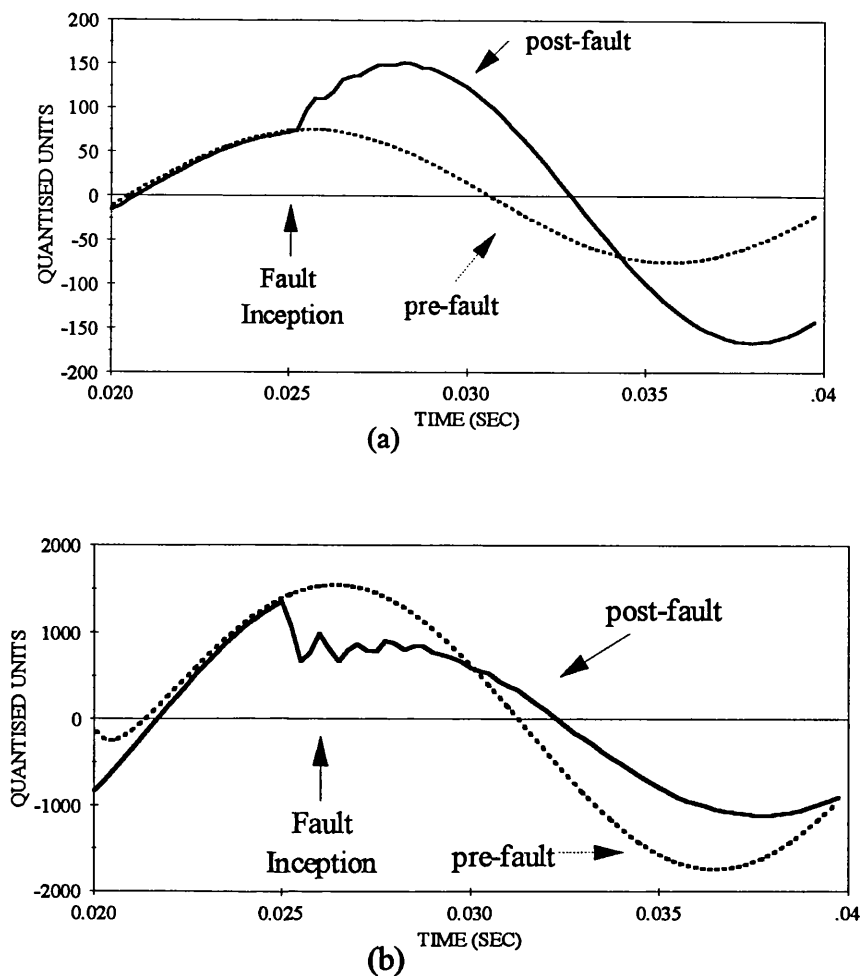
Figure 4.14 Current and voltage waveforms immediately after the fault and one cycle prior to the fault occurrence. A-phase fault at the middle of the line, S1=2.5GVA, S2=20GVA, R_f=20 Ω, pre-fault angle Vs/Vr=30 degree.
(a) Fault locator-end a-phase current.
(b) Fault locator-end a-phase line voltage.

4.8   Summary

In summary, the system simulation of the power system has been done using the EMTP software. It is vitally important that the system simulation be as accurate as possible within the bounds of practicality. In this respect, all the practical considerations, such as the effect of transducers and hardware errors, on the primary system fault data are included in the simulation.

Chapter 5

Accurate Fault Location Technique Based On Artificial Neural Networks

5.1 Introduction

Chapter one has outlined the importance and requirement for fast and accurate location of faults on electric power transmission lines and chapter three has described the technology of artificial neural networks. This chapter brings these two strands together and describes a new pattern recognition method for accurate fault location based on the application of artificial neural network technique. It possesses certain attractive features which are not attainable by the conventional methods. The technique is based on a modular approach and it is shown that the trained ANNs are able to make correct decision under various system and fault conditions. The extraction of the salient features from the simulation waveform is discussed. This original work is a necessary precursor to an AI based solution. The main simulation for data preparation and training process of the networks is done off-line and the fault location technique is based on an off-line application. Since the fault location estimation is performed off-line, computation time is not a major issue. However, the accuracy obtaining the location of the fault is of fundamental importance.

5.2   Motivation for Using ANNs

Artificial Neural Networks have emerged as a powerful pattern recognition technique. Since the need for pattern recognition arises whenever computers interact with the real world, ANNs are broadly useful in a range of applications. Like other pattern recognition techniques, ANNs act on data by detecting some form of underlying organisation not explicitly given or even known by human experts. The networks can recognise spatial, temporal or other relationships and can perform such task as classification, prediction and function estimation. This can bridge the gap between individual examples and general relationships. This characteristic has encouraged various researchers to apply ANNs to solve various power system problems such as load forecasting, security assessment, fault diagnosis, etc.

A neural network is characterized by its architecture, its processing algorithm and its learning algorithm. The architecture specifies the way the neurons are connected. The processing algorithm specifies how the neural network with a given set of weights calculates the output vector y for any input vector x. The learning algorithm specifies how the neural network adapts its weights for all given training vectors x.

The feed-forward multi-layer neural network with the use of supervised learning and common training rule of error back-propagation is used in this research. Supervised learning requires an external "teacher" that evaluates the behaviour of the system and directs the modifications [62]. The training is accomplished by adjusting the weights. This is done by presenting a set of patterns at the input, each with a desirable output pattern. Weights are then adjusted to minimize the error between the desired and actual output patterns. The standard back-propagation learning rule of Delta-rule, and the Hyperbolic tangent transfer function are used for training neural networks described herein.

5.2.1 Advantages of ANNs

Artificial neural networks (ANNs) are valuable on several counts. Firstly *they are adaptive*: they can take data and learn from it. Thus they infer solutions from the data presented to them, often capturing quite subtle relationships. This ability differs radically from standard software techniques because it does not depend on the programmer's prior knowledge of rules. Neural networks can reduce development time by learning underlying relationship even if they are difficult to find and describe. They can also solve problems that lack existing solution.

Secondly, *ANNs can generalize*: they can correctly process data that only broadly resembles the data they were trained on originally. Similarly, they can handle imperfect or incomplete data, providing a measure of fault tolerance. Generalization is useful in practical applications because real world data is noisy.

Thirdly, *the networks are non-linear*: they can capture complex interactions among the input variables in a system. In a linear system, changing a single input produces a proportional change in the output, and the input's effect depends only on its own value. In a non-linear system, the effect depends on the values of other inputs, and the relationship is a higher-order function. In this respect, systems in the real world are often non-linear.

Fourthly, *ANNs are highly parallel*: their numerous identical, independent operations can be executed simultaneously. Parallel hardware can execute them hundreds or thousands of times faster than conventional microprocessors and digital signal processors. Now that special-purpose parallel computers and chips have become available for neural network implementations, even large networks can achieve real-time speeds, and even everyday products can employ an embedded network. This increase in speed and economy makes many applications practical for the first time, encouraging further deployment.

5.2.2 Disadvantages of ANNs

In spite of several advantages, motivating the application of ANNs in the field of power system problems, there are still some drawbacks in their application. Some of these disadvantages are associated with the general application of neural network in any field, while others are specific to the application in power system problems. For example, the inability for extrapolation beyond the area which is trained for, is inherent characteristic to ANNs application in any field.

As the network size increases, the training time is longer. This appears as a critical constrain on the way of ANNs application. The nature of training data has a dominating effect on the learning performance of ANN, therefore, more effort is still required to develop sophisticated techniques for preparation of training data which can result in fast learning performance.

Other disadvantages of ANNs can be outlined as: there is no definite way of choosing the optimum architecture, there is no definite way of finding the best solution and the solution depends upon the accuracy of the training set.

5.3   Neural Network Based Scheme

Artificial neural networks have the ability to learn the desired inputs/outputs mapping based on training examples, without looking for an exact mathematical model. Once an appropriate ANN has been trained, the interconnections or links of the ANN will contain a representation of the non-linearity of desired mapping between inputs and outputs. Feature extraction is the first step to any pattern recognition method to effectively reduce the size of the neural network and improve its performance. In order to catch the features in the accurate fault location technique, the instantaneous three phase voltages and currents, which contain fault information at different frequencies, are used to train the ANN.

The basic configuration of the ANN-based fault location technique is shown in figure 5.1. The method is based on utilising voltage and current waveforms at the fault locator end of the line only and the signals employed are based on phase values. The effect of transducers - current transformers (CTs) and capacitor voltage transformers (CVTs), and hardware errors such as anti-aliasing filters and quantisation are taken into account, so that the information processed throughout the fault locator algorithm is very close to real-life situation; this is achieved through a data pre-processing stage whereby the primary system waveforms of voltages and currents are subjected to a full circuit emulation of the transducers/analogue interface modules via their practical frequency responses as described in chapter 4. The resultant data is then passed through a model of an analogue to digital (A/D) converter before being processed through the fault locator algorithm.
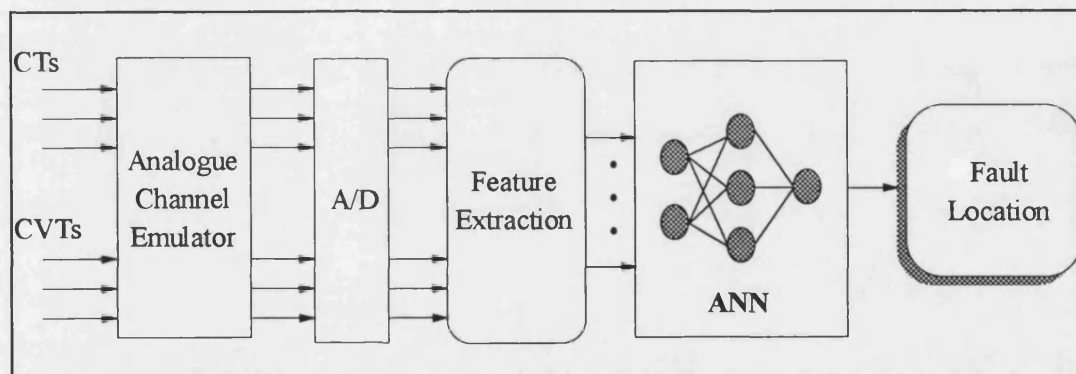
Figure 5.1 Basic configuration of the ANN-based fault location technique.

5.4   Data Pre-processing

5.4.1 Need for Pre-processing

The problem of developing a fault location technique, based on identifying the characteristics of the faulted waveforms, is essentially one of pattern recognition. The application of ANN to fault location scheme consists of four basic tasks:

1)   Collecting or producing sets of sample of fault voltage and current

waveforms.

2)   Pre-processing the data and extracting the useful features.

3)   Selecting and building the most appropriate ANN.

4)   Using the processed sample data to train the neural network and then testing the network on separate sets of processed data.

Pre-processing is an integral part of this strategy since it conditions the raw data into a form suitable for input into the ANN. The training cases for a typical 400 kV transmission system are generated through the use of EMTP. The simulation generates samples of voltage and current waveforms on the three phases. Since the fault transients generated on transmission system contain a wide range of frequency components, it is impractical to use the time-domain waveforms as the input to an ANN. Hence, certain parameters of the identified characteristics must be extracted to fully represent the state of the transmission line.

As described in chapter 4, the simulation is based on a sampling frequency of 4 kHz and after convolving the primary system data with the unit impulse responses of the transducers and voltage/current interface modules, the digital data is quantised through a 12-bit A/D for subsequent processing in the fault location algorithm.

5.4.2   Producing Sets of Sample of Fault Voltage and Current Waveforms

In the learning process of ANN-base fault location technique, it is essential to have sufficient and practical training data in order for the ANN to be well-trained. In this respect, by repeatedly analysing the EMTP simulation samples under various system and fault conditions and processing the resulting data, training patterns for the ANN were set up. As described in section 4.6, parameters such as effect of fault type, differing source capacities at both ends of the line, fault impedance, fault inception time and fault position, which influence the transient phenomena, were varied. Figures 5.2 and 5.3 typify the output of A/D voltage and current waveforms generated at end S (in figure 4.1) of the line under an 'a'-phase-earth fault at the

midpoint of the line and 'a'-'b' phase fault near end R (in figure 4.1) respectively.
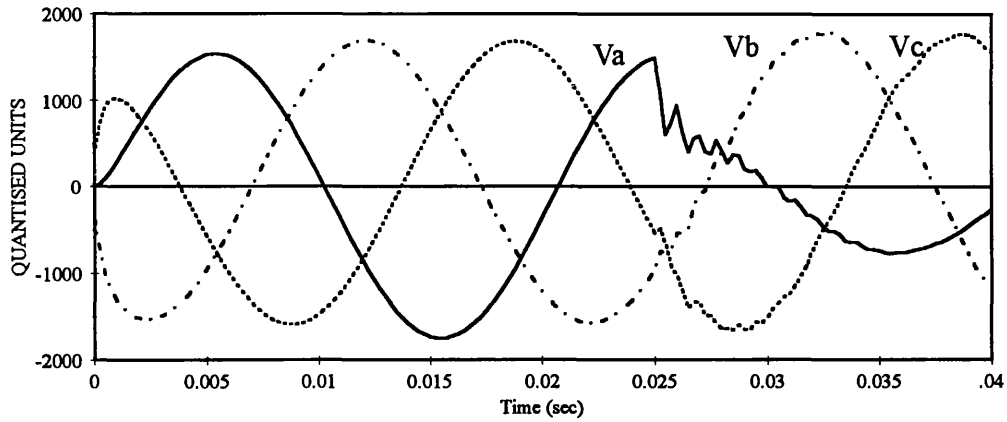
(a)
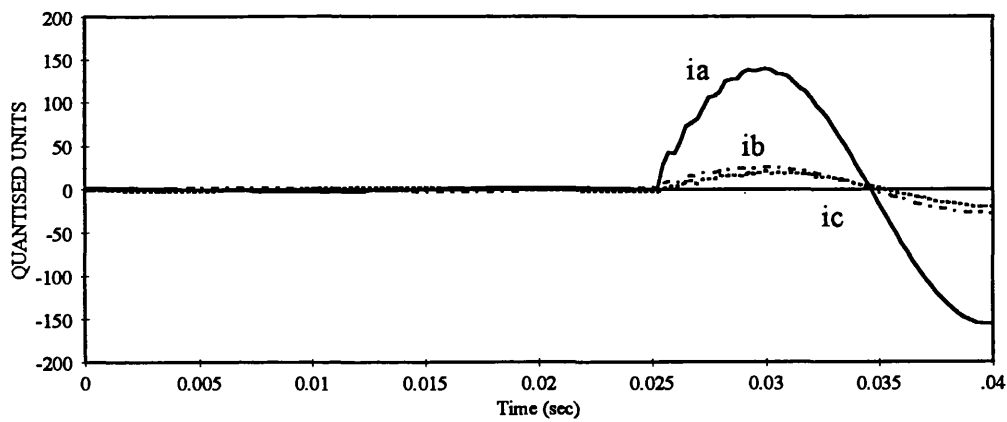
(b)

Figure 5.2 Output of the A/D for 'a'-phase-earth fault at the midpoint of the line.

(a) The three phase voltages.

(b) The three phase currents.
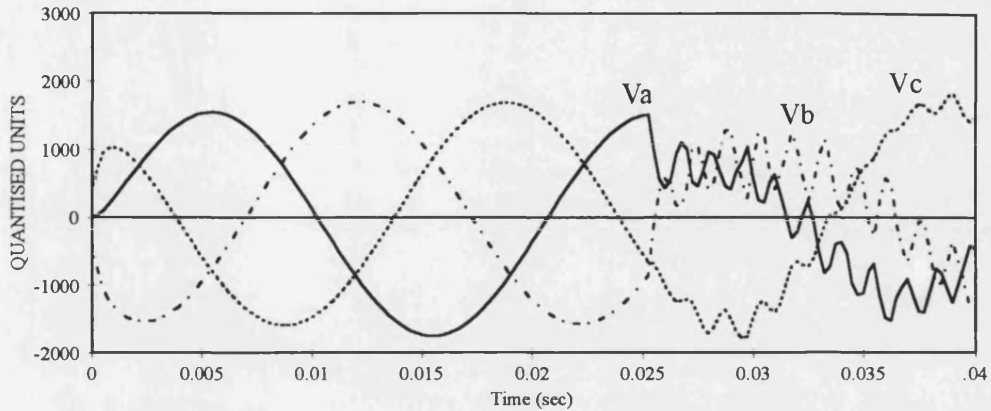
(a)
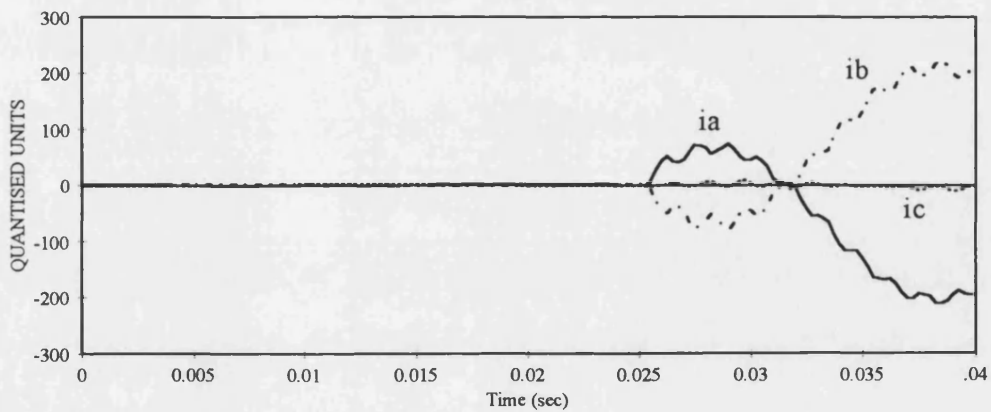
(b)

Figure 5.3 Output of the A/D for 'a'-'b'-phase fault at the remote end of the line.

(a) The three phase voltages.

(b) The three phase currents.

5.5   Feature Extraction

As a first step in any pattern classification technique, feature extraction is used to reduce the dimension of the raw data and extract useful information in a concise form. For the ANNs considered in this thesis, this process leads to a considerable reduction in the size of the networks, thereby significantly improving the performance and speed of the training process.

5.5.1 Data Reduction

Reduction in the amount of data is ultimately related to the type and amount of data available to represent the problem. In order to prevent the network becoming too large, the amount of data should be reduced. The number of inputs to a feed-forward network determines the number of nodes in the input layer of the network. In general training time required for a feed-forward ANN is related exponentially to the size of the network, and this constrains the size of the network. This indicates that a smaller number of inputs to the ANN and therefore features would be ideal. However, it is essential that the salient information is not removed from the input data.

5.5.2 Training Time

Training time is a main concern of ANN design, specially if the size of the problem is large and it is often required to update the learning process by change the training patterns. By training time we mean the time required for preparation of training data and learning process of ANN. Proper selection of training data has a profound effect on the learning ability and training time of an ANN. Furthermore, the sensitivity and causality of input/output patterns, can affect the convergence of training, which means that the type of input data would provide the best results in the output. For example, existence of irrelevant redundant data in the training pattern can slow down the process of training. However, long training time of ANN which is taken off-line can be justified by the fast operating characteristic of that in the working mode at on-line.

5.5.3 Feature Extraction Algorithm

Feature selection is more of an art than a science. The goal of feature selection is to eliminate as much unnecessary information as possible while still retaining the salient information in a compact form. Useful features are those which vary widely from class to class, are easy to measure and calculate and which are not correlated with

other features. This process is difficult to automate and must be based on an intuitive understanding of the problem. Although there exist some well-established techniques of feature extraction algorithms, in general whether or not a feature can be selected in reality, is problem dependent.

For development of this accurate fault location technique, an extensive series of studies revealed that the most distinct characteristics of the waveforms are those associated with the variation of the frequency components over time. Therefore the technique adopted here for feature extraction is the one based on time domain frequency decomposition of voltage and current waveforms using the Discrete Fourier Transform (DFT); a one cycle window was employed for this purpose.

5.5.4 Frequency Decomposition

The faulted voltage and current waveforms of the transmission line vary with time, and the frequency components within the waveforms evolve with time during the progression of the fault. Frequency transforms which take an input array and produce a frequency domain representation are a powerful technique for examining the behaviour of sequential waveforms. The basic merit of a frequency domain representation is that the signal in question can be fully represented, over an interval, by the superposition of a number of frequency harmonics. To obtain the frequency spectra of a discrete array, DFT is used. It transforms the input array signal into an array of complex coefficients. These coefficients specify the amount of each frequency harmonic required. The fourier transform utilises the property that harmonics of the fundamental frequency are orthogonal in order to calculate the values of the coefficients of the frequency spectrum.

5.5.5 Discrete Fourier Transform (DFT)

The DFT is the basis of all discrete-time spectral analysis. It represents a discrete-time signal $\{x(n)\}$ by a function $X(f)$ (or $X(\omega)$) in the frequency domain [63]. It is

a simple extension of Fourier transform concept, but relies heavily upon the Fourier series although time and frequency domains are interchanged. The DFT general formula is given as:

$$X(\omega) = \sum_{n=-\infty}^{+\infty} x(n) \cdot e^{j(-\omega T_s n)} \qquad (5.1)$$

where ω is the angular frequency, T_s is the sampling intervals and n is the sample number. The infinite summation is lost by using a windowing function $w(n)$ to limit the summation to N samples of $x(n)$. The section which is used for analysis lies in the region $0\leq n\leq(N-1)$. Effectively the original signal x(n) is being viewed through a rectangular window w(n), and

$$w(n) = \begin{cases} 1 & 0\leq n\leq(N-1) \\ 0 & elswhere \end{cases} \qquad (5.2)$$

The signal presented for analysis is then:

$$x'(n) = x(n) \cdot w(n) \qquad (5.3)$$

Calculation of the DFT on N samples from the time domain produces N/2 positive-frequency phasors and N/2 negative-frequency phasors, given N in total, although for a real signal these two sets will be conjugates. The interval along the frequency axis is Ω_s rad/sec or δ_s Hz. This then is the fundamental frequency, or the frequency different between any adjacent pair of phasors. The prime parameters of the DFT is then given by:

$$N \cdot \Omega_s = \omega_s \qquad (5.4)$$

or,

$$N \cdot \delta_s = f_s \qquad (5.5)$$

where f_s is the sampling frequency.

Now that the frequency scale has been discretised, the DFT equation can be rewritten in a new form. Incorporating the rectangular window into equation 5.1,

$$X(k\Omega_s) = \sum_{n=0}^{N-1} x(n) \cdot e^{-jk\Omega_s T_s n} \tag{5.6}$$

The exponent reduces to $-2\pi kn/N$ and it is usual to refer to the frequency variable only by the index k. Thus the equation is normally rewritten as:

$$X(k) = \sum_{n=0}^{N-1} x(n) \cdot W^{-kn} \tag{5.7}$$

where;

$$W = e^{\frac{j2\pi}{N}} \tag{5.8}$$

The W is called the twiddle factor and holds the key to the evaluation of the DFT, and forms the basis for the transformation.

5.5.6 Spectral Analysis

Figure 5.4 depicts the frequency spectra of the three-phase voltages and currents for the fault condition shown in Figure 5.2; likewise, Figure 5.5 shows the frequency spectra (again as observed at end S, in figure 4.1) for an 'a'-'b'-phase fault near end R, in figure 4.1, (shown on figure 5.3). It is apparent from the foregoing that the frequency spectra are distinctly different for the two types of fault. In this respect, it is important to note that the frequency spectra attained vary quite significantly under different types of fault, fault location, fault inception angle, etc.

In these simulations, points taken over one cycle of the 50Hz fundamental correspond to 80 samples of data in the time domain, which maps to 40 frequency magnitudes in the frequency domain. This represents a sampling rate of 4 kHz. This 40 dimensional feature space can then be further reduced by using empirical information, such as the CVT frequency response to discard frequencies above 700 Hz.

From the variation of different frequency components over the training set as shown in figure 5.4 and 5.5, it can be seen that the 50Hz components is the most significant, followed by the DC component. The application of this variance criteria is used to select frequencies to be presented to an ANN for it to attempt to learn and solve the problem of accurate fault location for transmission lines.
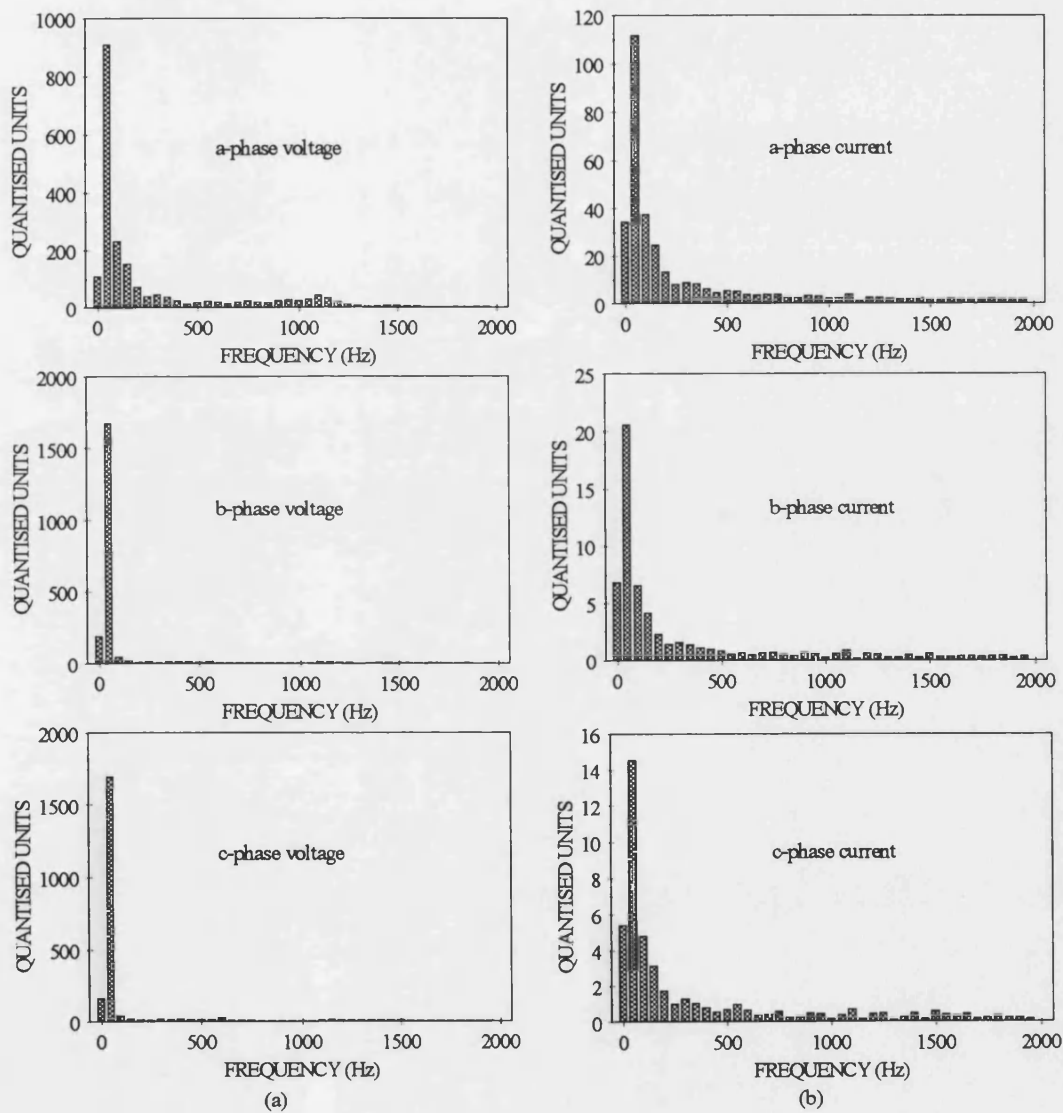
Figure 5.4 Frequency spectra for an 'a'-phase-earth fault at the midpoint.

(a) Spectra of three-phase voltages.

(b) Spectra of three-phase currents.
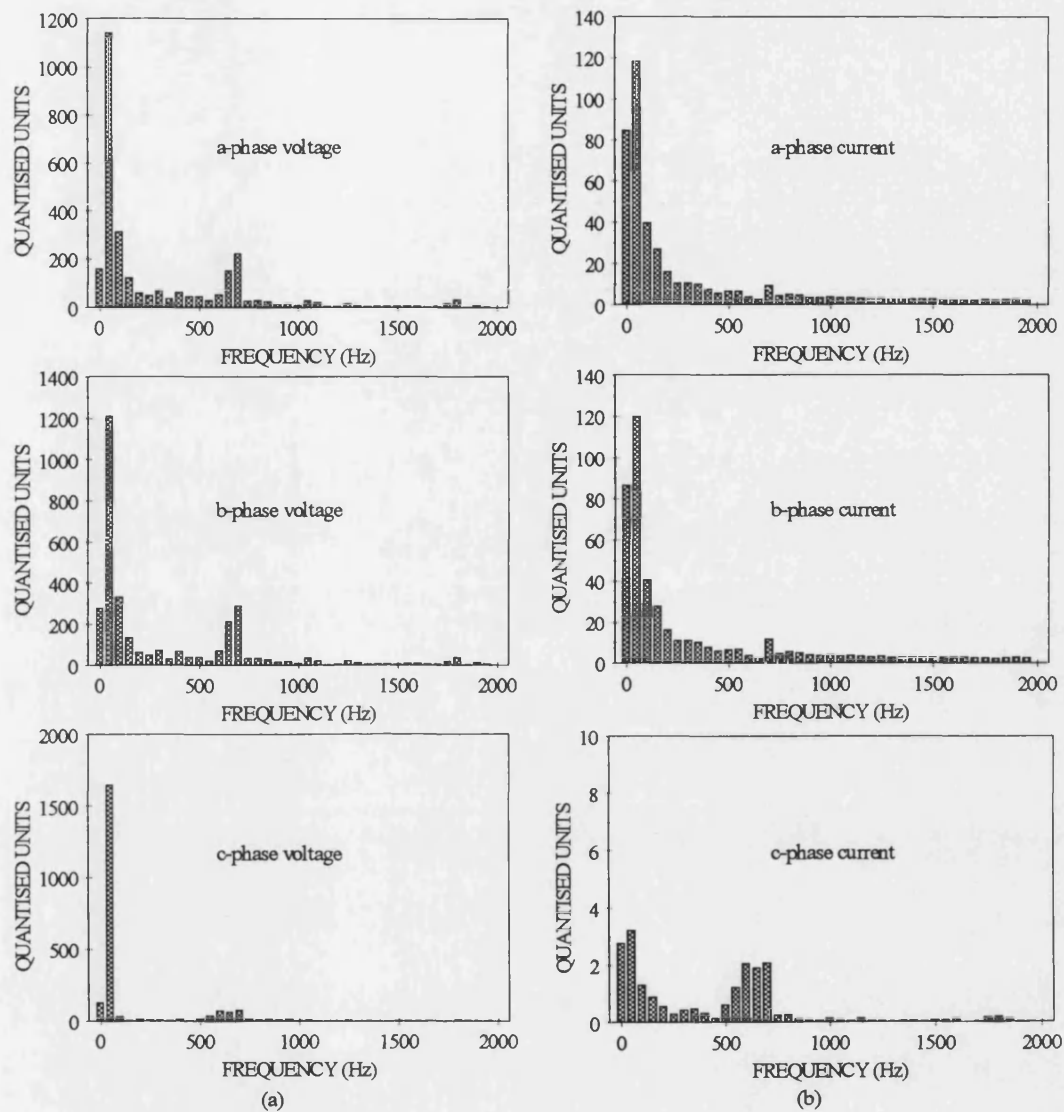
Figure 5.5 Frequency spectra for an 'a'-'b'-phase fault at the remote end.

(a) Spectra of three-phase voltages.

(b) Spectra of three-phase currents.

5.5.7 Training Data

In order to design a neural network, it is vitally important to train it correctly and then test it. In supervised learning ANNs are trained from a set of data examples which are associated with a desired outcome. These data examples can be considered as a vector which represents the state of the input. For example, a data example **X**

can be represented as:

$$X = \begin{pmatrix} x_1 \\ x_2 \\ . \\ . \\ x_n \end{pmatrix} \qquad\qquad (5.9)$$

The training set will consist of many training examples that will allow the ANN to learn to solve the task required and be capable of generalisation. When expressed as a vector, it is clear that each data example **X** can be considered as a point in **n** dimensional space. An ANN will attempt to find a mapping from this; this involving training the problem space into the solution space. For the accurate fault location problem considered in this chapter, it is required to map from the training set the exact location of the fault on transmission lines. However, the problem lies in two parts; fault type classification and fault location.

The inputs to the ANN comprise of a set of features based on the three-phase voltages V_a, V_b, V_c and three-phase currents I_a, I_b, I_c. With regard to the procedure for feature selection, an acceptable simple criterion used here is that a variable as a feature for the ANN input should provide more information for fault type classification and fault location than those not selected. In this respect, an extensive series of studies have revealed that the following frequency components (attained through the previously mentioned time-domain frequency decomposition of the fault waveforms) are representative of the vast majority of different system and fault conditions encountered in practice:

1)   DC Component.

2)   Fundamental Component.

3)   Components over 100 - 350 Hz range.

4)   Components over 400 - 1000 Hz range.

These are then converted into four features for each measured signal, those associated

with (3) and (4) above comprising of the summated signal energy at all discrete frequencies within their appropriate range; with this approach, it becomes possible to confine the number of inputs into the ANN to 24 elements for the 6 signals.

Examples of inputs into the ANN for two different fault conditions are shown in figure 5.6.
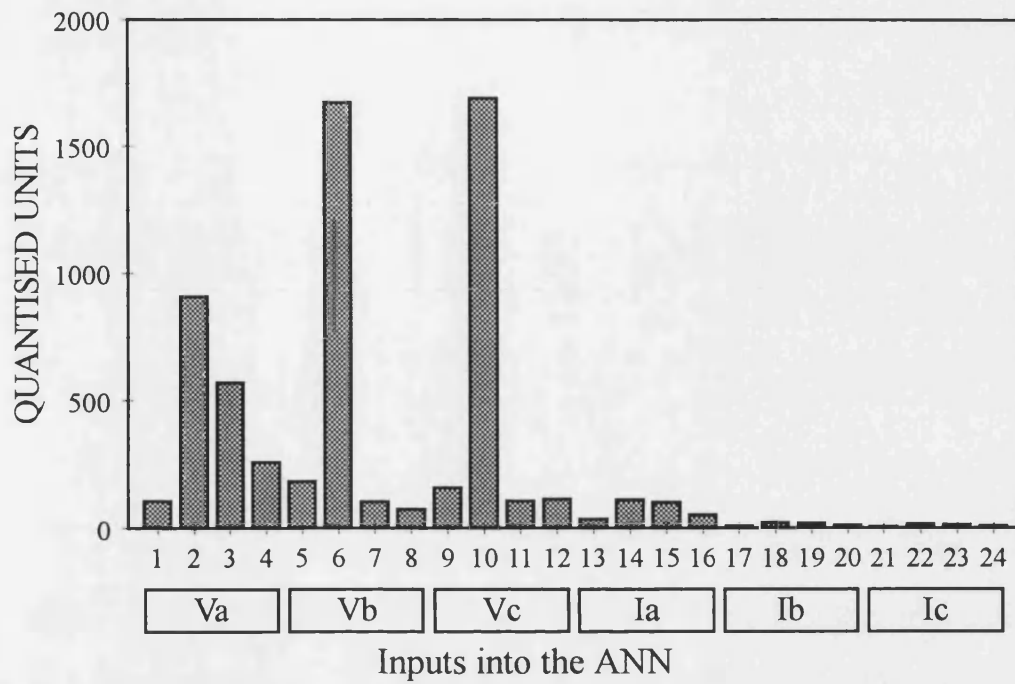
(a)
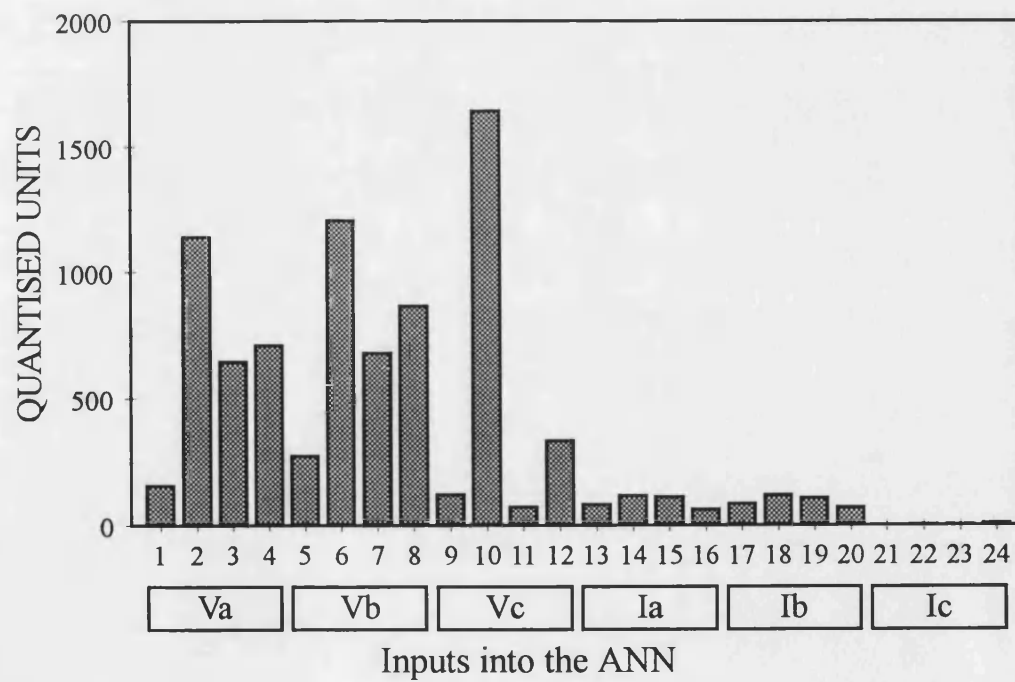
(b)

Figure 5.6 Examples of inputs into the ANN.

(a) 'a'-phase-earth fault at the midpoint (fault condition shown in figure 5.2).

(b) 'a'-'b'-phase fault at the remote end (fault condition shown in figure 5.3).

After the appropriate features have been selected, a large number of simulations were performed off-line to generate a good representative data for training and testing the ANN, which cover wide system and fault conditions; accurate fault location is the process which requires fine training an ANN. Thus the ANN should be trained by data under a known fault type and fault positions. Figure 5.7 shows a set of training data for a specific fault condition. The distance to fault was varied from 0 to 100% of the line length, at regular intervals of 10%. The training data has been scaled to the neurodynamic range and is presented to the network randomly.
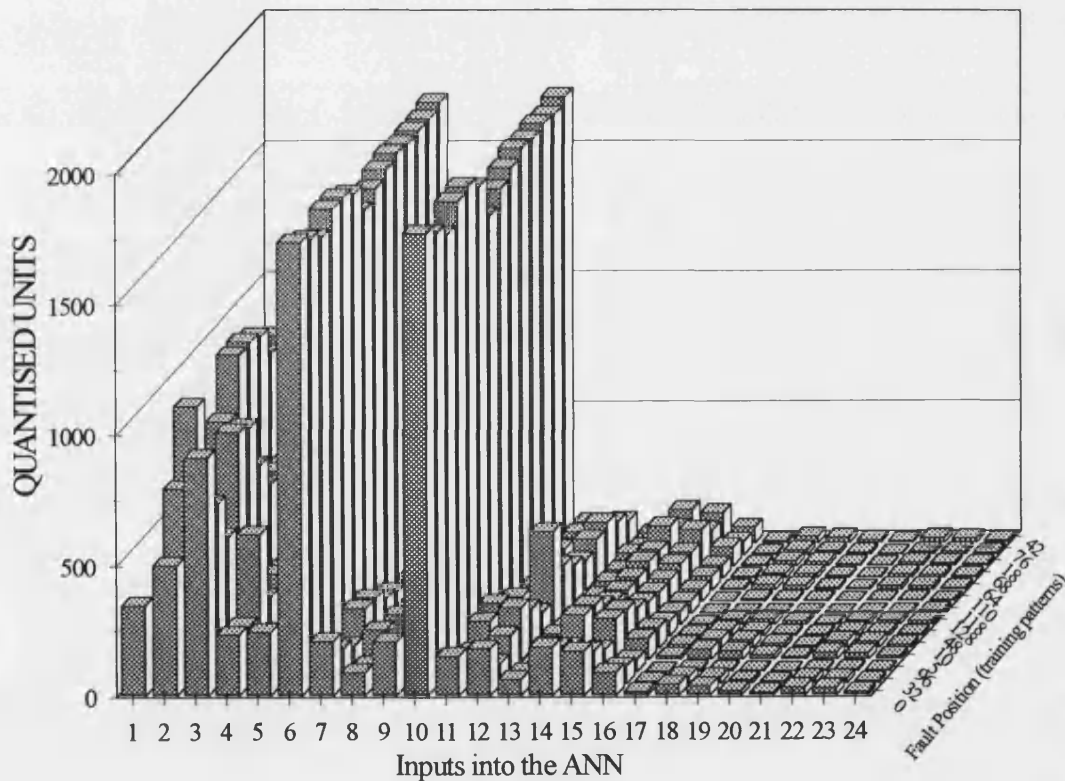
Figure 5.7 Training data for 'a'-phase-earth fault, sending end s.c.l. = 2.5GVA, receiving end s.c.l. = 20GVA, fault resistance = 1Ω, fault inception angle = 90 °.

The performance of the ANN is then tested using both patterns within and outside the training set. This is particularly so with reference to the speed of convergence and accuracy attained, essentially to ascertain if modification to the ANN structure or

further training is necessary. The approach adopted here is based on the error-back-propagation training algorithm whereby an input pattern corresponding to a particular fault condition is fed to the ANN and the output of the network is compared with the desired output pattern corresponding to that fault condition.

5.5.8 Scaling of input/output

For effective training of the ANN, scaling of both the input and output values is required. Scaling refers to the desired range of values required at the input and output of the network. The range into which the values must be scaled are primarily defined by the transfer functions in the nodes. If the input value to a node is large then the output of the node, defined by the transfer function, will be in an area of the function where the output is almost saturated. This means that the network is unable to learn. Similarly, the network may perform better when output values are within a certain range. For example, in training a back-propagation network, whose output layer has a sigmoid transform, will function better if desired output values are between 0 and 1.

The same scaling method must be used for both training and testing data. A linear scaling which for a variable X in the range of $[X_{min}, X_{max}]$ will assign the value A in the range of $[A_{min}, A_{max}]$ is adopted to linearly scale the inputs to the network. This scaling is suitable for the transfer function. Thus the general equation to scale the inputs is:

$$A = \left[\frac{A_{max} - A_{min}}{X_{max} - X_{min}}\right] (X - X_{min}) + A_{min} \tag{5.10}$$

The required network output value must indicate the class to which the input belongs. In the fault location problem, the training target output values were set to the actual distance to the fault on the line, and scaled in the range from 0 to 1 ie 1 corresponds to 100% of the line length.

5.6   ANN Topology for Accurate Fault Location

In order to find the best network topology for accurate fault location under all practically encountered different system and fault conditions, an extensive series of studies have revealed that it is not satisfactory to merely employ a single ANN and attempt to train it with a large amount of data. A much better approach is to separate the problem into two parts: firstly to employ and train a single ANN to indicate on which phase(s) the fault is and whether there is ground involved in a particular fault, irrespective of the actual fault position at this stage; secondly, in order to achieve a good generalisation, to use separately designed ANNs (one for each type of fault) to accurately locate the actual fault position associated with all the commonly encountered types of fault on EHV transmission lines; these are of course all driven from the single ANN designed at the first stage and the input data for the ANNs is generated the same way as that for the single ANN. Although this modular approach requires many networks, they are nonetheless quite simple in architecture, much easier to train and require significantly less training data than would otherwise be the case if simply one single ANN were to be employed; more importantly (as shown later), the accuracy achieved in fault location is significantly enhanced. Figure 5.8 illustrates the accurate fault locator scheme based on ANNs.
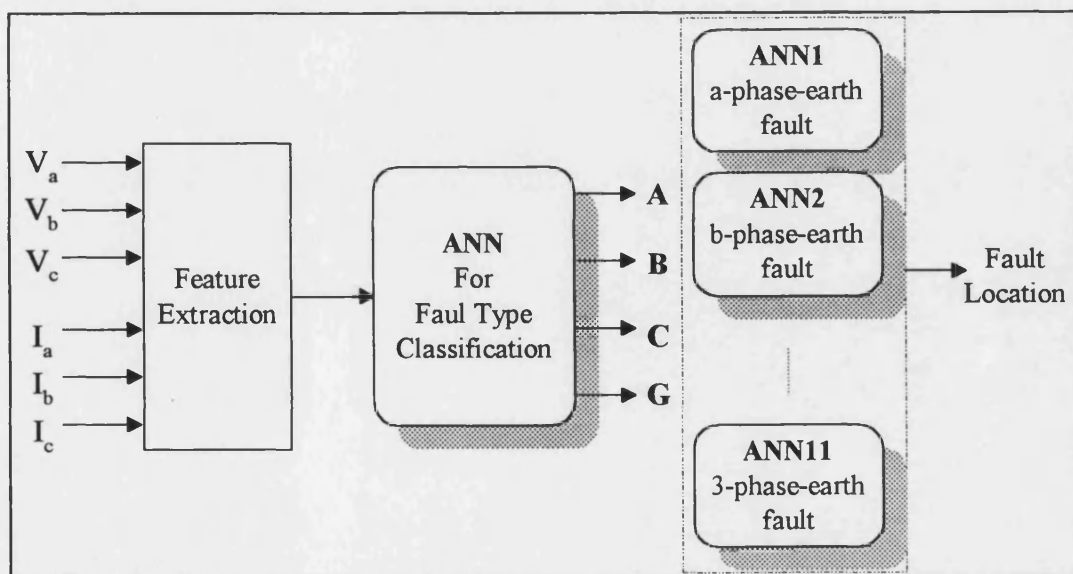
Figure 5.8 Schematic diagram of fault location technique based on ANNs.

5.6.1   Network Architecture

There are many types of ANNs but the most commonly used are the previously discussed (in chapter 3) multilayer feed-forward networks (MFNs). A typical layout of such a network was shown in figure 3.6. It is a fully-connected three-layer (input, hidden, and output) feed-forward ANN, which has been used in fault classification and fault location problem. The network architecture chosen depends on the problem being addressed. The number of inputs to the network is determined by the number of elements or features in the input vector.

Having one or more hidden layers allows the network to make more complex associations between input and output [64]. The number of nodes required in the hidden layer(s) depends on the complexity of the relationship between the inputs and outputs. If there are too many nodes in the hidden layer(s) the network will simply learn all of the input/output relationships individually without learning to generalise relationships for previously encountered data. If, however, there are not enough nodes in the hidden layer(s), then the network will not be able to learn to classify the inputs correctly. This applies similarly to the number of adjustable weights; too many weights will allow the network to learn all of the training set explicitly, and too few will not allow it to classify inputs correctly.

Considering the complexity of the accurate fault location problem and the amount of data available, in order to determine the appropriate size of the hidden layers, different combinations of the following network training methods were chosen and tested:

☐   different connections (full or non-full) between the processing elements.

☐   different number of hidden layers.

☐   different hidden neurons in each layer.

☐   different transfer functions (sigmoid, linear, and hyperbolic tangent).

☐   different learning set data (sequential or random) in training the network.

☐   different error back-propagation schemes.

5.6.2   Fault Type Classification

The fault type classification technique is based on training a three-layer perceptron by the Delta-Bar-Delta learning algorithm [65]. The outputs of the ANN comprise of four variables A, B, C and G; of these, a value close to unity for any of the first three variables corresponds to the appropriate a, b or c phases being faulty and a near unity value of G signifies that ground is involved in a fault. This ANN logic is depicted in table 5.1.

ANN-logic for output representation				
A	B	C	G	TYPE OF FAULT
0	0	0	0	no fault
1	0	0	1	a-phase-earth fault
0	1	0	1	b-phase-earth fault
0	0	1	1	c-phase-earth fault
1	1	0	0	a-b-phase fault
0	1	1	0	b-c-phase fault
1	0	1	0	a-c-phase fault
1	1	0	1	a-b-phase-earth fault
0	1	1	1	b-c-phase-earth fault
1	0	1	1	a-c-phase-earth fault
1	1	1	0	3-phase fault
1	1	1	1	3-phase-earth fault

Table 5.1 ANN-logic for output representation of fault type classification technique.

The ANN architecture is based on 24 inputs, 4 outputs and 14 neurons in the hidden layer as shown in figure 5.9.

The training patterns for different fault types were selected considering different system and fault conditions for three fault positions on the line (near end S in figure 4.1, midpoint and near end R in figure 4.1). The performance of the ANN is then evaluated using various test cases for different fault positions.
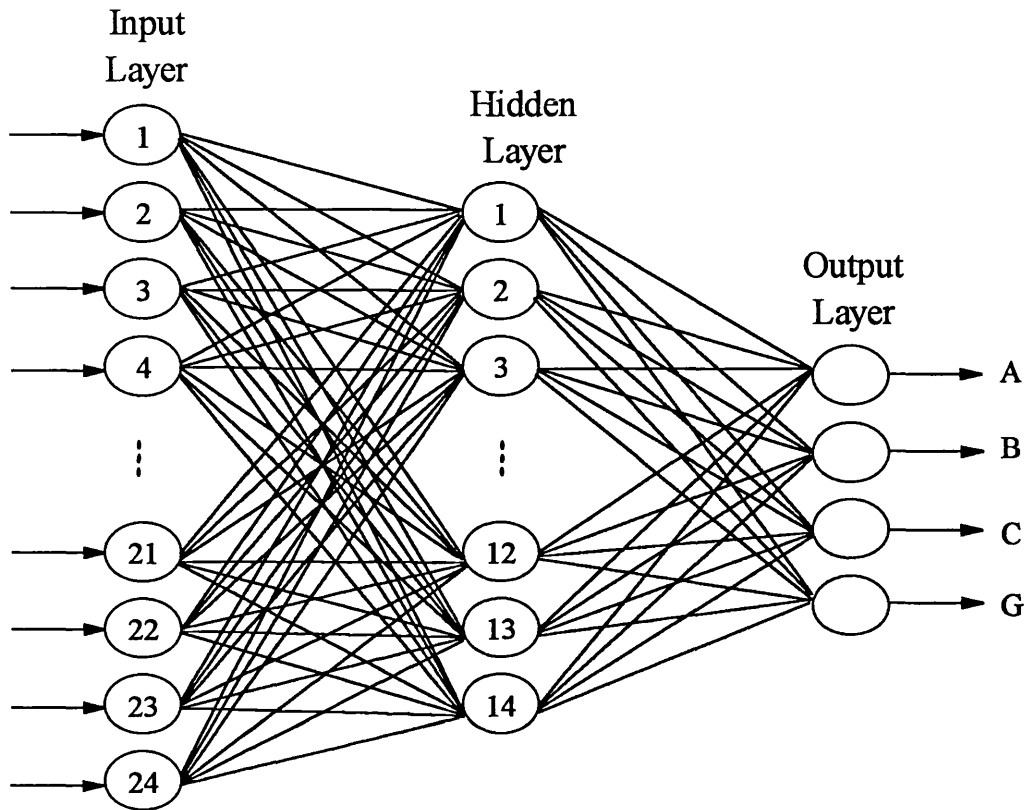
Figure 5.9 ANN architecture for fault type classification.

5.6.3   Fault location

As mentioned in section 5.6.2 and shown in figure 5.8, separate ANNs are designed to accurately locate fault position for each type of fault under all practically encountered different system and fault conditions. They are all driven from the single ANN designed to classify the fault type and the input data for the ANNs is generated the same way as that for the single ANN.

The MFNs shown in figure 5.10, with 24 neurons in the input layer and 1 in the output layer were chosen, where the output shows the location of the fault. The number of hidden neurons vary slightly for each ANN. ANNs are trained with different training data to cater for all types of commonly encountered faults.
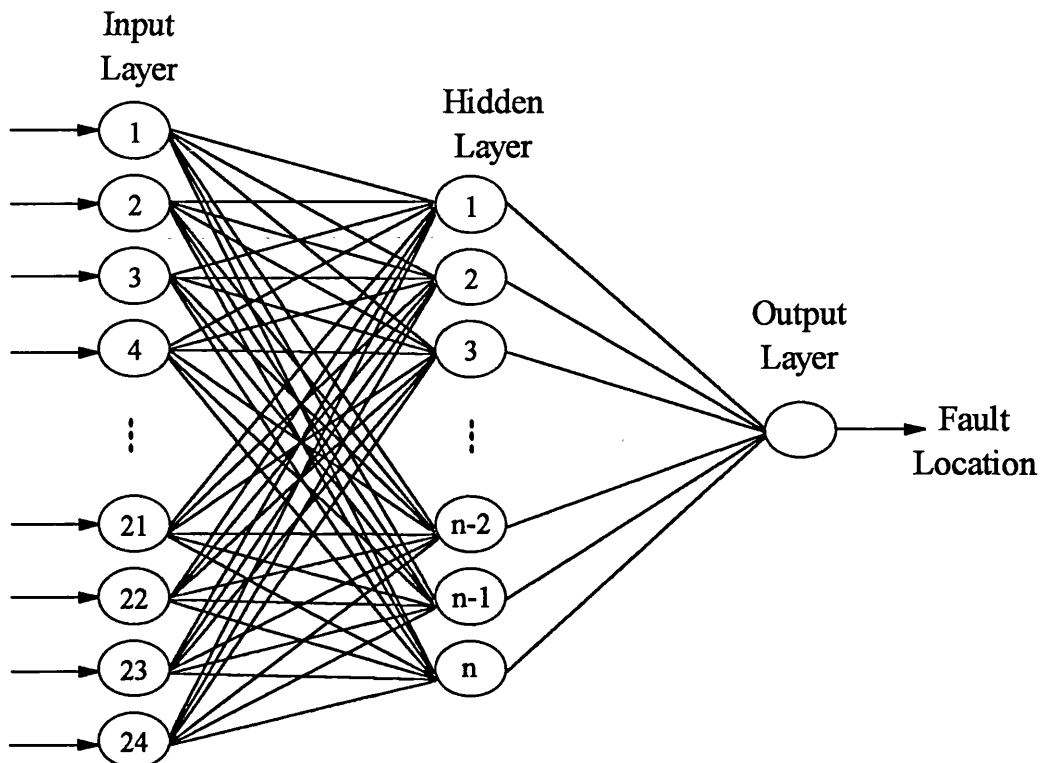
Figure 5.10 Structure of the ANNs for fault location.

5.7   Summary

An accurate fault location technique based on ANN is developed in this chapter. A single ANN is trained to classify the fault type and separate ANNs are designed to accurately locate the actual fault position associated with all the commonly encountered types of fault on EHV transmission lines.

Data pre-processing of the simulated waveforms is discussed and the time-domain frequency decomposition of voltage and current waveforms using DFT is adopted in the feature extraction process. In this respect, four features for each measured signal are selected as inputs to the ANNs.

Chapter 6

Fault Location Technique Based On
Fuzzy Neural Networks

6.1 Introduction

This chapter describes a fault location technique using fuzzy neural networks (FNN). The technique is essentially an extension of the one described previously in chapter 5, in which a hybrid approach based on integration of fuzzy logic and artificial neural networks (ANNs) is adopted. Like before it which utilises voltage and current fault data at one line end only and comprises of two stages: the first stage is based solely on an artificial neural network (ANN) in order to classify fault types and the second stage is based on a FNN whereby fuzzy logic is employed to process the information for a second ANN for the purposes of accurately locating a fault on the line. It is clearly shown that with this integrated approach, the accuracy in fault location is significantly improved over other techniques solely based on ANN architectures.

ANN-based techniques have the potential advantage over conventional techniques in significantly improving the accuracy in fault location. This is so by virtue of the fact that ANNs have the capability of non-linear mapping, parallel processing and learning; these attributes make them ideally suited for providing a high accuracy in fault location under a wide variety of different systems and fault conditions.

However, there are still a number of contingencies under which an ANN-based fault location technique's performance can be adversely affected. The technique presented herein thus proposes the use of fuzzy logic to further improve the accuracy of an ANN-based fault location technique.

6.2 Introduction to Fuzzy Logic

6.2.1 Fuzzy Logic Technology

The enormous success of commercial applications, which are at least partially dependent on fuzzy technologies, has led to a surge of curiosity about the utilisation of fuzzy logic for scientific and engineering applications. Over the last ten years, fuzzy models have taken over more conventional technologies in many scientific applications and engineering systems, especially in control systems and pattern recognition. The success in the application of fuzzy technology has been such that the interest in this subject area is growing.

6.2.2 Characteristics of Fuzzy Logic System

Fuzzy logic provides an inference morphology that enables approximate human reasoning capabilities to be applied to knowledge-based systems, such as perceptual and linguistic attributes. Also, this theory provides a mathematical strength to capture the uncertainties associated with human cognitive processes like thinking and reasoning.

6.2.2.1   Fuzzy set

Fuzzy set theory, introduced by Zadeh in 1965 [67], is an extension of conventional set theory. It provides a mathematical tool for dealing with linguistic variables (also called fuzzy variables). In traditional (or nonfuzzy) set theory, the sets considered are defined as a collection of objects having some very general property; nothing special

is assumed or considered about the nature of the individual objects. On the other hand, fuzzy variable has a degree of membership or degree of truth which for the range of a variable, is described by a membership function.

6.2.2.2   Fuzzy set representation

It is more convenient to as recall the definition of ordinary sets which henceforth will be referred to crisp sets. For the sake of future definition of fuzzy sets, the crisp sets are defined by introducing membership functions. Specifically, if U is a universe of discourse, then a crisp set A in U is characterized by a membership function, denoted as μ_A, which is defined as follows:

$$\mu_A(x) = \begin{cases} 1 & \text{if } x \in A \\ 0 & \text{if } x \notin A \end{cases} \tag{6.1}$$

Therefore, the membership function corresponding to a crisp set will only take values 0 or 1. Hence according to this perspective, the world is viewed as black or white. On the other hand, a fuzzy set F defined in a universe of discourse U is characterized by a membership function μ_F which takes values in the closed interval [0,1]. According to this definition, it is clear that a crisp set is also a fuzzy set. However, the inverse is not necessarily true as illustrated by the following example.

Example:

U ≡ Positive real numbers.

A ≡ The crisp set of positive real numbers.

F ≡ The fuzzy set of positive real numbers "much" greater than 1.

Membership functions for A and F are shown in figure 6.1.
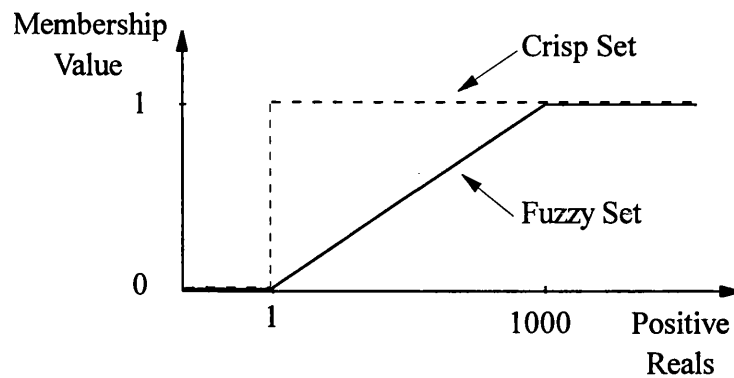
Figure 6.1 The crisp and fuzzy sets of "positive" real numbers.

6.2.2.3   Linguistic Variable and Hedges

An Important application of fuzzy sets is in "computational linguistic" whose aim is to calculate with natural language statements in a similar way as logic calculates with logical statements. Fuzzy sets and linguistic variables can be used to determine the meaning of this natural language, which can then be manipulated. A linguistic variable is assigned values which are expressions such as words, phrases or sentences. As an example of the linguistic variable size, terms such as small, medium, and large can be employed to describe the variable size on a linear scale. This is shown in figure 6.2.
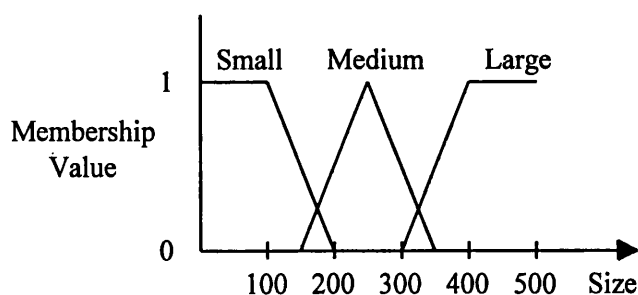
Figure 6.2 Fuzzy membership function for linguistic variable size.

A linguistic hedge or modifier is an operation that modifies the meaning of a term, or more generally, of a fuzzy set. Thus, a larger set of values will be generated for any particular linguistic variable. For example, the small size fuzzy set could be

defined as: very small, very very small, more or less small, not very small and so on.

6.2.2.4   Fuzzy Set Operations

The set theoretical operation of union ($\cup$), intersection ($\cap$), and complement for fuzzy sets are defined via their membership functions. Let A and B denote a pair of fuzzy sets in X with membership functions $\mu_A(x)$ and $\mu_B(x)$, respectively. The membership function $\mu_{A \cup B}(x)$ of the union $A \cup B$ and the membership function $\mu_{A \cap B}(x)$ of the intersection $A \cap B$ are defined as follows:

$$\mu_{A \cup B}(x) = \max\left(\mu_A(x) , \mu_B(x)\right) \tag{6.2}$$

$$\mu_{A \cap B}(x) = \min\left(\mu_A(x) , \mu_B(x)\right) \tag{6.3}$$

The complement of the fuzzy set A is defined by the membership function:

$$\mu_{\bar{A}}(x) = 1 - \mu_A(x) \tag{6.4}$$

6.2.3   Fuzzy Logic Systems

Figure 6.3 shows a fuzzy logic system (FLS), which comprises of four principal components: a fuzzification interface, a fuzzy rule base, an inference engine, and a defuzzification interface.
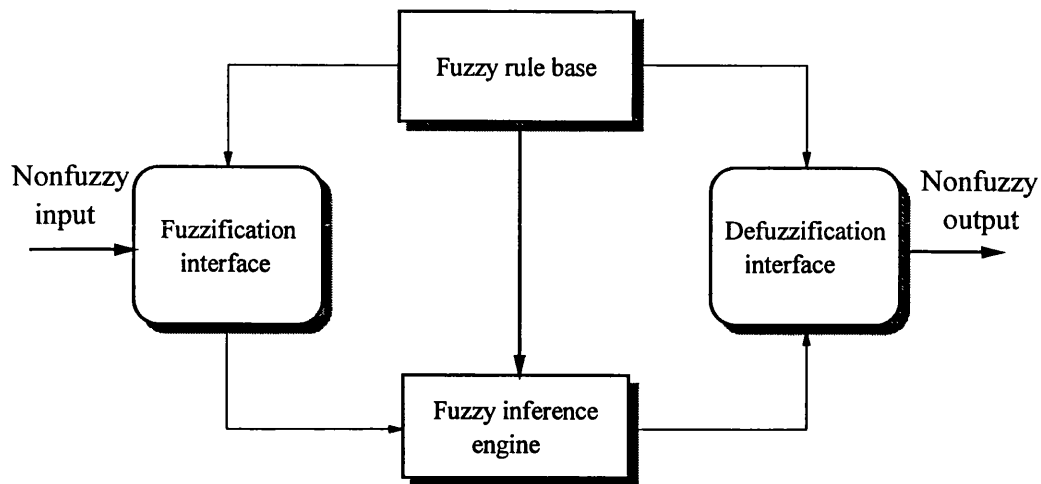
Figure 6.3 The general structure of FLS.

1) Fuzzification interface involves the following functions:

■   Measures the values of input variables.

■   Performs a scale mapping that transforms the range of values of input variables into corresponding universe of discourse.

■   Performs the function of fuzzification that converts input data into suitable linguistic values which may be viewed as labels of fuzzy sets.

2) Fuzzy rule base consists of a set of linguistic control rules written in the form:

"IF a set of conditions are satisfied,

THEN a set of consequences are inferred".

3) The fuzzy inference engine is a decision-making logic performing the inference operations of the fuzzy rules. Based on the fuzzy IF-THEN rules in the fuzzy rule base and the compositional rule of inference [68], the appropriate fuzzy sets are inferred in the output space. There are two principal methods of inference in fuzzy systems: the max-min inference and the max-product inference. Many other techniques are mentioned in the literature. Each method of composition of fuzzy relations reflects a special inference machine and has its own significance and applications. The max-min method is the one used by Zadeh in his original paper on

approximate reasoning using natural language IF-THEN rules.

In most fuzzy problems, the rules are generated based on post experience. Concerning problems that deal with fuzzy engines or fuzzy control, one should know all possible input-output relationships even in fuzzy terms; the input-output relationships, or rules, are than easily expressed with IF-THEN statements, such as:

IF A and/or B THEN C

Here "and/or" signifies logical union or intersection, A and B are fuzzified inputs, and C is action for the rule.

The following common methods are among those proposed in the literature for composition operation $B = A \circ R$, where A is the input defined on the universe X, B is the output defined on universe Y, and R is a fuzzy relation characterizing the relationship between specific inputs (x) and specific outputs (y):

$$\text{max-min} \qquad \mu_B(y) = \max_{x \in X}\{\min[\mu_A(x), \mu_R(x,y)]\} \qquad (6.5)$$

$$\text{max-}product \qquad \mu_B(y) = \max_{x \in X}[\mu_A(x) \cdot \mu_R(x,y)] \qquad (6.6)$$

$$\text{max-max} \qquad \mu_B(y) = \max_{x \in X}\{\max[\mu_A(x), \mu_R(x,y)]\} \qquad (6.7)$$

$$\text{min-max} \qquad \mu_B(y) = \min_{x \in X}\{\max[\mu_A(x), \mu_R(x,y)]\} \qquad (6.8)$$

$$\text{min-min} \qquad \mu_B(y) = \min_{x \in X}\{\min[\mu_A(x), \mu_R(x,y)]\} \qquad (6.9)$$

$$\text{max-}average \qquad \mu_B(y) = \frac{1}{2}\max_{x \in X}[\mu_A(x) + \mu_R(x,y)] \qquad (6.10)$$

Graphical representation

Let A, B and C denote fuzzy set in universe of discourse U, V and W respectively, then figures 6.4 and 6.5 illustrate the graphical interpretation of the max-min and max-product inference methods for a simple single-rule system i.e. IF A and B THEN C.
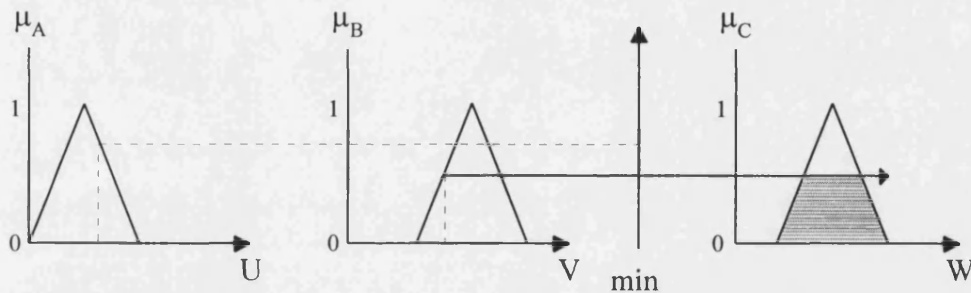
Figure 6.4 Graphical interpretation of max-min inference method.
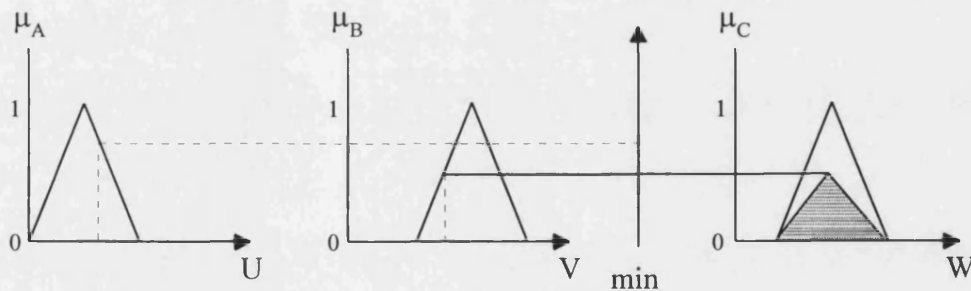
Figure 6.5 Graphical interpretation of max-product inference method.

4) Defuzzification interface performs the following functions:

- A scale mapping that converts the range of values of output variables into corresponding universe of discourse.
- Defuzzification that yield a nonfuzzy (crisp) control action from an inferred fuzzy control action.

A commonly used defuzzification rule is the centroid method, according to which the defuzzification interface produces a crisp output defined as the centre of gravity of the distribution of possible action.

6.2.4 Fuzzy Logic Applications to Power Systems

As previously discussed in chapter 1, a Power System consisting of a number of generating plants, busbars and transmission lines exhibits a high order of non-linearity. Because of its very nature, fuzzy logic would seem to be directly applicable to the analysis and control of power systems. However, work in this area has been rather limited. But, because of the constraints imposed upon most power utilities throughout the world due to economic and environmental reasons, there is increased interest in the subject of expert systems and fuzzy logic in running power networks more efficiently, even though this may entail on-line operation near to stability limits.

The fuzzy logic approach has been applied in one form or another to a range of power system problems, which Control staff deal with on a day to day basis, such as power system stability control, power system stability assessment, power system optimization, power system protection, etc.

6.3 Hybrid Intelligent Systems

Recent developments have involved combining the relative powers of AI techniques to solve power system problems. Because of the nature of various types of power system problems, different types of solution may be required. The real world power system problems may neither fit the assumption of a single AI technique nor be effectively solved by the strengths and capabilities of a single AI technique. In this respect, to solve complex power system problems with a high level of accuracy and reliability, two or more AI techniques are combined to increase their strength and overcome each other's weaknesses and generate hybrid solutions.

By integration of various AI techniques, hybrid intelligent systems as shown in figure 6.6 are developed. It is now becoming apparent that hybrid intelligent systems are very important in overcoming the drawbacks associated with purely symbolic AI-based representations for dealing with complex real world problems.
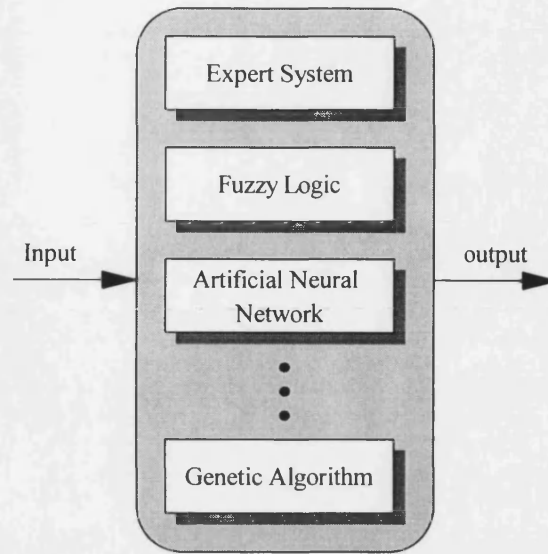
Figure 6.6 Hybrid intelligent systems.

The hybrid intelligent systems can be developed in a variety of ways. Some types of hybrid system can be summarised as: fuzzy neural networks, fuzzy expert systems, fuzzy controlled genetic algorithm, genetic based fuzzy systems and genetic neural networks. In recent years, hybrid intelligent systems have been applied to various power system problems such as: load forecasting [69,70], static security assessment [71] and power system stability [72]. To establish the basic concepts of the accurate fault location technique described in this chapter, fuzzy neural networks are discussed in the following section.

6.3.1   Fuzzy Neural Networks

Over the last decade, several parallel advances have been made in two distinct AI techniques: fuzzy logic and ANNs. While fuzzy logic provides an inference mechanism under cognitive uncertainty, ANNs offer exciting advantages such as learning, adaptation, fault-tolerance, parallelism and generalization. The ANNs, comprising of neuron like processing elements, are capable of coping with computational complexity, non-linearity and uncertainty. In view of this versatility of ANNs, it is believed that they hold great potential as building blocks for a variety

of behaviours associated with biological neural networks.

One of the important characteristics of ANNs is that they can classify inputs. Furthermore, the ANN can continuously classify and also update classifications. On the other hand, FLS can deal with fuzzy information and is capable of providing crisp outputs. However, in FLS there is no learning and, even vaguely, the input-output relationships (the fuzzy rules) must be known in advance.

In fact, concepts of fuzzy logic and ANNs integrate very well to give birth to emerging area of research called "fuzzy neural networks". Paradigms based upon this integration are believed to have considerable potential in the area of medical diagnosis, control systems, pattern recognition, and system modelling. Two possible models of FNN are schematically shown in figure 6.7(a) and 6.7(b). In figure 6.7(a), the fuzzy interface block provides an input vector to the ANN with response to logistic values. In this respect, the ANN can be trained to yield desired outputs, extract the fuzzy rules and learn membership functions from the training data. On the other hand, in the scheme presented in figure 6.7(b), an ANN derives the fuzzy inference mechanism ie., the ANN adjusts the fuzzy parameters.

In FNN, the ANN part is primarily used for its learning and classification capabilities and for pattern association and retrieval. The ANN part automatically generates fuzzy logic rules and membership functions during the training period. In addition, even after training, the ANN keeps updating the membership functions and fuzzy logic rules as it learns more and more from its input signals. Fuzzy logic, on the other hand, is used to infer and provide a crisp or defuzzified output when fuzzy parameters exist.

(a)

(b)
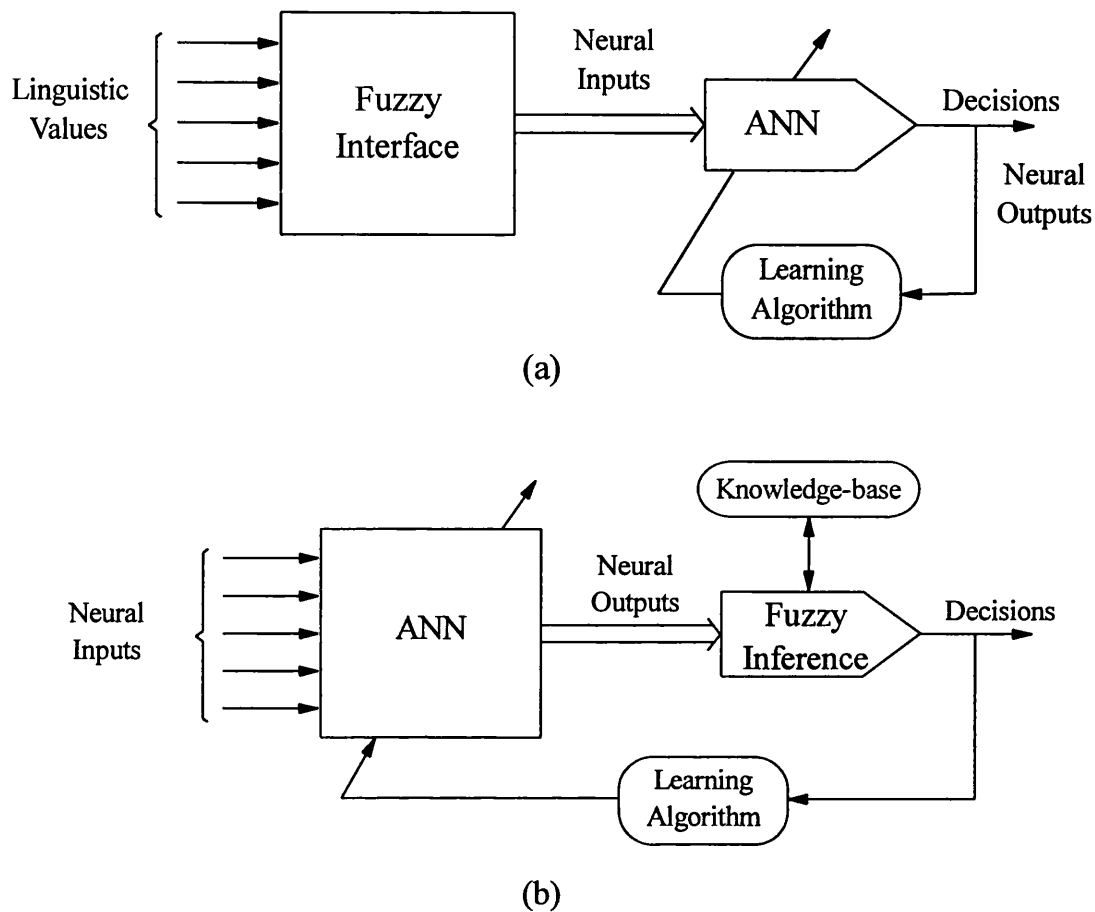
Figure 6.7 Two models of fuzzy neural networks.

(a) Feedforward architecture: ANN responds to the fuzzy inputs.

(b) Feedback architecture; ANN drives the fuzzy inference mechanism.

6.4　Fuzzy NN based fault location Scheme

6.4.1　Basic Configuration of the Technique

The FNN-based fault locator as developed in this work scheme is shown in figure 6.8. The technique consists of two stages: (i) fault type classification based solely on ANN architecture and (ii)　precise location of a fault on the line based on an integrated network comprising fuzzy logic and an ANN.

The method is based on utilising voltage and current waveforms at the fault locator end of the line only and the signals employed are based on phase values. The effect of transducers - current transformers (CTs) and capacitor voltage transformers (CVTs), and hardware errors such as anti-aliasing filters and quantisation are taken into account, so that the information processed throughout the fault locator algorithm is very close to real-life situation; this is achieved through a data pre-processing stage as discussed previously in chapter 5.
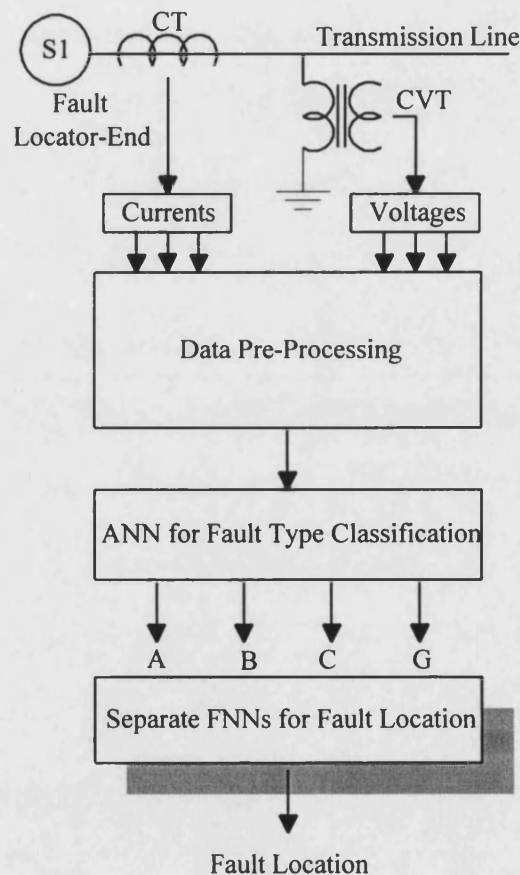
Figure 6.8 FNN-based fault location scheme.

The fault type classification technique is essentially the same as that described in section 5.6.2, where it was used in the fault location technique based solely on ANNs. As discussed before, separately designed FNNs, one for each type of fault and as shown in figure 6.8, are used herein, to accurately locate the actual fault position

associated with all the commonly encountered types of fault on EHV transmission lines; as discussed later, this approach further improves the accuracy of the fault location technique over that based solely on ANNs.

6.4.2   FNN Fault Locator Structure

The fuzzy logic is classified as an extension of binary Boolean Logic [73]. It is a class in which the transition from membership to non-membership is gradual rather than abrupt. As mentioned before, both the ANN and the fuzzy logic have some drawbacks when used on their own. The ANN can produce mapping rules from empirical training data sets through learning, but the mapping rules in the network are not visible and are difficult to understand. On the other hand, since the fuzzy logic does not have learning capability, it is difficult to tune the rules. In order to overcome these difficulties, the link between symbolic processing (fuzzy) and numerical processing (neural) has been investigated in recent years, and this has resulted in hybrid architectures based on integrating the representational ability of fuzzy systems [68,73], often referred to as a fuzzy neural network (FNN).

Figure 6.9 illustrates the FNN considered herein. The FNN carries out fuzzy inference with ANN structure, and adjusts the fuzzy parameters using ANN learning. The ANN has been trained to extract the best rules and to learn membership functions from the training set.

The structure of the FNN is determined by the functions used to represent the linguistic fuzzy variables; these are employed to set up fuzzification, ANN learning and defuzzification strategies. The centre of gravity defuzzification algorithm is used to produce a crisp output which indicates the actual fault location on a transmission line.

The information flow through a FNN can be clearly seen from figure 6.9. A crisp input (a single value rather than fuzzy or probability distribution) is presented to the

network, and the memberships of the multivariate fuzzy input linguistic variables (represented by fuzzy sets) are calculated. The confidence in each of the fuzzy output linguistic variables is then determined, and the network output is obtained by defuzzifying the information.

The FNN employed comprises of three components: fuzzifier, ANN learning and defuzzifier.
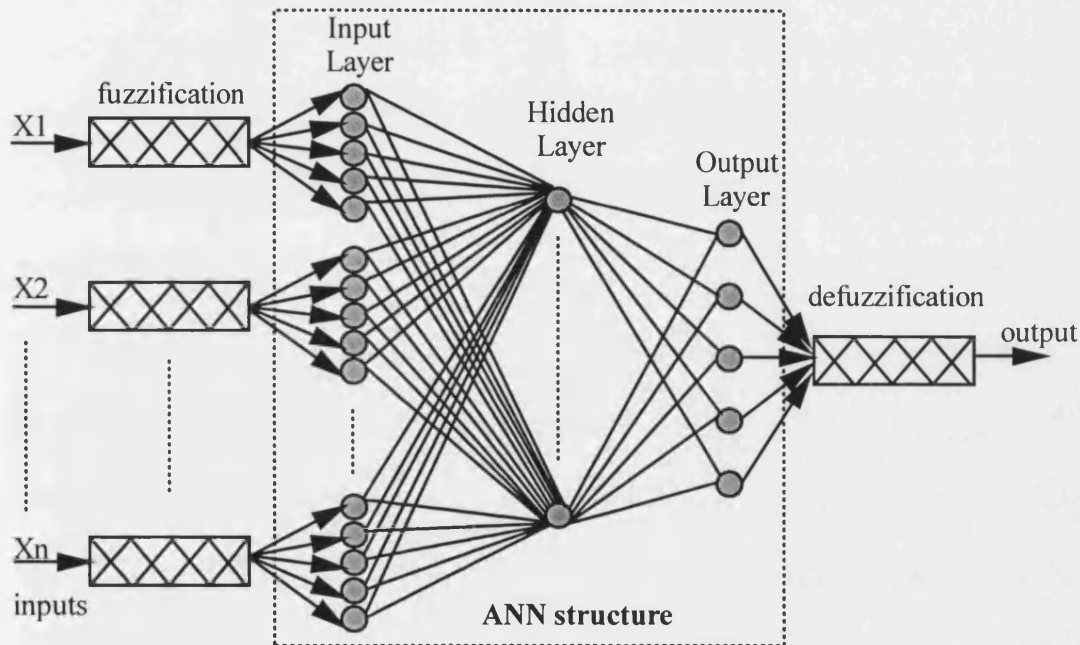
Figure 6.9 Fuzzy Neural Network Structure.

6.4.2.1   Fuzzification

A fuzzification operator has the effect of transforming crisp data into fuzzy sets; symbolically:

$$x = fuzzifier(\ x_o\ ) \qquad\qquad\qquad (6.11)$$

where x_o is a crisp input value from a process; x is a fuzzy set and the fuzzifier represents a fuzzification operator. The triangular membership functions are used to

define the fuzziness of the system.

6.4.2.2   Acquisition of fuzzy knowledge and inference by neural networks

The operation of a FNN can best be understood by considering the basic configuration of a fuzzy logic system (FLS) with pre-processing (fuzzifier or encoder) and reformation (defuzzifier or decoder) as shown in figure 6.10. In such a system, a set of linguistic rules or conditional statements in the form of: "IF a set of conditions is satisfied, THEN a set of consequences are inferred" are employed; the fuzzifier maps the crisp sets in the input universe U to a fuzzy set in U, and the defuzzifier maps the fuzzy sets in the output universe V of pure fuzzy logic system's output, to the crisp sets in V. However, it is virtually impossible to define these rules in a FLS on its own from the training set; this is so by virtue of the fact that the training data is highly complex in nature and is constituted by the interaction of many variables under different system and fault conditions. An integrated structure whereby the inference engine in figure 6.10 is replaced by an ANN (as shown in figure 6.9) is a much better alternative to deal with the problem and this is the approach adopted in the technique presented herein. The main attribute of such a structure is that the ANN automates the process of determining the membership function parameters and learns the best rules from the training set. After the training process, the resultant weights and biases become the principle base and the ANN takes over as the inference engine.
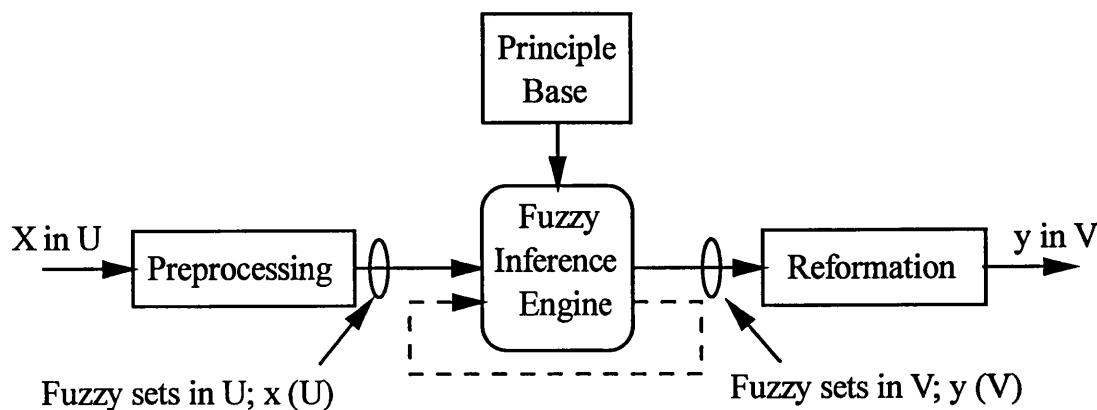
Figure 6.10 Basic structure of a fuzzy logic system.

The structure of the ANN employed within the FNN has one hidden layer and an output layer comprising of five nodes. It is a feedforward, fully connected network in which a hyperbolic tangent function is employed as the activation function. As mentioned before, once a fault has been classified to be of a particular type by the fault-classification ANN at the first stage, the appropriate FNN is then enabled for fault location identification at the second stage of the technique. In this respect, it should be noted that there are different FNNs employed (each with a slightly different architecture in terms of the number of hidden neurons and of course different training data) to cater for all types of commonly encountered faults.

Extracted features through spectrum analysis of the training data, described in the pre-processing stage in section 5.4, are converted into fuzzy sets; these are then used as inputs to train each ANN. The location of the fault is coded into a number of fuzzy membership functions determined by the desired resolution. In this study, five membership functions have been used. The number of output neurons of each ANN are the same as the number of the fuzzy membership functions.

6.4.2.3   Defuzzification

As shown in figure 6.9, the defuzzifier produces a crisp output from the fuzzy set which in turn is the output of the ANN learning block. In the defuzzification process, each membership function is weighted by the state of the corresponding output neuron of the ANN. The location of the fault is then obtained using centroid defuzzification as given by:

$$Fault\ Location = \frac{\sum_{i=1}^{n} y_i \mu_B(y_i)}{\sum_{i=1}^{n} \mu_B(y_i)} \tag{6.12}$$

where:

n is the number of quantization level of the output,

y_i is the output value at the quantization level i,

$\mu_B(y_i)$ is the value of membership function of the output fuzzy set at y_i .

6.4.3 Training data

Training data for FNN is obtained essentially the same way as that described in section 5.5.7. As for the fault location technique based solely on ANN structure, the inputs to the ANN comprise of a set of features based on the three-phase voltages V_a, V_b, V_c and three-phase currents I_a, I_b, I_c. With regard to the data pre-processing stage shown in figure 6.8, the following four frequency components are also considered here as the best features for each measured signal to generate the inputs to FNNs.

1) DC Component.

2) Fundamental Component.

3) Components over 100 - 350 Hz range.

4) Components over 400 - 1000 Hz range.

Figure 6.11 illustrates the frequency components for the "a"-phase current for a variety of fault conditions. From this, it can be seen that the training data is highly complex and different classes in the training set have overlap. Thus, by using fuzzy logic, this problem of overlap can be overcome by mapping of the membership of different data points in the different classes.
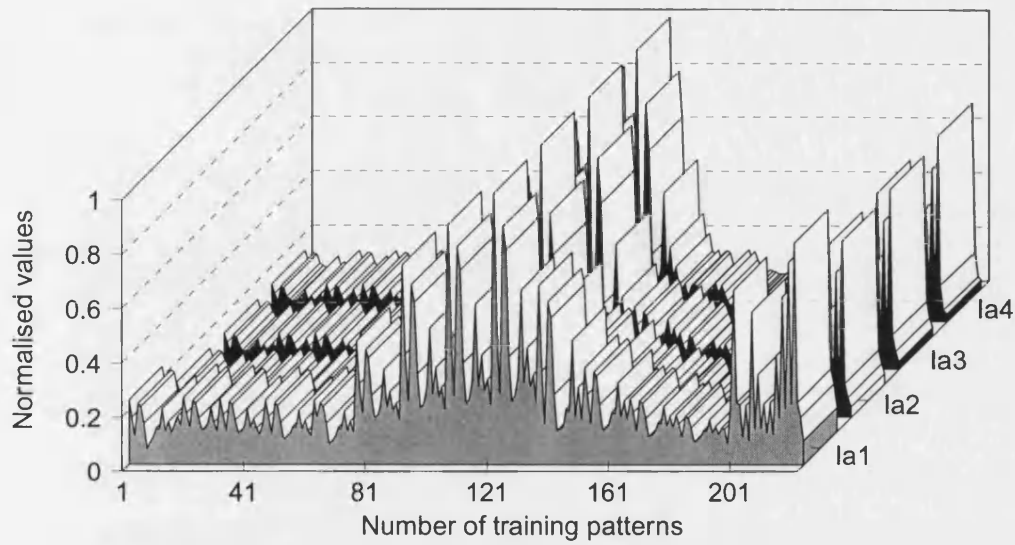
Figure 6.11 Frequency components for a-phase current.

6.4.3.1 Fuzzification of crisp information for the FNNs

This section describes how triangular membership functions describing the fuzziness of the transmission system are used to convert the previously described extracted features into fuzzy sets for the FNN and these are shown in figure 6.12(a). In order to facilitate this process, the overhead transmission line is divided into five sections as shown in figure 6.12(b). Each output neuron corresponds to the value of the membership function. As can be seen for a fault at say 48 km of the line, the membership function (and the ANN output) is [0 0.5 0.5 0 0].
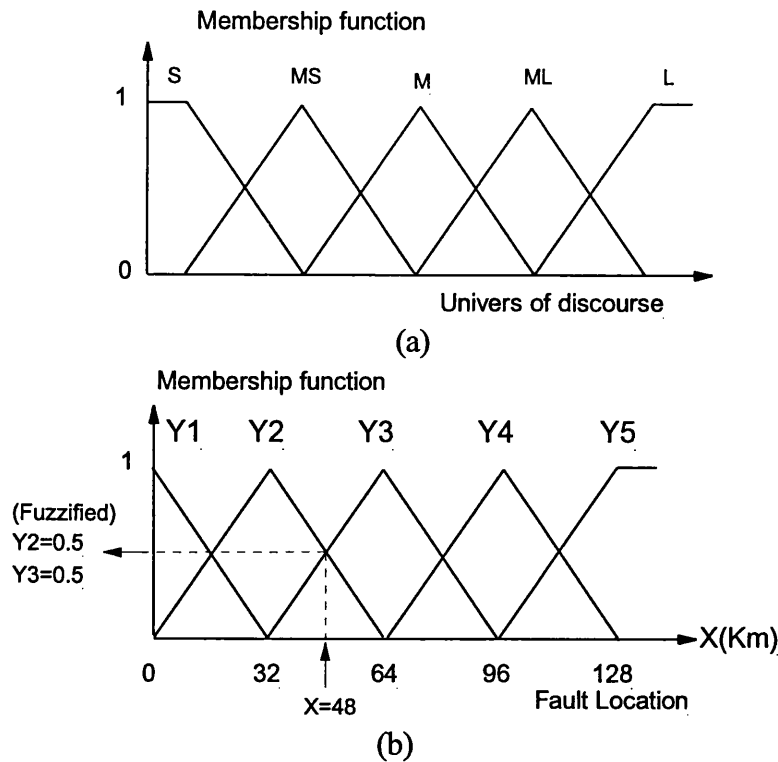
Figure 6.12 Input/output membership functions.

(a)   Membership functions of linguistic values(S: small, MS: medium small, M: medium, ML: medium large, L: large).

(b)   Membership functions for the fuzzification mapping of the output neurons.

Inputs to ANN are fuzzy sets $(S_1, S_2, ..., S_n)$ in the universe of discourse $(X_1, X_2, ..., X_n)$ respectively. These fuzzy sets are obtained by converting the DC and other frequency components attained through the frequency decomposition of the time-domain waveforms. As shown in figure 6.12(a), five linguistic terms as "small", "medium small", "medium", "medium large" and "large" are used to convert the crisp values to fuzzy inputs. In this respect, the structure of ANN consists of 60 neurons in the input layer and five neurons in the output layer. The FNN has been trained to yield desired fuzzy outputs. Table 6.1 illustrates the linguistic values of inputs and the fuzzy outputs for an 'a'-phase to ground fault occurring at the middle of the line and an 'a'-'b'-phase fault occurring at the remote end of the line; the frequency spectra associated with these faults are shown in figure 5.4 and 5.5 respectively. The training data for the FNN consists of fuzzy inputs/outputs with respect to these

linguistic terms and their membership functions. The location of the fault is then obtained using centroid defuzzification with respect to the membership functions shown in figure 6.12(b).

Fault Type	Frequency Component	Linguistic Values For Inputs						Fuzzy Outputs				
		i_a	i_b	i_c	V_a	V_b	V_c	Y1	Y2	Y3	Y4	Y5
a-phase-earth fault	DC	MS	ML	ML	M	ML	ML	0	0	1	0	0
	50 Hz	M	L	ML	MS	ML	M					
	100-350 Hz	MS	ML	M	S	MS	ML					
	400-1000 Hz	MS	M	S	MS	M	L					
a-b-phase fault	DC	L	ML	MS	S	MS	M	0	0	0	0	1
	50 Hz	L	M	MS	MS	ML	L					
	100-350 Hz	M	L	ML	MS	ML	L					
	400-1000 Hz	MS	M	ML	M	MS	ML					

Table 6.1 Fuzzy input/output training data representation.

6.5   Summary

The applications of fuzzy logic and fuzzy logic systems are reviewed. Structures of hybrid intelligent systems with practical emphasis on fuzzy neural networks are discussed in this chapter.

An integrated approach comprising fuzzy logic and ANNs for accurately locating faults on a transmission line, and further improve on the accuracy attainable from fault location techniques based solely on ANN architectures, is also discussed in this chapter. The technique consists of two stages: (i) fault type classification based solely on ANN architecture and (ii) precise location of a fault on the line based on FNNs.

Chapter 7

Performance Evaluation Of The Fault Location Techniques

7.1 Introduction

This chapter is concerned with the performance evaluation of the two proposed fault location techniques described in the previous two chapters. The chapter has been divided into two main parts to describe the performance of each technique. In the first part, the performance evaluation of the ANN topology for accurate fault location technique is discussed and the analysis of the results for fault type classification and fault location based solely on ANN architectures are presented. The second part is principally concerned with quantifying the improvements affected the accuracy through the employment of a fault location technique based on an integrated approach comprising fuzzy logic and ANN called fuzzy neural network (FNN).

The effects of differing source capacities, fault resistance, fault inception time, fault type, etc on the accuracy are examined for each technique.

It should be mentioned that the results presented in this chapter have been selected from an extensive series of training and test set examples from simulations of faults, generated as described in chapter 4. They attempt to represent, in the best suitable

way, the overall performance of the fault locator under a whole variety of system and fault conditions encountered in practice.

In order to obtain the results, customised programs were written in FORTRAN and C languages, and standard software packages such as DADiSP [74] (for waveform analysis) and Neural Works Professional II Plus [75] (for setting up ANN architectures) were used.

7.2 Performance Evaluation of the Technique Based Solely on ANNs

7.2.1 Preprocessing of Training / Test Data

In order to demonstrate the effectiveness of the proposed approach, it is necessary to pre-process training/test data. In this respect, as mentioned before, the required training and test data was generated for faults using EMTP software and then pre-processing the resulting data. Each case in the training set represents a different fault condition. Approximately, 3000 training/test set examples were prepared to evaluate the performance of the technique. Roughly, 60% of these cases were used for training of the ANNs, and the other 40% were used for the subsequent testing.

An illustrative study

as discussed before, the performance of the ANN depends on the training/test data, in this respect, it is important to fully examine the outputs of each process implemented for a typical fault condition. Figure 7.1 shows such waveforms when an a-phase-earth fault has occurred at the middle of the line. Figures 7.1(a) and 7.1(b) show the primary system voltage and current waveforms, at the fault locator end of the line. Figures 7.1(c) and 7.1(d) show the effect of CVTs and CTs on the voltage and current waveforms, respectively, it is apparent that the CVT has a significant influence on the voltage waveforms in that the high frequency transients are heavily attenuated; the corresponding analogue channel outputs are shown in figures 7.1(e) and 7.1(f). These waveforms are the same shape as the CVTs and CTs outputs,

except that the magnitudes are scaled down to ±8.5 volts for the voltage waveforms and ±2 amps for the current waveforms. The resultant data is then passed through a 12 bit A/D converter and the output signals are shown in figures 7.1(g) and 7.1(h). The A/D converter gives ±2048 quantum levels with 4.88 mV quantum level accuracy.

Figure 7.2 depicts the frequency spectra of the three-phase voltages and currents for the fault condition shown in figure 7.1, and the inputs into the ANN are shown in figure 7.3. As expected the dominant component in each signal is of the power frequency ie. 50 Hz. These are obtained through the previously described feature extraction technique employed, whereby four features for each measured signal are extracted from the frequency spectra shown in figure 7.2.
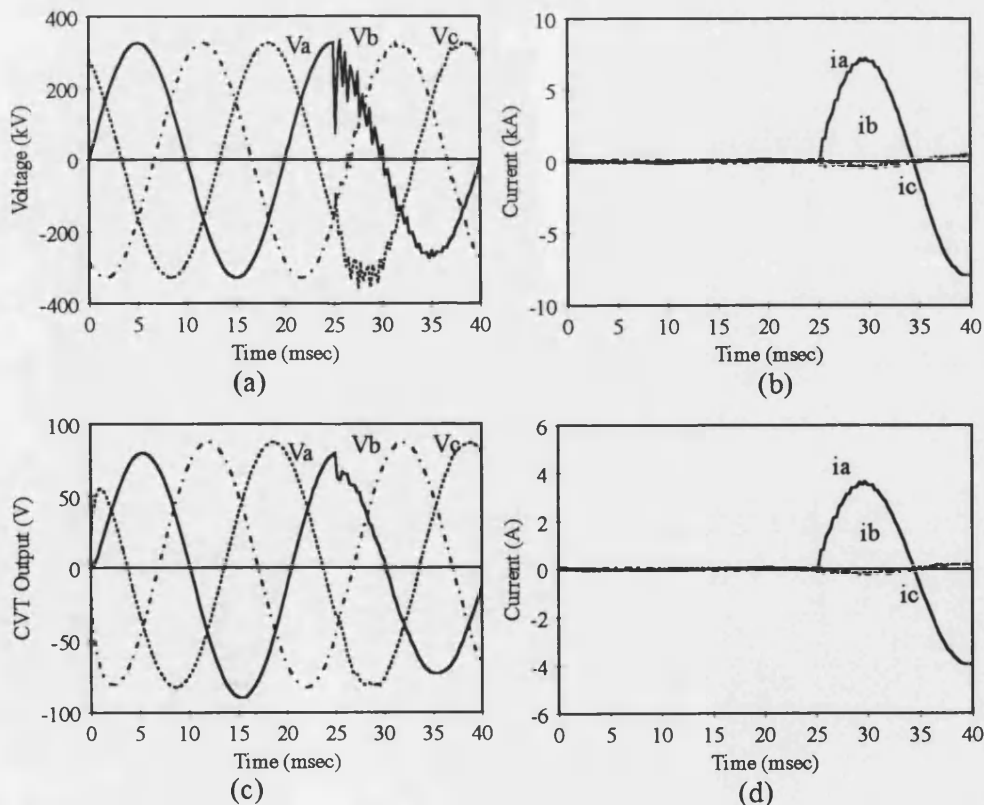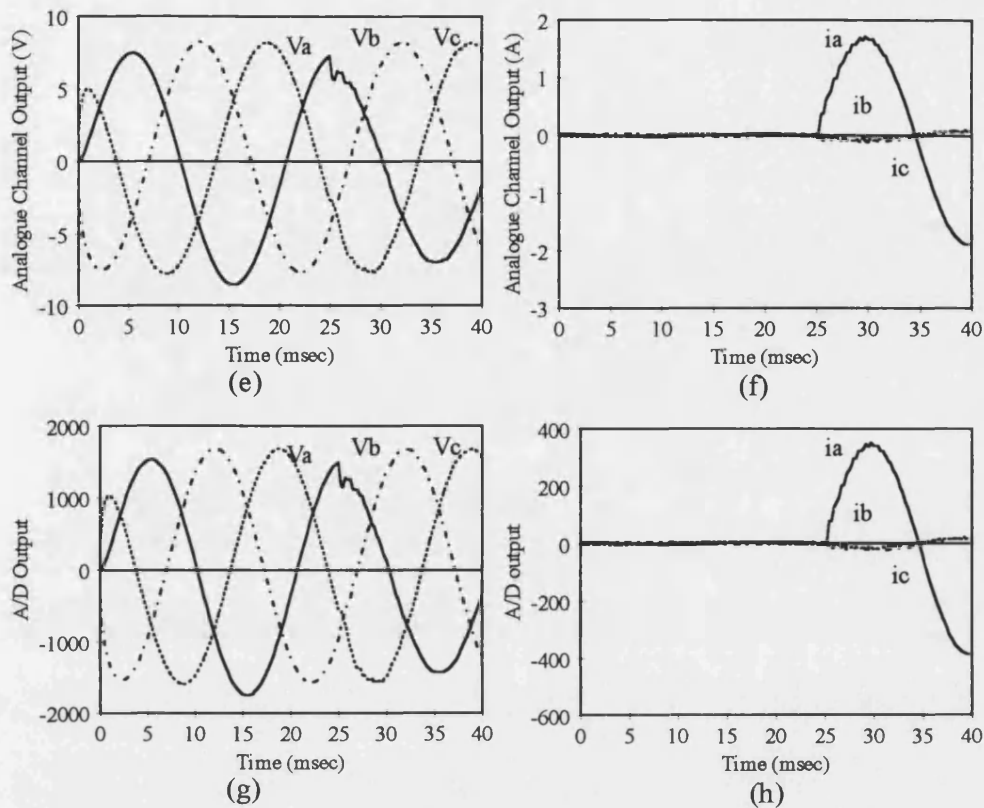
Figure 7.1 Example of data pre-processing for ANN training; a-phase-earth fault at the middle of the line, s.c.l. at the sending-end=20GVA, s.c.l. at the receiving-end=2.5GVA, R=1Ω.

(a) and (b) Primary system voltage and current waveforms.

(c) and (d) CVTs and CTs outputs.

(e) and (f) Analogue channel outputs.

(g) and (h) A/D outputs.
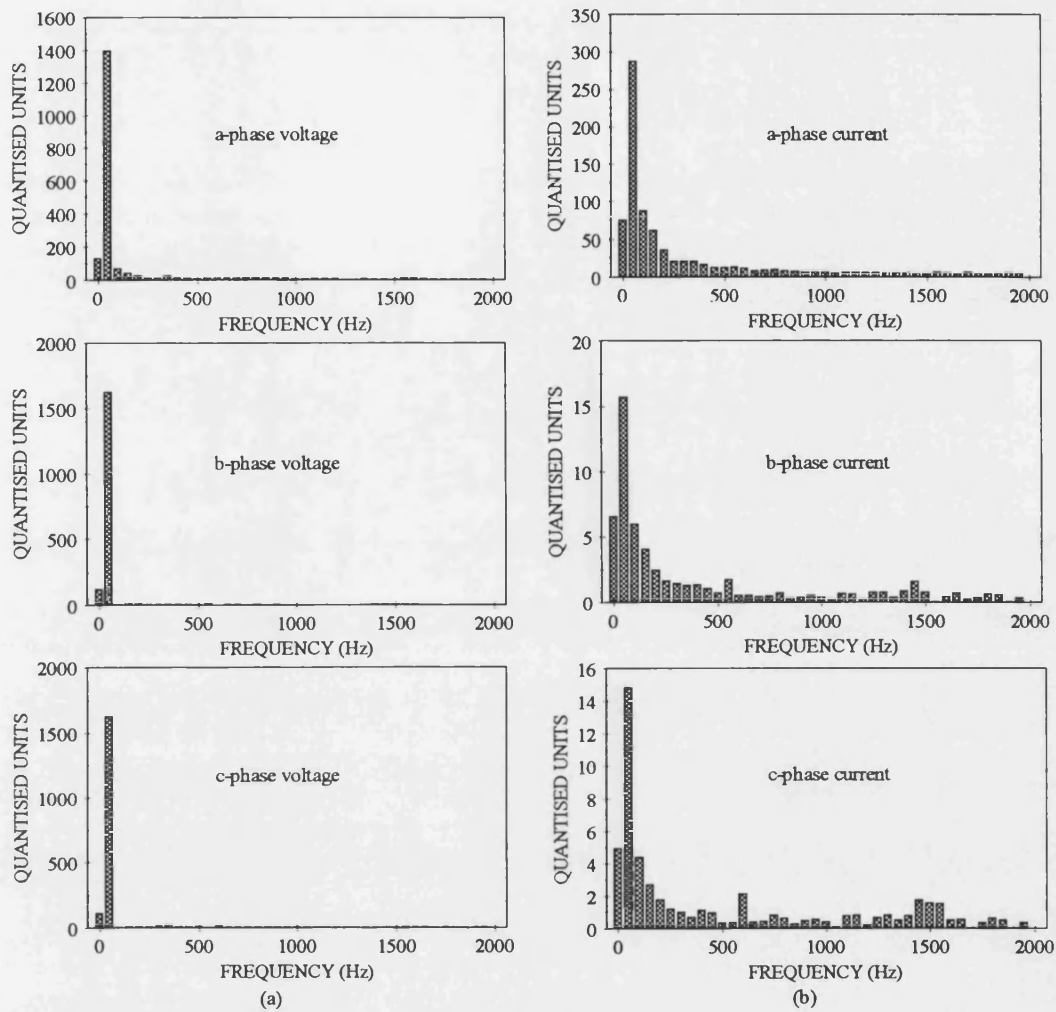
Figure 7.2 Frequency spectra for fault condition on figure 7.1.

(a) Spectra of three-phase voltages.

(b) Spectra of three-phase currents.
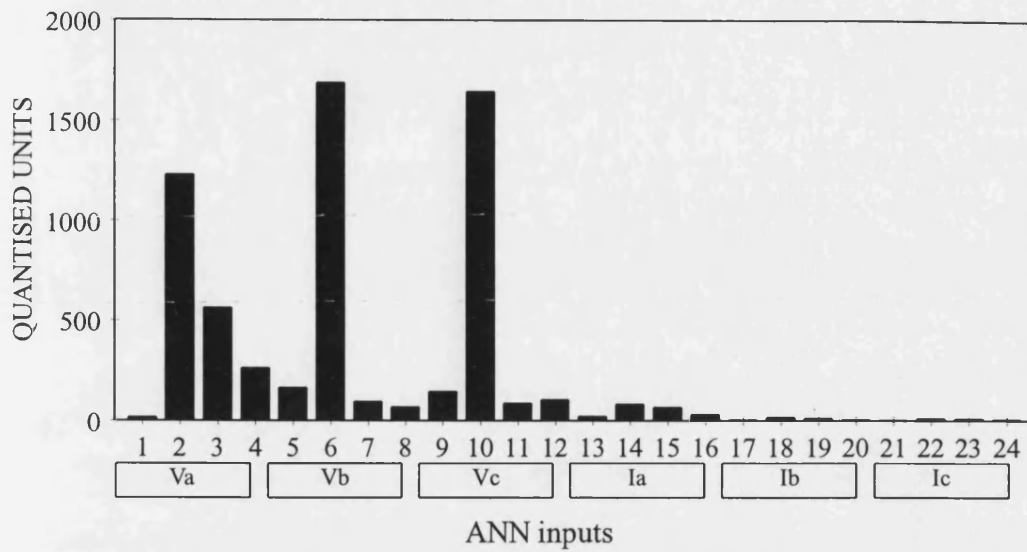
Figure 7.3 Inputs into the ANN for the fault condition on figure 7.1.

7.2.2 Feature Extraction

The feature extraction process is independent of the ANN architecture except for the fact the number of feature extracted constrains the number of inputs into the ANN and therefore simplifies its architecture. As mentioned in chapter 5 section 5, a frequency decomposition approach was adopted as the feature extraction process, utilising the following frequency components: DC components, fundamental components, components over 100-350 Hz range and components over 400-1000 Hz range. The four frequency components for 'a'-phase voltage, representing a vast majority of different system and fault conditions, are shown in figure 7.4. The peak of these frequency components vary with respect to each fault condition.
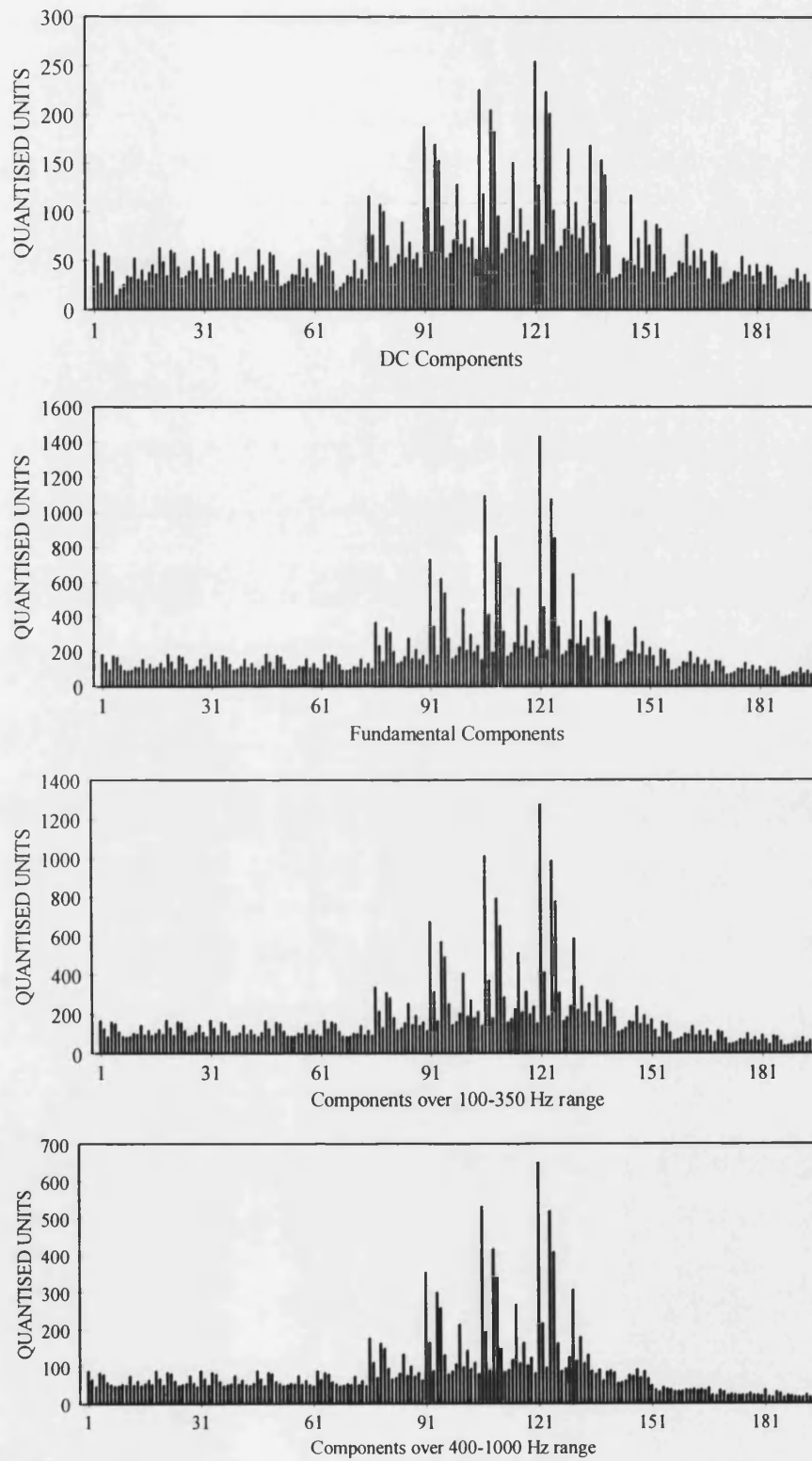
Figure 7.4 Frequency components for 'a'-phase voltage under different fault conditions.

7.2.3   ANN Topology for Fault Classification/Location

In order to find the best network topology for accurate fault location under all practically encountered different system and fault conditions, various ANN topologies were experimented with. The main functions that an ANN has to perform in this application are:

- Fault type classification.
- Fault location.

The first approach to the problem of accurate fault location on EHV transmission lines was based on a single ANN to both classify the type of the fault and locate the fault position. Figure 7.5 illustrates the structure of this algorithm which shows the input vectors and the nature of the outputs as discussed in chapter 5 section 6.
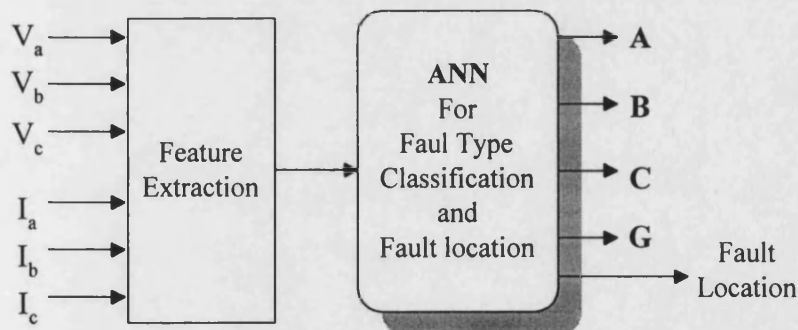
Figure 7.5 Structure of fault location algorithm using a single ANN.

A multi-layer feed-forward ANN using supervised learning and common training rule of error-back-propagation was used for this technique. Here, the structure of the ANN consists of 24 neurons in the input layer and 5 in the output layer. ANN training was conducted using 1500 fault patterns generated under different system and fault conditions.

In order to provide an indication of the ANN learning performance, the root mean square (RMS) error over a training epoch has been plotted against the number of

training iterations as shown in figure 7.6, and the performance of the fault location output for one set of examples (100 training patterns) is shown in figure 7.7. The performance and speed of the training process depends upon the size of the network and the amount of data (training patterns) presented to the network.

In order to improve the performance of the training, various ANN structure were designed and tested. However, as shown in figures 7.6 and 7.7, the network cannot converge within the required RMS error criterion of 0.01 and it does not have the generalisation capability. It is thus impractical to merely employ a single ANN and attempt to train it with a large amount of data. Obviously, the network failed to converge and produce the correct results. In this respect, a much better approach, as mentioned in section 5.6, is to separate the problem into two parts:

1) Use a single ANN for fault type classification

2) Use separate ANNs (one for each type of fault) for fault location.
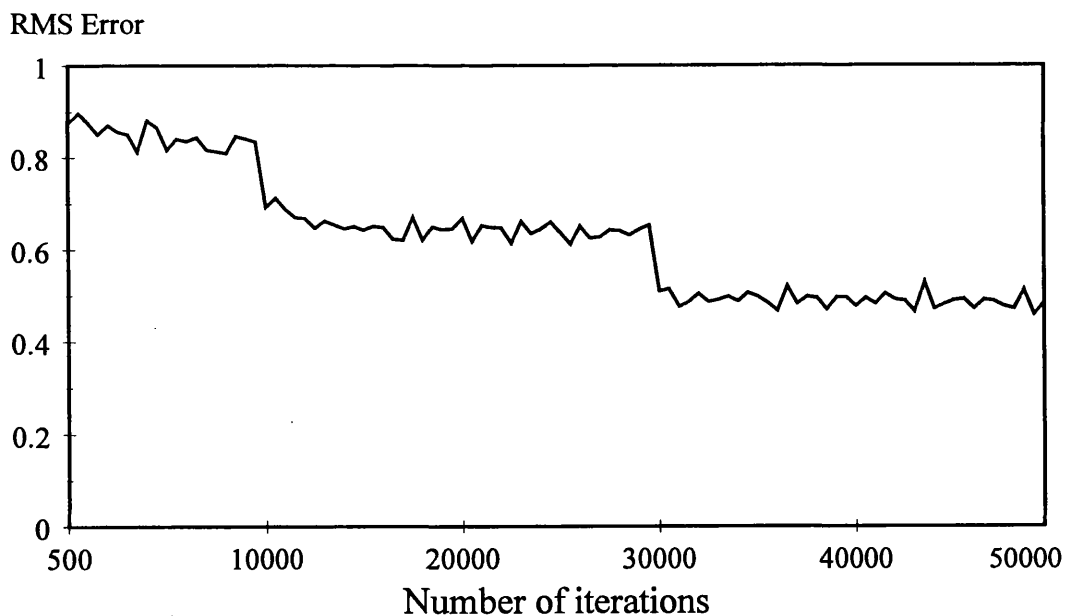
RMS Error

Figure 7.6 ANN RMS error (convergence capability of ANN).
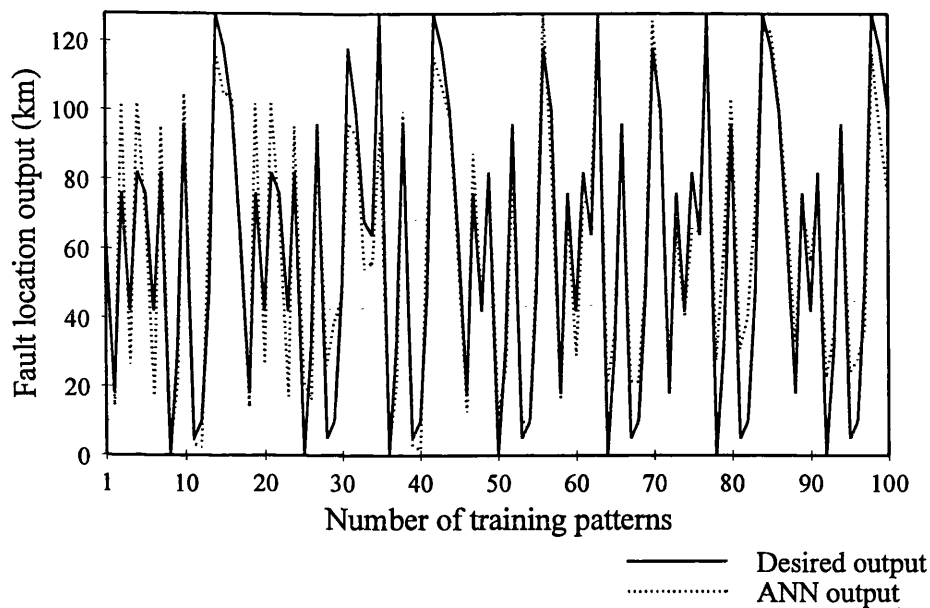
Figure 7.7 Performance of the fault location for a set of training examples (generalisation capability of ANN).

7.2.4 Performance of ANN for Fault Type Classification

A three-layer perceptron based on the Delta-Bar-Delta learning algorithm was trained for the fault type classification problem. In this study, 60 training patterns were used in the training set and the performance of the ANN was then evaluated using various unseen cases.

The first task in this approach was the selection of the most appropriate ANN architecture. In this respect, a range of ANN architectures were trained and tested. The general performance was good for even simple types of network, and is so by virtue of the good separation of classes provided by the feature extraction process, and the good selection of logic for the output of the ANN. The RMS error is plotted in figure 7.8, which indicates a very good performance of the ANN learning and fast convergence of the training process. The generalisation capability of the ANN for four typical output values is illustrated in figure 7.9. This shows a good generalisation capability which is due to the good selection of the training set. One iteration during training took about 4 milliseconds, therefore, the total training time

was about 32 seconds corresponding to 8000 iterations. It should be mentioned, these computing time are for a 486-66 MHz PC. Of course this time would be shorter for a more powerful PC.

RMS Error

Number of iterations
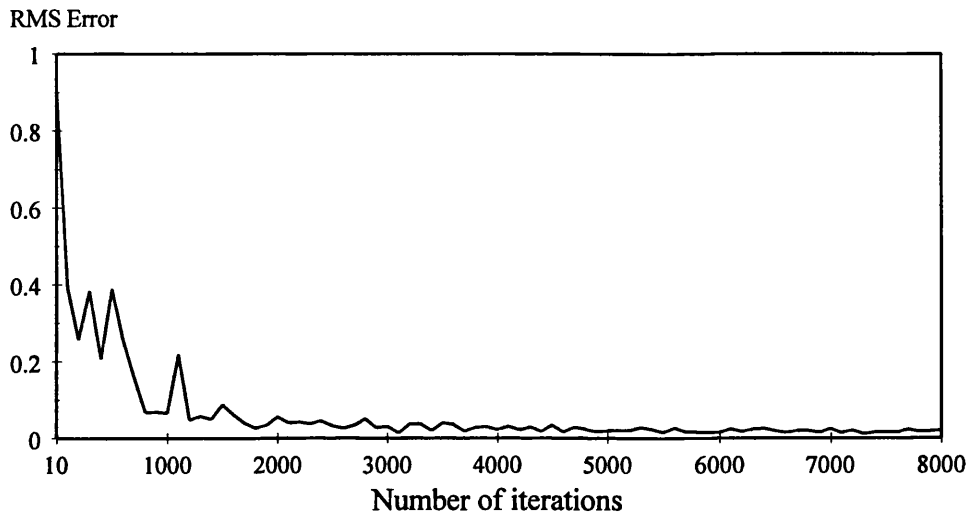
Figure 7.8 Convergence capability of the ANN.

7.2.4.1   Analysis of Test Results

Following the training of the ANN, a separate set of test patterns were supplied as input to the ANN involved in the fault-type classification in order to evaluate its performance. Table 2 gives some examples of the test results. The left four columns are the desired outputs, ideally '1' or '0' (corresponding to the fault types as indicated by the logic shown in Section 5.6.2), and the right four columns are the actual outputs of the ANN; each test case comprises of four different fault positions at distances of 8, 62, 96 and 120 km, respectively from end S (see figure 4.1). It is evident from the results that although the ANN gives a high accuracy, there are small fluctuations in the actual ANN outputs around '1' and '0'; since in practice this cannot be avoided, small threshold levels have to be built into the ANN algorithm in order to minimise the degree of uncertainty. In this application, these levels were set such that if the output fell within the range <0.1 then it would be classed as '0' ie, a healthy phase indication, and if it fell within the range >0.9 then it was classed as unity ie, a faulted phase indication.
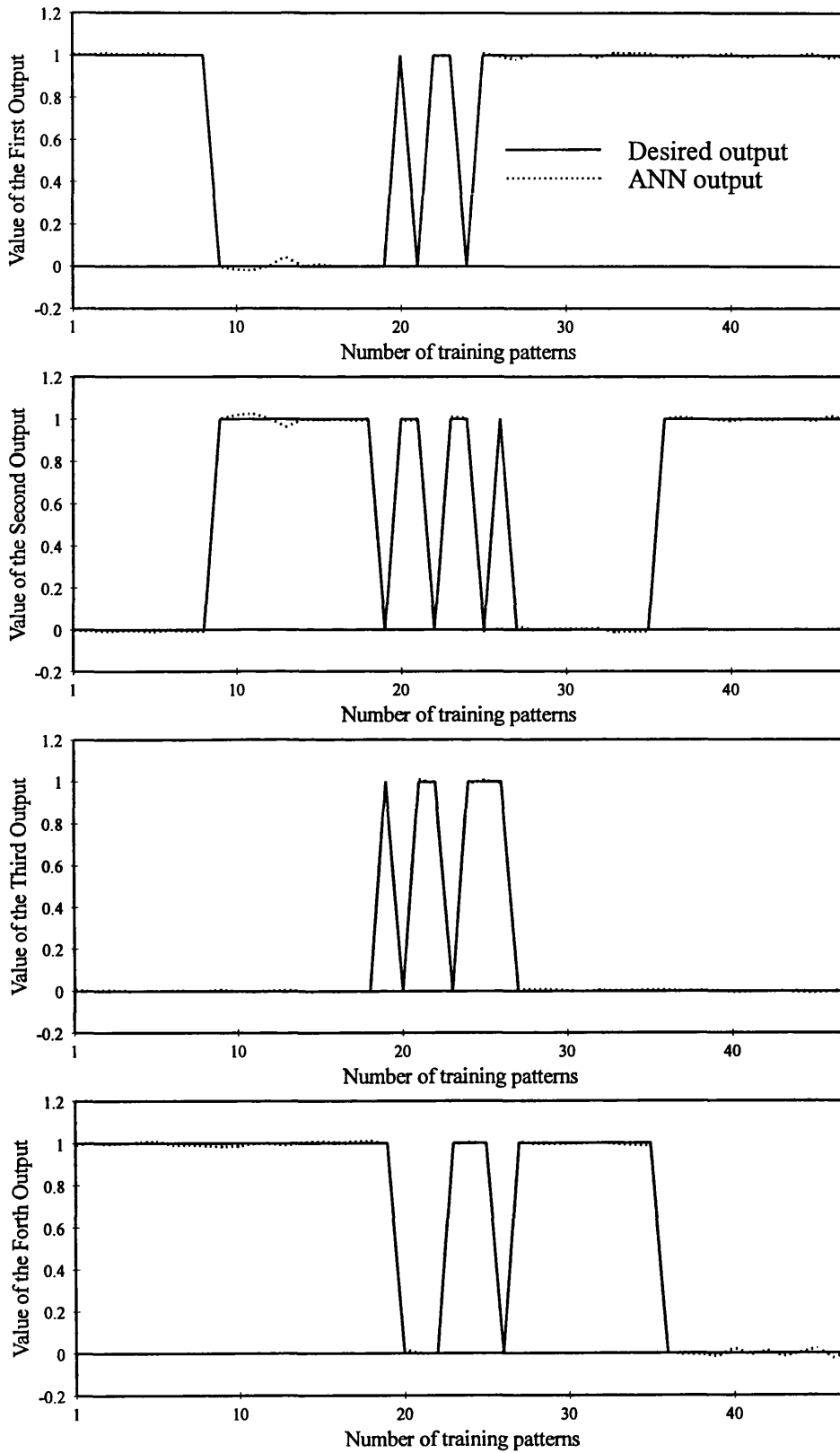
Figure 7.9 Generalisation capability of the ANN training.

Test Cases	Desired Output				Actual Output			
Case 1 S1=2.5GVA S2=20GVA Rf=1Ω	1.0000	0.0000	0.0000	1.0000	1.0110	-0.0055	0.0021	0.9971
	1.0000	0.0000	0.0000	1.0000	1.0096	-0.0038	0.0090	0.9923
	1.0000	0.0000	0.0000	1.0000	1.0021	-0.0089	0.0568	0.9803
	1.0000	0.0000	0.0000	1.0000	1.0326	-0.0253	0.0128	0.9913
Case 2 S1=2.5GVA S2=20GVA Rf=100Ω	1.0000	0.0000	0.0000	1.0000	0.9763	0.0045	-0.0042	1.0057
	1.0000	0.0000	0.0000	1.0000	0.9761	0.0163	0.0162	1.0187
	1.0000	0.0000	0.0000	1.0000	0.9959	0.0047	-0.0050	1.0091
	1.0000	0.0000	0.0000	1.0000	0.9469	0.0212	0.0113	1.0215
Case 3 S1=2.5GVA S2=20GVA Rf=100Ω	1.0000	1.0000	0.0000	1.0000	1.0104	1.0045	-0.0617	1.0055
	1.0000	1.0000	0.0000	1.0000	1.0044	1.0087	-0.0280	1.0770
	1.0000	1.0000	0.0000	1.0000	0.9899	1.0089	0.1032	0.9969
	1.0000	1.0000	0.0000	1.0000	1.0008	1.0210	-0.0054	1.0229
Case 4 S1=20GVA S2=2.5GVA	1.0000	1.0000	0.0000	0.0000	0.9999	1.0020	-0.00045	0.0025
	1.0000	1.0000	0.0000	0.0000	1.0103	0.9915	-0.0054	0.0235
	1.0000	1.0000	0.0000	0.0000	0.9873	1.0136	-0.0015	-0.0241
	1.0000	1.0000	0.0000	0.0000	1.0016	0.99609	0.0085	0.0041
Case 5 S1=15GVA S2=20GVA Rf=50Ω	0.0000	1.0000	1.0000	1.0000	0.0032	0.9603	1.0646	0.9174
	0.0000	1.0000	1.0000	1.0000	-0.0141	1.00214	0.99878	0.9680
	0.0000	1.0000	1.0000	1.0000	0.0095	1.0114	1.0211	1.0090
	0.0000	1.0000	1.0000	1.0000	-0.0130	0.9324	0.9750	1.0275
Case 6 S1=2.5GVA S2=20GVA Rf=1Ω	1.0000	0.0000	1.0000	1.0000	1.00121	-0.0021	0.9457	1.0098
	1.0000	0.0000	1.0000	1.0000	0.9940	0.0012	0.9321	1.0010
	1.0000	0.0000	1.0000	1.0000	1.0190	-0.0190	0.9540	0.9121
	1.0000	0.0000	1.0000	1.0000	1.0013	0.0021	1.0210	1.0010
Case7 S1=2.5GVA S2=20GVA Rf=1Ω	1.0000	1.0000	1.0000	1.0000	1.0204	1.0166	1.0074	0.9687
	1.0000	1.0000	1.0000	1.0000	1.0306	1.0223	0.9823	0.9446
	1.0000	1.0000	1.0000	1.0000	1.0378	1.0363	1.0002	1.1146
	1.0000	1.0000	1.0000	1.0000	1.0126	1.0021	1.0698	1.0668

Table 7.1 Test cases for fault type classification.

7.2.4.2   Performance Evaluation

In order to quantitatively evaluate the performance of the fault classification technique, three indices are proposed as follows:

Error index (EI) = No. of error decisions / No. of total tests

Single Confidence Index (SCI) = Desired - Iactual / desired

Average Confidence Index (ACI) = Sum of SCI / No of tests

Table 7.2 presents the overall performance of tests carried out over 200 system and fault conditions, which indicates that the overall confidence index is 99.66% with no single error decision.

		A	B	C	G
Single Confidence Index	Min	99.8%	99.98%	99.82%	99.2%
	Max	99.9%	99.9%	99.9%	99.9%
Average Confidence Index		99.8%	99.5%	99.85	99.55%
Overall Confidence Index	99.66%		Error Index		0%

Table 7.2 Performance evaluation of fault type classification.

7.2.5   Performance of Fault Location

This section presents the performance evaluation of the fault location technique under different system and fault conditions. The trained ANNs involved in the second stage of the fault location technique were tested with a separate set of test data *unseen* by the ANNs before. As mentioned in chapter 5, this stage comprises of a number of ANNs (each corresponding to a different type of fault), the appropriate ANN being activated by the outputs from the ANN in the first stage (as described above in section 7.2.4).

7.2.5.1   ANN Structure

Through a series of tests and modifications, the optimal number of hidden neurons in the single hidden layer for the best performance of each ANN was obtained. Table 7.3 typifies the number of hidden neurons used to design the structure of each ANN. As mentioned in chapter 5, 24 neurons in the input layer and 1 in the output layer were chosen, where the output shows the location of the fault.

Type of Fault	Number of hidden Neurons
a-phase-earth fault	15
b-phase-earth fault	15
c-phase-earth fault	15
a-b-phase fault	18
b-c phase fault	18
a-c phase fault	18
a-b-phase-earth fault	20
b-c-phase-earth fault	20
a-c-phase-earth fault	20
3-phase fault	14
3-phase-earth fault	16

Table 7.3 Optimal number of hidden neurons for each ANN.

Determining the best net size

The degree of freedom of the ANN equal to the number of inter connection / size, and therefore proportional to the number of hidden neurones, must be matched, in some sense, to the complexity of the classification boundary. Currently, in the absence of parameter / theoretic guidance, the only proposed method of determining the best number of hidden neurons is by comparative cross validation among several ANNs. As shown in figure 7.10 (for four typical fault type), moving from a small number of hidden neurons to a large number should decrease the overall probability

of error while maintaining an equivalent error performance for the best and training data. When the perceptron's performance on training data begins to lag when the number of hidden neurons increase, the process of memorization may have started. There is always a range where the error of the ANN is relatively unchanged. This should be the best range for ANN structure.
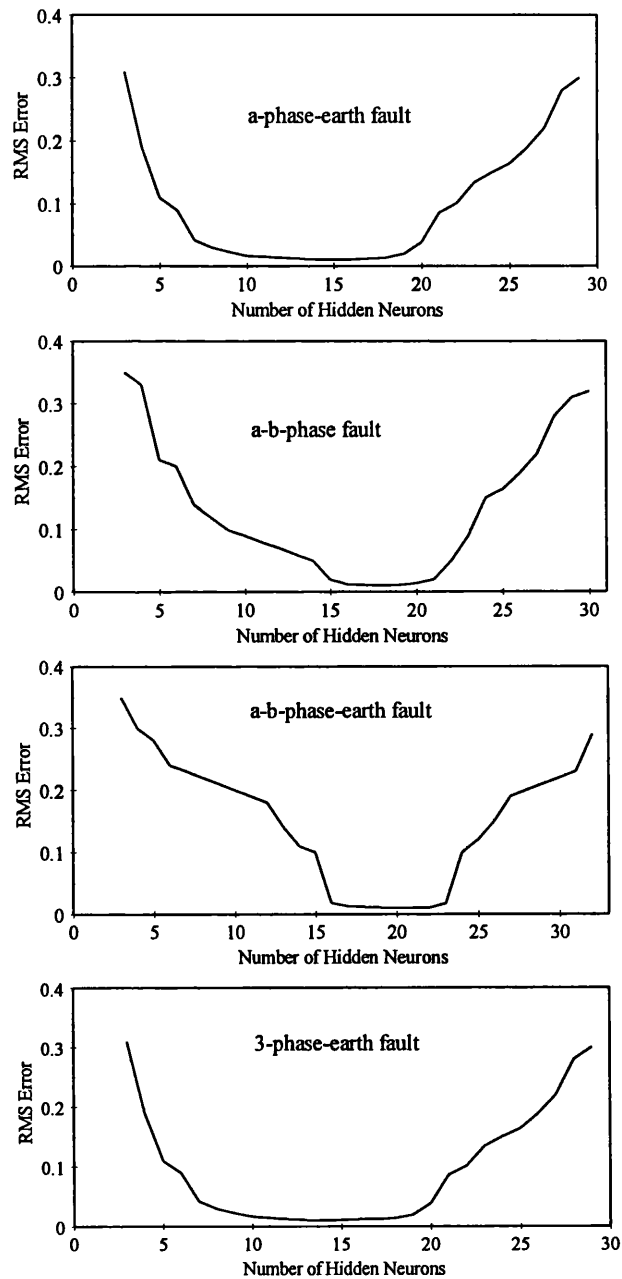
Figure 7.10 RMS errors vs number of hidden neurons.

7.2.5.2   ANN Training

ANN training was conducted using different training sets for each type of fault. In this respect, an extensive series of studies have shown that each ANN training based on a set of approximately 150 different training patterns are sufficient to cater for all practically encountered different system and fault conditions.The networks were then trained by randomly processing the training patterns using the back-propagation learning algorithm. It is important to adopt this approach because if the data is presented in a sequential fashion, and similar data is grouped together, then the network may start to loose what it has learned from one end of the data set to another. At the start of the data set, it learns one set of relationships and as it moves towards the end of the data set, it learns a different set of relationships, forgetting what it learned at the start. RMS error criteria is used herein to evaluate the learning performance. The learning performance for the ANNs representing: a-phase-earth fault, a-b-phase fault a-b-phase-earth fault, and 3-phase-earth fault is shown in figure 7.11. In all cases, it is shown that the ANNs reached the required RMS criterion of 0.01% in approximately 30 000 learning iterations. The epoch of 100 was chosen to show the performance of each network for all training iterations. A smaller epoch such as one is also useful for viewing the performance of the network classification type, because the largest individual errors are often more important than the rms error.

In general, the rms error becomes lower as training progresses, as shown in figure 7.11. Although this process is slower in large networks, in such networks, the error reduces further. Training data which produces consistently larger errors than average is typically taken from samples around the boundaries of each class of patterns, or at the limits for that class.
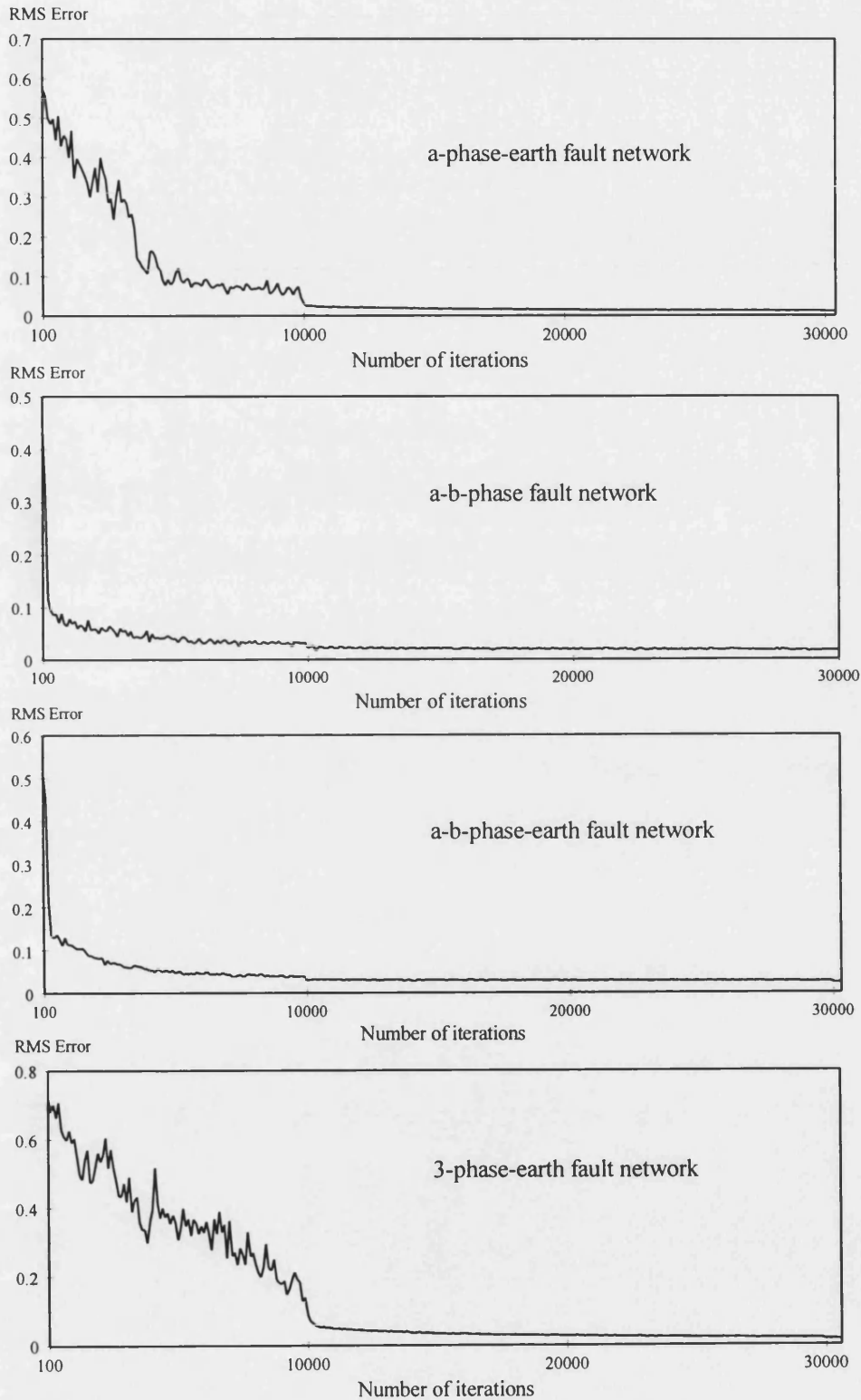
Figure 7.11 Performance of ANNs training for different types of fault.

7.2.5.3   Analysis of Test Results

Separate sets of test data were supplied as input to each ANN involved in the fault location stage in order to evaluate their performance under different fault and system conditions. The error for fault location is expressed as a percentage of the length of the line, and is given as:

$$\% \ error = \frac{actual \ location \ - \ desired \ location}{length \ of \ the \ line} \times 100$$

Effect of source capacity: As discussed in section 4.6, the source parameters, particularly their capacities, significantly affect the fault transient waveforms. Therefore, it is vitally important to verify the effect of source capacity on the performance of the proposed fault location technique. Tables 7.4 and 7.5 show the effect of source capacity on the accuracies attained for some examples of test results. The source capacities are varied from a large value to a very small value at each end of the line in both tables respectively. In order to illustrate the performance of the fault location technique under varying source capacities, three different fault positions at distances of 0, 64, and 128 km, respectively from end S (shown in figure 4.1), are used to show the results for each type of fault. A small fault resistance of 1 Ω for the faults involving earth, and a fault inception angle of 90° is used in all the test cases.

It is clearly evident from the results that the accuracy achieved in fault location is high, being < 2% in all the test cases. The technique also retains its high accuracy at low capacities for different types of faults. This is a major advantage particularly since source capacities constantly change according to the load demand.

Fault Type	SCL at S (GVA)	SCL at R (GVA)	Desired Output (km)	Actual Output (km)	% Error
a-earth fault	2.5	20	0.0000	1.8721	1.46
a-earth fault	10	20	64.0000	63.0123	0.77
a-earth fault	20	20	128.0000	126.3265	1.31
a-b-phase fault	20	20	0.0000	0.9532	0.74
a-b-phase fault	15	20	64.0000	65.8760	1.46
a-b-phase fault	0.5	20	128.0000	130.3410	1.82
a-b-earth fault	5	20	0.0000	1.1085	0.86
a-b-earth fault	10	20	64.0000	62.5670	1.11
a-b-earth fault	15	20	128.0000	129.6541	1.29
3-phase-earth fault	0.5	20	0.0000	1.9470	1.52
3-phase-earth fault	10	20	64.0000	63.6650	0.26
3-phase-earth fault	15	20	128.0000	127.0101	0.77

Table 7.4 Effect of source capacity on accuracy for differing source capacities at the sending-end (end S) of the line.

Fault Type	SCL at S (GVA)	SCL at R (GVA)	Desired Output (km)	Actual Output (km)	% Error
a-earth fault	20	20	0.0000	0.7210	0.56
a-earth fault	20	10	64.0000	65.1803	0.92
a-earth fault	20	20	128.0000	129.6565	1.29
a-b-phase fault	20	0.5	0.0000	1.1501	0.89
a-b-phase fault	20	15	64.0000	62.4670	1.19
a-b-phase fault	20	20	128.0000	125.8032	1.71
a-b-earth fault	20	2.5	0.0000	0.8500	0.66
a-b-earth fault	20	10	64.0000	66.0891	1.63
a-b-earth fault	20	20	128.0000	127.5540	0.34
3-phase-earth fault	20	0.5	0.0000	1.4501	1.13
3-phase-earth fault	20	15	64.0000	64.7501	0.58
3-phase-earth fault	20	20	128.0000	129.2181	0.95

Table 7.5 Effect of source capacity on accuracy for differing source capacities at the receiving-end (end R) of the line.

Effect of fault resistance: It is vitally important to ascertain if the fault location estimation is significantly influenced by changes in fault resistance. In order to examine the accuracy of fault location algorithm to different fault resistances, a series of unseen test cases were created. The tests cases were carried out varying the fault resistance from 1 to 200 Ω for one particular type of fault. The effect of fault resistance is not studied for phase-phase faults, since in practise the fault resistance for such type of faults rarely exceeds 1 Ω.

Table 7.6 shows the effect of fault resistance on the accuracies attained for the transmission system shown in figure 4.1 subject to an a-phase-earth fault and a-b-earth fault respectively, at 64 km from end S. Table 7.7 illustrates the same effect for 3-phase-earth fault near end R (the error attained in this case is due to the fact that the line considered is untransposed). It is clearly evident from the results that the ANNs give accurate evaluation of fault position that is largely independent of the fault resistance. An extensive series of tests have shown that this is the case for all types of fault involving fault resistance. This is a very significant advantage over conventional techniques, particularly those based on impedance to fault measurements, which tend to produce excessive errors when dealing with resistive faults.

Desired Output (km)	Rf (Ω)	a-phase-earth fault		a-b-phase-earth fault	
		Actual Output (km)	% Error	Actual Output (km)	% Error
64.0000	0	64.7843	0.61	64.9456	0.73
64.0000	25	62.8941	0.86	65.3210	1.03
64.0000	50	63.0453	0.74	62.1204	1.46
64.0000	75	66.1014	1.64	65.3450	1.05
64.0000	100	65.6548	1.30	62.7541	0.97
64.0000	125	61.8124	1.71	66.2140	1.73
64.0000	150	62.3127	1.31	62.0191	1.54
64.0000	175	66.1440	1.67	61.6401	1.84
64.0000	200	61.7140	1.78	66.5012	1.95

Table 7.6 Effect of fault resistance on fault location's accuracy, ANNs test examples for a-phase-earth fault and a-b-phase-earth fault.

Desired Output (km)	Rf (Ω)	3-phase-earth fault	
		Actual Output (km)	% Error
128.0000	0	127.1201	0.68
128.0000	25	129.4510	1.13
128.0000	50	129.5912	1.24
128.0000	75	126.8940	0.875
128.0000	100	129.6019	1.25
128.0000	125	126.5461	1.13
128.0000	150	126.3219	1.31
128.0000	175	130.1210	1.65
128.0000	200	130.6140	2.04

Table 7.7 Effect of fault resistance on fault location's accuracy, ANN test examples for 3-phase-earth fault.

Effect of fault inception angle: For the results presented hitherto, the faults have been applied either at an instant corresponding to voltage maximum or at zero voltage in the faulty phase or phases. The former of the two is the worst case from the point of view of travelling wave distortion. The other extreme, i.e. when the fault is applied at zero voltage, distortion is extremely small in the voltage waveforms because there is not a large and sudden voltage change at the point of the fault, however, the latter results in a large DC offset in the current waveforms.

It is thus important to verify the performance of ANNs for faults at different inception angles to those studied previously. The effect of fault inception angle variation on the accuracies attained is thus examined for all types of fault. Tests were performed for faults applied at instances corresponding to voltage maximum, at 45° angle, and at zero voltage on the faulty phase or phases. Table 7.8 presents the overall performance of tests carried out over 20 different test cases for each type of fault, which indicates that the fault location technique maintains a high degree of accuracy which is almost independent of the fault inception angle. This feature is important since in practice, faults can occur at any point on wave i.e. the fault inception angle cannot be defined in advance. This study clearly demonstrates that the fault location algorithm is virtually immune to any errors caused by either the higher frequency transients, which are associated with faults near voltage maximum or DC offsets caused by faults near voltage zero.

Fault Type	% Error		
	0o angle	45o angle	90o angle
a-earth fault	1.85	1.90	2.00
b-earth fault	1.71	1.58	1.38
c-earth fault	1.69	1.71	1.62
a-b-phase fault	1.68	1.80	1.95
b-c-phase fault	1.46	1.53	1.64
a-c-phase fault	1.34	1.65	1.41
a-b-phase-earth fault	1.88	2.00	1.44
b-c-phase-earth fault	1.12	1.35	1.63
a-c-phase-earth fault	1.22	1.51	1.50
3-phase fault	1.66	1.36	1.54
3-phase-earth fault	1.81	1.59	2.00

Table 7.8 The effect of fault inception angle on the accuracy. Maximum % error for all type of faults for different fault conditions. Faults applied at different angles with respect to 'a'-phase.

External faults: In any fault locator, although a high accuracy for internal faults is of primary concern, nonetheless, it should also be stable under external faults. For the fault location technique described herein, an external fault produces an estimation which is consistently very much higher than that expected for an internal fault, results shown in table 7.9 being a typical example. It is evident, from the results that when the ANNs give such abnormally high values, then it can be safely assumed that the fault is external. Studies have shown that the aforementioned is the case for all practically encountered external faults.

Fault Type	Fault Location (km)	
	Behind the Busbar at end S	beyond the Busbar at end R
a-phase-earth fault	-801	1024
a-b-phase-earth fault	-756	981

Table 7.9 Performance of ANNs under external faults.

Effect of line configuration: As mentioned before, the 400 kV vertical single-circuit configuration lines commonly encountered in the UK, are used to create the training and test data. However, it is also important to examine the performance of the fault location technique for faults on other configurations. Table 7.10 typifies the degree of accuracy attained for a 400 kV vertical double-circuit line and 500 kV horizontal single-circuit line under 'a'-phase-earth fault. The results clearly demonstrate that the technique retains its high accuracy for distance estimation for different line configurations, the magnitude of errors in terms of accuracy being less than about 2% for most of the fault conditions studied. This is a major advantage and indicates that the technique is robust and can be used for different transmission systems.

Desired Output (km)	Rf (Ω)	400 kV Vertical double-circuit		500 kV Horizontal single-circuit	
		Actual Output (km)	% Error	Actual Output (km)	% Error
0	1	0.9210	0.72	1.2401	0.97
18	10	16.8491	1.15	19.3510	1.05
48	50	46.8910	0.86	49.6204	1.26
64	100	65.4104	1.10	62.7150	1.00
68	50	67.5148	0.38	69.8401	1.44
80	10	81.6084	1.25	78.2840	1.34
90	10	88.1020	1.48	92.1101	1.65
100	1	101.1014	0.86	101.7111	1.33
128	100	125.8140	1.70	130.3505	1.83

Table 7.10 Effect of line configuration on the accuracy for a-phase-earth fault, s.c.l. at the sending-end=10GVA, s.c.l. at the receiving-end=20GVA.

Transmission line length: The EHV transmission line lengths can vary considerably in length. Therefore, it is vitally important to ascertain as to what extent the fault location accuracy is affected as a result of a change in the line length. Table 7.11 illustrates the performance of the ANN-based technique for 'a'-phase-earth faults when subjected to the line lengths of 80, 100 and 150 km respectively. The system configuration shown in figure 4.1 is used to create the test cases.

The results summarised in table 7.10 and 7.11 clearly demonstrate that the accuracy of the fault location technique described herein is little affected by changing the line configuration and line length.

It should be also mentioned that the performance of the ANN for fault type classification in the first stage of the technique is little affected by a variation in line configuration or line length.

Line Length (km)	Rf (Ω)	Desired Output (km)	Actual Output (km)	% Error
80	1	0.0000	0.8219	1.02
80	1	60.0000	59.2037	0.99
80	1	64.0000	65.3210	1.65
100	1	0.0000	1.2050	1.20
100	1	64.0000	62.1078	1.89
100	1	100.0000	97.9841	2.01
150	1	10.0000	13.0120	2.00
150	1	64.0000	61.5014	1.66
150	1	150.0000	158.4540	2.30

Table 7.11 ANN performance for a-phase-earth fault for different line length.

7.3   Performance Evaluation of the Technique Based on FNNs

This section is concerned with the performance evaluation of the integrated approach comprising fuzzy logic and ANNs for locating faults on transmission lines. It should be mentioned here that like the previous case, this approach also comprises of two stages: a fault type classification stage and a fault location stage. In this respect, the fault type classification stage is exactly the same as that employed previously; it is the second stage ie. fault location stage, which is based on FNNs.

7.3.1 Fuzzification of the Training Data

In order to obtain the training data for FNNs, the previously discussed frequency components considered as the best features for each measured signal, are converted to fuzzy sets using triangular membership functions. The membership functions used to convert the frequency components of 'a'-phase current (shown in figure 6.11) are illustrated in figure 7.12 and the corresponding fuzzy sets for an 'a'-phase-earth fault at 0, 64 and 128km, respectively from end S (in figure 4.1), are shown in table 7.12. These fuzzy sets are used as the inputs to train the ANNs and the desired fuzzy outputs are defined based on the membership function shown in figure 6.12 (b).
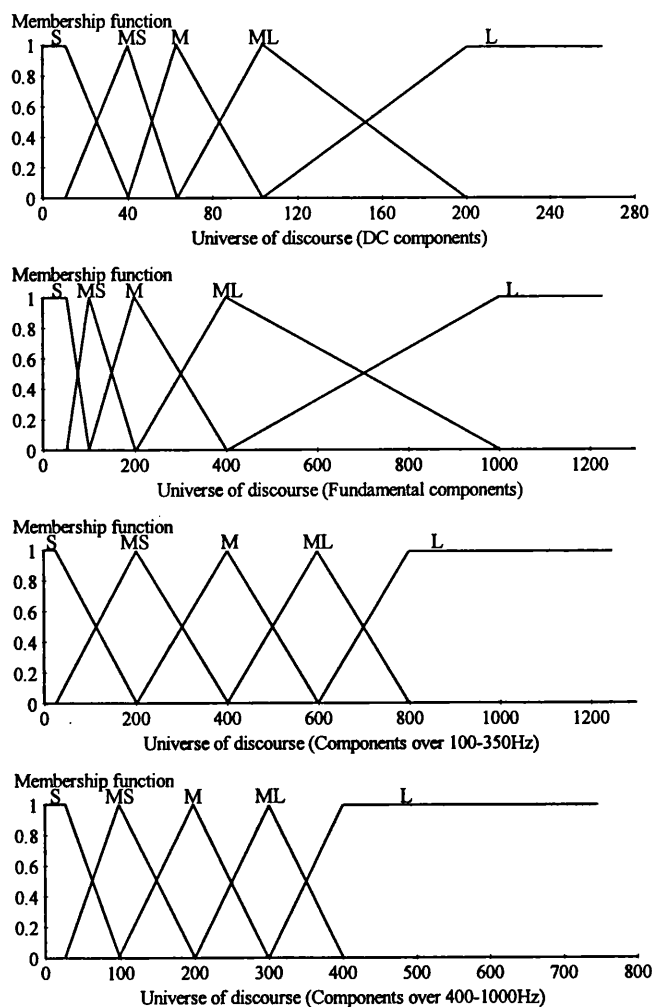
Figure 7.12 Membership functions for fuzzification of 'a'-phase current.

Membership functions of linguistic values (S: small, MS: medium small, M: medium, ML: medium large, L: large).

Fault Position (km)	Frequency Component	Crisp Data	Fuzzy Input Data				
0	DC	60.82	0.00	0.16	0.84	0.00	0.00
	Fundamental	183.71	0.00	0.00	0.00	0.00	1.00
	100-350 Hz	167.75	0.00	0.00	0.00	0.00	1.00
	400-1000 Hz	87.58	0.33	0.67	0.00	0.00	0.00
64	DC	101.81	0.19	0.81	0.00	0.00	0.00
	Fundamental	52.77	0.00	0.00	0.00	0.59	0.41
	100-350 Hz	6.82	0.00	0.00	0.3	0.7	0.00
	400-1000 Hz	20.56	0.81	0.19	0.00	0.00	0.00
128	DC	15.00	0.83	0.17	0.00	0.00	0.00
	Fundamental	94.50	0.00	0.00	0.71	0.29	0.00
	100-350 Hz	89.04	0.00	0.16	0.84	0.00	0.00
	400-1000 Hz	51.88	0.45	0.55	0.00	0.00	0.00

Table 7.12 Fuzzification of the 'a'-phase current for a-phase-earth fault.

7.3.2 FNN Training

FNN training is conducted using different training sets for each type of fault. Training patterns are the same as those used to train the ANNs in the previous section. In order to evaluate the performance of the training process, the RMS error criteria of 0.01 is used. Figure 7.13 illustrates the performance of the training process for an 'a'-phase-earth fault and 'a'-'b'-earth fault. It is clearly shown that the networks have a very good training performance and convergence capability. This could be attribute to good separation of classes provided, by using fuzzy sets as the training data.
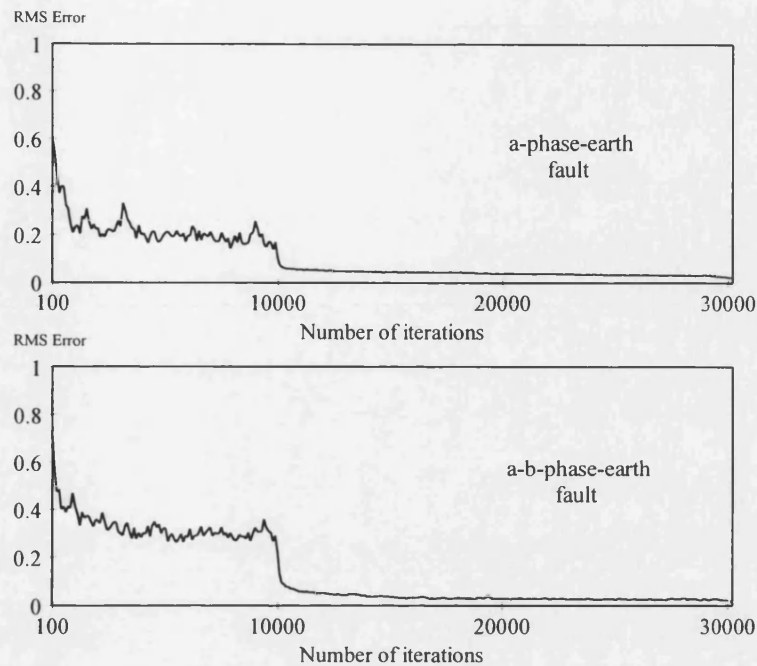
Figure 7.13 RMS error vs training iterations for FNNs.

7.3.3 Defuzzification

The location of the fault is obtained using centroid defuzzification as given by equation 6.12. Table 7.13 illustrates defuzzification of the fuzzy outputs for different 'a'-phase-earth fault test cases.

Desired Output(km)	ANN Fuzzy Outputs					Defuzzification
1.00	0.9308	0.0781	-0.0246	0.02138	-0.0115	1.50
32.00	0.0770	0.9102	0.0236	-0.0160	0.01911	31.10
92.00	0.0188	0.0005	0.1191	0.8248	0.0500	91.99
8.00	0.7424	0.3023	-0.0514	0.0351	-0.0172	7.47
48.00	-0.0288	0.5756	0.4254	0.0312	-0.0145	47.30
120.00	0.0082	-0.0212	0.0013	0.2688	0.7449	120.31
96.00	0.0101	0.0050	0.0733	0.8443	0.0761	94.81
18.00	0.4379	0.56815	0.0040	0.0127	-0.0060	18.58

Table 7.13 Defuzzification of fuzzy outputs for a-phase-earth fault examples.

7.3.4 Analysis of Test Results

Like in the previous case, the trained FNNs involved in the second stage of the fault location technique were tested with a separate set of test data *unseen* by the FNNs before. As mentioned before, this stage comprises of a number of FNNs, each corresponding to a different type of fault, the appropriate FNN being activated by the outputs from the ANN in the first stage. Table 7.14 gives some examples of the test results.

Fault Type	SCL at S1-GVA	SCL at S2-GVA	Rf (Ω)	Desired Output (Km)	Actual Output (Km)	% Error
a-phase-earth fault	2.5	5	1	18.0000	18.5701	0.44
a-phase-earth fault	2.5	5	1	48.0000	47.3402	0.51
a-phase-earth fault	2.5	15	1	0.0000	1.118426	0.92
a-phase-earth fault	2.5	15	50	5.0000	4.4394	0.43
a-phase-earth fault	15	2.5	1	100.0000	99.4633	0.42
a-phase-earth fault	20	2.5	100	82.0000	83.3833	1.0
a-phase-earth fault	20	2.5	100	100.0000	99.0838	0.72
a-b-phase fault	20	2.5	-	100.0000	99.5221	0.37
a-b-phase fault	15	2.5	-	64.0000	62.7108	1.00
a-b-phase fault	5	20	-	62.0000	61.0615	0.73
a-b-phase-earth fault	5	20	20	62.0000	61.0615	0.73
a-b-phase-earth fault	20	5	50	62.0000	62.8382	0.65
a-b-phase-earth fault	10	20	100	8.0000	9.3341	1.04
3-phase fault	2.5	20	-	0.0000	1.3010	1.01
3-phase fault	10	20	-	64.000	63.2100	0.61
3-phase fault	20	20	-	128.0000	126.9105	0.85
3-phase-earth fault	20	2.5	100	42.0000	42.0944	0.85
3-phase-earth fault	2.5	20	50	64.0000	65.2010	0.94
3-phase-earth fault	20	2.5	100	82.0000	83.3833	1.0

Table 7.14 Fault location results obtained from testing FNNs under different fault condition.

It is clearly evident from the results that the accuracy achieved in fault location is very high, being <1% in the majority of cases. An extensive series of studies have shown that the fault location technique described herein maintains this high accuracy

and robustness under a vast majority of different system and fault conditions; equally importantly, the improvement attained over the previous technique based solely on ANNs ie, without the integration of fuzzy logic and an ANN, is very significant, as indicated by the results shown in the following section. In practice, this improvement in accuracy is vitally important since it would considerably narrow the span of a line length which would be necessary to be scrutinised; this in turn would expedite the precise location of a fault thereby enabling the line to be restored to normal quickly.

7.3.4.1   Improvement on the Accuracy of Fault Location

This section demonstrates the improvement in the accuracy attained over the fault location technique based on ANNs. In order to illustrate the effect of different system and fault conditions, the FNNs are tested with the same sets of testing data as used in the previous technique based solely on ANN architectures and the results are compared in terms of the maximum percent error obtained for each technique.

7.3.4.2   Effect of Source Capacity

The overall performance of both techniques under differing source capacities is shown in table 7.15. It should be mentioned that the degree of accuracy attained herein, for each type of fault, is based on the same tests applied to both techniques. This is apparent that there is a significant reduction in error in the case of the FNN-based technique, this being reduced from about 2.5% (in the case of ANN-based technique) to $\cong 1\%$.

Fault Location Technique	% Maximum Fault Location Error			
	a-phase-earth fault	a-b-phase fault	a-b-phase-earth fault	3-phase-earth fault
ANN	2.20	2.51	2.62	2.51
FNN	1.00	0.90	1.01	1.00

Table 7.15 Effect of source capacity for different types of fault under 50 test cases for each type of fault.

7.3.4.3   Effect of Fault Resistance

FNNs were tested for all types of fault involving fault resistance. The results in table 7.16 clearly show a very high accuracy for fault location and further improvement in the accuracy. This is again a significant achievement over the previous technique. The maximum percent of error obtained in table 7.16 is based on the same test cases applied to both techniques.

Fault Location Technique	% Maximum Fault Location Error		
	a-phase-earth fault	a-b-phase-earth fault	3-phase-earth fault
ANN	2.00	2.50	2.01
FNN	1.00	1.00	1.01

Table 7.16 Effect of fault resistance for different types of fault.

7.3.4.4   Effect of Fault Inception Angle

In order to evaluate the performance of FNNs for faults at different inception angles, the test cases presented in table 7.8 were used to examine the accuracy of the fault location for different types of fault under variations in the fault inception angle. Table 7.17 gives a summary of the results. It is apparent that the accuracy attained by the FNN fault location technique is largely independent of the fault inception angle and also shows improvement on the accuracy of the previous fault location technique.

Fault Location Technique	Inception Angle	% Maximum Fault Location Error			
		a-phase-earth fault	a-b-earth fault	a-b-phase fault	3-phase-earth fault
ANN	0	1.85	1.88	1.68	1.81
FNN	0	1.00	1.02	0.95	1.00
ANN	45	1.90	2.00	1.80	1.59
FNN	45	1.01	1.00	0.90	1.01
ANN	90	2.00	1.63	1.95	2.00
FNN	90	1.00	1.02	1.00	1.02

Table 7.17 Effect of fault inception angle on the accuracy of both techniques.

7.3.4.5   Effect of External Faults

Like the previous case, the FNNs were tested for external faults behind the busbar near end S and beyond the busbar near end R (in figure 4.1), and same results as those shown in table 7.9 was obtained. Henceforth, an error orders of magnitude higher than that expected for an internal fault indicates the existence of an external fault.

7.3.4.6   Effect of Line Configuration

Like the previous case, FNNs were tested with a set of unseen data (same test cases as the previous technique) comprising faults at different positions on the line for 400 kV vertical double-circuit lines and 500 kV horizontal single-circuit lines. Table 7.18 summarises the results and shows the improvement on the accuracy based on the new approach.

Fault Location	% Maximum Fault Location Error	
Technique	Vertical double-circuit	Horizontal single-circuit
ANN	1.70	1.83
FNN	0.90	1.00

Table 7.18 Test results for a-phase-earth fault on different line configurations.

7.3.4.7   Effect of Transmission Line Length

In order to evaluate the performance of FNNs for faults on different transmission line lengths, the same test cases as shown in table 7.11 were used to examine the accuracy of the results. Table 7.19 illustrates the results attained on the accuracy for different line lengths; here again, aforementioned case, there is a vast improvement in accuracy.

Fault Location	% Maximum Fault Location Error		
Technique	Line length (km)		
	80	100	150
ANN	1.65	2.01	2.5
FNN	0.90	1.01	1.10

Table 7.19 Test results for a-phase-earth fault on different transmission line length.

7.4   Summary

The performance evaluation of the two AI-based fault location techniques is discussed. Through a series of tests and modifications, it is shown that a single ANN can very accurately classify the type of fault on the EHV transmission lines under all practically encountered system and fault conditions. In order to illustrate the effectiveness of the ANN fault location technique, each ANN was tested with a separate set of unseen data and their performance on the accuracy of the results are presented.

The results presented herein, clearly show that an FNN gives a high accuracy in fault location under a whole variety of different system and fault conditions, and further improves on the accuracy attainable from fault location techniques based solely on ANN architectures.

CHAPTER 8

Conclusions And Future Work

8.1 Introduction

This thesis presents a novel fault locator for EHV transmission systems based on artificial intelligence techniques, and shows a vastly improved performance over conventional techniques. The technique addresses some of the common problems in fault location and can be applied to a whole variety of practically encountered system and fault conditions, without sacrificing the high accuracy requirements.

8.2 Previous work

A number of special algorithms have been proposed in the literature to the problem of transmission lines fault location and these have been developed for two- and three-terminal transmission lines. These have been divided into algorithms which use data from one end of the line only and those that employ data from the two ends. There are, however, many disadvantages to these algorithms: fault resistance is not taken into account, there is a need to synchronise register devices located at both ends of the line (in the case of two- or three-ended measurements), the effect of line capacitance is disregarded, pre-fault loading condition is considered totally balanced, etc.

8.3   Artificial Neural Networks

Application of ANNs to power system problems is an interesting subject which has attracted many researchers. Due to highly nonlinear nature of power system problems, different types of solution may be required. In this respect, ANNs have shown the potential to deal with non-linearity because of the parallelism. In the case of fault location, ANNs provide an encouraging prospect to accurate fault location problem on EHV transmission systems. Amongst various forms of ANNs, the multi-layer network is the most promising, in particular, its integration with fuzzy logic is a new and interesting concept for solving many complex power system problems.

8.4   Fuzzy logic and ANN

Fuzzy logic and ANNs work together, ANN classify and learn rules for fuzzy logic and fuzzy logic infers from unclear ANN parameters. Incorporating fuzzy principles into ANN gives more user flexibility and a more robust system. Fuzziness in this case means more flexibility in the definition of the system; boundaries can be described more generally, not crisply; inputs can be described more vaguely, yet better control can be achieved.

8.5   Fault Location Techniques

Two fault location techniques are discussed in this thesis, that are very effective in overcoming the disadvantages aforementioned and improve the accuracy of the fault location over that attained with traditional techniques. The method is based on utilising voltage and current waveforms at the fault locator end of the line only and the signals employed are based on phase values. The first technique is based solely on ANNs and consists of two parts: (i) employment of an ANN for fault type classification and (ii) utilisation of separate ANNs (one for each type of fault) to accurately locate the actual fault position associated with all the commonly encountered types of fault on EHV transmission lines. In order to further improve the

accuracy in fault location, an integration of fuzzy logic and ANN is adopted in the second technique.

The techniques, although based on CAD, nonetheless take into account the practical limitations associated with voltage / current transducers and hardware so that the performance attained is close to that which would be expected from a hardware model under service conditions.

8.6   Performance

- The choice of feature extraction scheme is critical to the time taken for the neural network to train, and more importantly to the results emanating from the actual testing. In this respect, although there are many methods available for extracting the features, an extensive series of studies have shown that the one based on frequency domain decomposition is best suited for the application discussed herein and this is one adopted here. Moreover, series of tests have revealed that the four frequency components namely DC components, fundamental components, components over 100-350 Hz range and components over 400-1000 Hz range, are the most significant in that they are representative of the vast majority of different system and fault conditions and then are the ones employed as input features into the ANNs; this feature extraction methodology is near optimal in both correctly classifying the type of fault and in defining the fault position on EHV transmission systems with a high degree of accuracy.

- The overall performance of the ANN for fault type classification under a vast majority of different system and fault conditions, has indicated a confidence index of about 99.66% with no single error decision. This clearly shows that the ANN is very effective in classifying all types of fault on EHV transmission systems.

■   It has been observed that for the majority of cases studied, the maximum fault location error attained via the first technique ie., the one based solely on ANN architecture, is less than 2%. It is also evident from the results that the best accuracies are always found for single-phase-earth fault (most commonly encountered) when compared to other types of fault.

■   It is clearly shown that the technique retains its high degree of accuracy under differing source capacities at both end of the line. This demonstrates the flexibility of the proposed algorithm which is a major achievement over the conventional techniques, particularly in view of the fact that source capacities can vary at random depending upon the local requirements.

■   It is also shown that the fault locator gives an inherently accurate evaluation of fault position that is not significantly influenced by changes in fault resistance and fault inception angle. The former is a very significant advantage over conventional techniques, particularly those based on impedance to fault measurements, which tend to produce excessive errors when dealing with resistive faults.

■   For the fault locator described, an external fault always produces an estimation which is consistently very much higher than that expected for an internal fault. This very important feature of the algorithm makes it totally immune to any mal-operation for external faults.

■   The technique has been tested for a typical vertical double-circuit and a horizontal single circuit configurations encountered in practice. It is found that the technique has the ability to retain a high degree of accuracy for the other configurations under different fault conditions and this in term verifies the robustness of the fault locator algorithm developed.

■   The technique also gives an acceptable degree of accuracy for transmission

lines with different line lengths.

8.6.1 Improvement on the Accuracy

The second part of the tests are concerned with presenting the performance evaluation of the FNN fault location technique. This is a novel fault locator for EHV transmission systems, based on an integrated approach, and shows a vastly improved performance over conventional techniques, this technique, comprising fuzzy logic and ANNs, gives an accuracy of <1% under a vast majority of different system and fault conditions encountered in practice and is a considerable improvement over other artificial intelligence techniques in particular the one based solely on ANN architectures as discussed previously; this is a major advantage in practice since it would expedite the exact location of a fault by significantly reducing the span of a line length that would have to be scrutinised.

8.7 Future Work

8.7.1 Testing the Proposed Algorithm with Data from a Real System

As emphasised in the thesis, an extensive series of tests have been conducted to ascertain the accuracy of the proposed AI-based techniques under different system and fault conditions, using the EMTP software and a data pre-processing stage; every effort has been made to develop the techniques using extensive training and test data covering the vast majority of different system and fault conditions. As a next logical step, the algorithm should be tested with real input data captured from practical systems. This is important in view of the fact that although the technique takes into account the practical limitations associated with voltage / current transducers and hardware errors such as anti-aliasing filters and quantisation and it is expected that it should retain the high degree of accuracy in fault location, in practice there is always a level of spurious noise present on the measured signals and this can have some bering on the performance achievable in practice.

8.7.2 Suggestion for Implementation of the Technique in a Real System

As emphasised earlier, the proposed technique is based on an off-line application and makes use of information from one-end only for the fault distance estimation and consequently a communication link is not necessary. In this respect, the data can be captured from a digital fault recorder which can be subsequently processed in the fault location algorithms (described in this thesis) on a standard PC in an off-line mode.

8.7.3 Application of the Technique to Three-Terminal Lines

Three-terminal lines (teed feeders), although attractive both from environmental and economical points of view, pose additional problems caused by the intermediate infeed from the third terminal and therefore require special attention. In this respect, accuracy requirements in fault locator is very important. The proposed AI-based fault location technique can be relatively easily extended for accurate fault location on EHV teed feeders.

8.7.4 Application of the Technique to Series-Compensated Lines

Requirement exists for a reliable fault locator to be used for accurate fault location on series-compensated transmission lines. Series capacitor compensation in long distance EHV transmission lines is a widely accepted method to compensate inductive reactance voltage drop, increase steady state and transient stability margin etc. There are, however, difficult problems encountered in locating faults on such lines, and these arise primarily due to the varying amount of capacitance in the circuit, which can cause mal-operation of distance relays and fault locators may not be able to accurately determine the fault position. Due to the entirely different principles used in the proposed fault location technique, there is a strong possibility of overcoming such problems using the aforementioned AI concepts. Such applications should therefore be investigated.

8.7.5 Application of the Technique to Power Distribution Systems

The need to locate permanent and transient faults in distribution systems have been essential for power companies to provide continuance service without any major outages. In such systems, although the level of transients during a fault is very low, the presence of local taps and remote infeed can adversely affect the performance of fault location technique. Application of ANNs and fuzzy logic to accurate fault location on distribution systems provides an attractive alternative and this aspect of the research should be investigated.

8.7.6 Alternative Training Methods: Genetic-Based ANN

Although error-back-propagation is the most widely used method to train multilayer perceptrons, it is not necessarily the best approach. Back-propagation is attractive because it can be performed within the ANN structure. However, the technique has a number of limitations. For example, since the error-back-propagation technique is not designed to be adaptive, all data must be used every time the weights are updated. If a set of old data becomes irrelevant, the ANN is retrained by using the entire new data set. Also, when new data is in conflict with old data, the effect of old data cannot be removed unless the ANN is retrained without the old data. The importance of some data cannot be easily weighted. In addition, if the size of the ANN is not adequately selected, or the convergence criterion is not realistic, thousands of iterations may be required to train a layered perceptron and in some cases, the required convergence error may never be achieved due to the ANN getting into a local minima. An alternative to the error-back-propagation is genetic algorithm (GA) which is an evolutionary algorithm based on the concept of natural selection and genetics. As an attractive alternative the application of GA (which relies on a convergence error based on a global minima) to improve the speed and performance of the ANNs in proposed AI-based techniques should be investigated.

Bibliography

[1]   Jones, D., "Analysis and Protection of Electrical Power System", Pitman Publishing, 1971.

[2]   Saha, M. M. and Erikson, L., "Microcomputer Based Accurate Fault Locator with Remote-End Feed Compensation", IEE Conference Publication, No. 249, pp. 193-198, April 1985.

[3]   Moharari, N. S. and Debs, A. S., "A Rule-Based Artificial Neural Networks Approach for Electric Load Forecasting", Proceeding of the 1993 North American Power Symposium, pp. 145-150, 1993.

[4]   Ebron, s., Lubkeman, D. L. and White, M., "A Neural Network Approach to the Detection of Incipient Faults on Power Distribution Feeders", IEEE Trans., Vol. 5, No. 2, pp. 905-914, 1990.

[5]   Aggarawal, R. K., Johns, A. T., Song, Y. H., Dunn, D. S., and Fitton, D. S., "Neural Network Based Adaptive Single-Pole Autoreclosure Technique for EHV Transmission Systems", IEE Proc.-Gener. Transm. Distrib., Vol. 141, No. 2, March 1994.

[6]   Aggarawal, R. K., Song, Y. H. and Johns, A. T., "Adaptive Three-phase Autoreclosure for Double-circuit Transmission Systems Using Neural Networks", IEE 2nd International Conference on Advances in Power System Control, Operation and Management, Hong Kong, December 1993.

[7]   Kezunovic, M., Rikalo, I. and Sobajic, D. J., "Neural Network Application to Real-Time and Off-Line Fault Analysis",

[8]   Kandil, N. , Sood, V.K. , Khorasani, K. and Patel, R.V. , "Fault Identification

in AC-DC Transmission System Using Neural Networks", IEEE Transaction on Power System, Vol. 7. No. 2, May 1992.

[9]   Friedrich, T., Dalstein, T. and Kulicke, B., "A Neural Time Zone Classifier for High Speed Protective Relaying", 29th University Power Engineering Conference, University College Galway Ireland, September 1994.

[10]   Sant, M.T. and Paithankar, Y.G., "On Line Digital Fault Locator For Overhead Transmission lines", IEE Proc., 127, No. 11, pp. 1181-1185, November 1979.

[11]   Takagi, T., Yamakoshi, Y., Yamaura, M. Kondow, R. and Matsushima, T., "Development of a New Type Fault Locator Using The One-Terminal Voltage and Current Data", IEEE Trans., PAS-101, No 8, pp. 2892-2898, August 1982.

[12]   Schweitzer, O., "Evaluation and Development of Transmission Line Fault Locating Techniques Which Use Sinusoidal Steady-State Information", Ninth Annual Western Protective Relay Conference, Spokane Washington, USA, 1982.

[13]   Takagi, T., Yamakoshi, Y., Yamaura, M. Kondow, R. and Matsushima, T., "A New Algorithm of an Accurate Fault Location for EHV/UHV Transmission lines: Part I-Fourier Transform Method", IEEE Trans., PAS-100, No 3, pp. 1316-1323, March 1981.

[14]   Takagi, T., Yamakoshi, Y., Yamaura, M. Kondow, R. and Matsushima, T., "A New Algorithm of an Accurate Fault Location for EHV/UHV Transmission lines: Part II-Laplace Transform Method", IEEE Trans., PAS-101, No 3, pp. 564-573, March 1982.

[15]   Wiszniewski, A., "Accurate Fault Impedance Locating Algorithm", IEE Proc., 130, Part C, No. 6, pp. 311-314, 1983.

[16]   Erikson, L., Saha, M.M. and Rockefeller, G.D., "An Fault Locator with Compensation for Apparent Reactance in the Fault Resulting from Remote-End Infeed", IEEE Trans., PAS-104, No. 2, pp. 359-368, February 1985.

[17]   Cook, V., "Fundamental Aspects of Fault Location Algorithms Used in Distance Protection", IEE Proc., 133, Part C, No. 6, pp. 359-368, September

1986.

[18]   Richards, G.G. and Tan, O.T. "An Accurate Fault Location Estimator for Transmission Lines", IEEE Trans., PAS-101, No. 4, pp. 945-950, April 1982.

[19]   Schweitzer, C. and Jachinowski, J.K. "A Prototype Microprocessor-Based System for Transmission Line Protection and Monitoring", Eight Annual Western Protective Relay Conference, 1981, Spokane, Washington, USA.

[20]   Johns, A.T. and Jamali, S., "Accurate Fault Location Technique for Power Transmission Lines", IEE Proc. Vol 137, Part C, No. 6, pp. 395-402, September 1990.

[21]   Sachdev, M.S. and Agarwal, R., "Accurate Fault Location Estimates from Digital Impedance Relay Measurements", IEE Conf. Publications 249, pp 180-184, 1985.

[22]   Sachdev, M.S. and Agarwal, R., "A Technique for Estimating Transmission line Fault Location from Digital Impedance Relay Measurement", IEEE Trans. on Power Delivery, Vol. 3, No. 1, pp 121-129, January 1988.

[23]   Girgis, A.A., Hart, D.G. and Peterson, W.L., "A new Fault Location Technique for Two- and Tree-terminal Lines", IEEE Trans. PWRD Vol. 7, No. 1, pp. 98-107, 1992.

[24]   Kezunovic, M., Mrkic, J. and Perunicic, B., "An Accurate Fault Location Algorithm Using Synchronized Sampling", EPSR, Vol. 29, No. 3, pp. 161-169, 1994.

[25]   Zamora, I., Minambres, J.F., Mazon, A.J., Alvarez-Isasi, R. and Lazaro, J., "Fault Location on Two-Terminal Transmission Lines Based on Voltages", IEE Proc. -Gener. Transm. Distrib., Vol. 143, No. 1, pp. 1-6, 1996.

[26]   Aggarawal, R. K., Coury, D. V., Johns, A. T., Kalam, A., "A Practical Approach to Accurate Fault Location on Extra High Voltage Teed feeders", IEEE Transaction on Power Delivery, Vol. 8, No. 3, July 1993.

[27]   Girgis, A.A., Johns, M.B., "A Hybrid Expert System for Faulted Section Identification, Fault Type Classification and Selection of Fault Location Algorithm", IEEE Trans. PWRD Vol. 4, No. 2, pp. 978-985, 1989.

[28]   Kanoh, H., Kaneta, M., and Kanemaru, K., "Fault Location for Transmission

Lines Using Inference Model Neural Network", IEE (Japan), Vol. 111, No. 7, 1991.

[29]   Kandil, N. , Sood, V.K. , Khorasani, K. and Patel, R.V. , "Fault Identification in AC-DC Transmission System Using Neural Networks", IEEE Transaction on Power System, Vol. 7, No. 2, May 1992.

[30]   Tylor, T., Tapp, J., Wall, J. and Lubkeman, D., "Applications of Knowledge-Based Systems to Power Engineering", Proce. of the 18th SSST, pp. 2-6, March 1986.

[31]   Rahman, S. and Bhatnagar, R., "An Expert System Based Algorithm for Short Term Load Forecasting", IEEE/PES 1987 Winter Meeting, New Orleans, Louisiana, February 1987.

[32]   Holland, J.H., "Adaptation in Natural and Artificial System", University of Michigan Press, Ann Arbor, 1975.

[33]   Hertz, J. , Krogh, A. and Palmer, R.G. , "Introduction to the Theory of Neural Computing", Addison Wesley, Reading, Ma, 1991.

[34]   Pao, Y.H. , "Adaptive Pattern Recognition and Neural Networks", Addison Wesley, Reading, Ma, 1989.

[35]   Kohonen, T., "Sels Organisation and Association Memory", Springer-Vaerlag, 1988.

[36]   Sobajic, D. and Pao, Y.H., "Artificial Neural-Net Based Dynamic Security Assessment for Electric Power Systems", IEEE Trans. on Power Systems, Vol. 4, No. 1, pp. 220-228, 1989.

[37]   Wong, K.P., Ta, N.P. and Attikiouzel, Y., "Transient Stability Assessment for Single-Machine Power Systems Using Neural Networks", IEEE TENCON'90 Proc., Hong Kong, pp. 32-36, 1990.

[38]   Wong, K.P., and Lau, B.S., "Fault Distance Estimation in Transient Stability Assessment: an Artificial Neural Network Approach", Proc. of Fourth Sym. on Expert Systems Application to Power Systems, Melbourne Australia, pp. 1-6, 1989.

[39]   Chen, C.R., and Hsul, Y.Y., "Synchronous Machine Steady-State Stability Analysis Using an Artificial Neural Networks", IEEE PES Summer Power

Meeting, Paper No. 90 SM 430-9 EC, 1990.

[40]   Mori, H., Tamaru, Y. and Tsuzki, S., "An Artificial Neural-Net Technique for Power System Dynamic Stability with the Kohonen Model", IEEE Trans. on Power Systems, Vol. 7, No. 2, pp. 856-864, 1992.

[41]   Park, D.C., El-Sharkawi, M.A. and Marks Π, R.J., "Electric Load Forecasting Using an Artificial Neural Networks", IEEE PES Summer Power Meeting, Paper No. 90 SM 377-2 PWRS, 1990.

[42]   Hsu, Y.Y. and Yang C.C., "Design of Artificial Neural Networks for Sort-Term Load Forecasting. Part I: Self Organising Feature Maps for Day Type Identification ", IEE Proc., Pt. C, Vol. 138, No. 5, pp. 407-413, 1991.

[43]   Hsu, Y.Y. and Yang C.C., "Design of Artificial Neural Networks for Sort-Term Load Forecasting. Part Π: Multilayer Feedforward Networks for Peak Load and Valley Load Forecasting ", IEE Proc., Pt. C, Vol. 138, No. 5, pp. 414-418, 1991.

[44]   Tomas, R.J. and Ku B.Y., "Approximation of Power System Dynamic Load Characteristics by Artificial Neural Networks ", Proc. First Int. Forum on Application of Neural Networks to Power Systems, Seattle, USA, pp. 172-182, 1991.

[45]   Neily, G., Barone, R., Josin, G. and Charney, D., "Joint VAR Controller Implemented in an Artificial Neural Networks Environment", Proc. First Int. Forum on Application of Neural Networks to Power Systems, Seattle, USA, pp. 271-276, 1991.

[46]   Feser, K., Braun, U., Engler, F. and Maier, A., "Application of Neural Networks in Numerical Busbar Protection Systems", Proc. First Int. Forum on Application of Neural Networks to Power Systems, Seattle, USA, pp. 117-121, 1991.

[47]   Khaparde, S., Kale, P.B. and Agarwal S.H., "Application of Artificial Neural Network in Protective Relaying of Transmission Lines", Proc. First Int. Forum on Application of Neural Networks to Power Systems, Seattle, USA, pp. 122-126, 1991.

[48]   Ori, H.,Tanaka, Y., Akimoto, Y. and Izui, Y., "Fault Diagnosis System for

GIS Using an Artificial Neural Networks", Proc. First Int. Forum on Application of Neural Networks to Power Systems, Seattle, USA, pp. 112-116, 1991.

[49] Hartana, R.K. and Richards, G.G., "Harmonic Source Monitoring and Identification Using Neural Networks", IEEE PES Winter Power Meeting, Paper No. 90 WM 283-6 PWRS, 1990.

[50] Mori, H., Uematsu, H., Tsuzuki, S., Kojima, Y. and Suzuki, K., "Identification of Harmonic Loads in Power Systems Using an Artificial Neural Networks", Proc. Second Sym. on Expert Systems Application to Power Systems, Seattle, USA, pp. 371-378, 1989.

[51] Chan, E.H.P., "Application of Neural-Network Computing in Intelligent Alarm Processing", IEEE Proc. PICA, pp. 246-251, 1989.

[52] Fischl, R., Kam, M., Chow, J.C. and Ricciardi S., "Screening Power System Contingencies Using a Back-Propagation Trained Multilayer Perceptron", Proc. ISCAS, Vol. 1, pp. 486-489, 1989.

[53] Mori, H., Kitani, N. and Tsuzuki, "Optimal Power Flow Calculation Using the Hopfield Net", Proc. Third Sym. on Expert Systems Application to Power Systems, Japan, pp. 328-335, 1991.

[54] Sasaki, H., Watanabe, M., Kubokawa, J., Yorino, N. and Yokoyama, R., "A Solution Method of Unit Commitment by Artificial Neural Networks", IEEE PES Summer Power Meeting, Paper No. SM 437-4 PWRS, 1991.

[55] Sasaki, H., Kubokawa, J., Watanaba, M., Yokoyama, R. and Tanabe, R., "A Solution of Generation Expansion Problem by Means of Neural Network", Proc. First Int. Forum on Applications of Neural Networks to Power Systems, Seattle, USA, pp. 219-226, 1991.

[56] Kim, Y.S., Eom, I.K., and Park, J.H., "Economic Power Dispatch for Piecewise Cpst Function Using Hopfield Neural Network", IEE Int. Conf. Proc., No. 348 on Advances in Power System Control, Operation and Management, Hong Kong, pp. 902-906, 1991.

[57] EMTP Group "Alternative Transients Program Rule Book", K.U. LEUVEN EMTP CENTRE, July 1987.

[58]   Johns, A.T. and Aggarwal, R.K. ,"Digital Simulation of Faulted e.h.v. Transmission Lines with Particular Reference to Very-High-Speed Protection", Proc. IEE, Vol. 123, No. 4, April 1976.

[59]   Gonen T. "Modern Power System Analysis", Wiley Interscience, NY, 1988.

[60]   GEC Alsthom, "Protective Relays Application Guide", GEC Alsthom Measurements Limited, pp. 56-61, 1987.

[61]   Lucas, J. R., Mclaren, P. G., et al, "Improved Simulation Model for Current and Voltage Transformers in Relay Studies", IEEE-PWRD, Vol. 100, No. 1, pp. 152-159, 1992.

[62]   Bressloff, P. C. and Weir, D. J., "Neural Networks", GEC Journal of Research, Vol. 8, No. 3, pp. 151-169, 1991.

[63]   Oppenheim, V. Willsky, A.S. and Young, I. T., "Signals and Systems", Prentice-Hall, 1983.

[64]   Lippmann, R. P., "An Introduction to Computing with Neural Nets", IEEE ASSP Magazine, pp. 4-22, April 1987.

[65]   Rumelhart, D.E., McClelland, J.L., "Parallel Distributed Processing. Explorations in the Micro Structure of Cognition. Volume 1: Foundations", MIT Press, Cambridge, Massachusetts 1986.

[66]   Rumelhart, D.E., McClelland, J.L., "Parallel Distributed Processing. Explorations in the Micro Structure of Cognition. Volume 2: Psychological and Biological Models", MIT Press, Cambridge, Massachusetts 1986.

[67]   Zadeh, L. A., "Fuzzy Sets", Information and Control, vol. 8, pp. 338-358, 1965.

[68]   Lee, C. C., "Fuzzy Logic in Control System: Fuzzy Logic Controller-Part I and II", IEEE Transaction on System, Man, and Cybernetics, Vol. 20, No. 2, pp. 404-435, 1990.

[69]   Dash, P. K., Liew, A. C., and Rahman, S. "Fuzzy Neural Network and Fuzzy Expert System for Load Forecasting", IEE Proc. Gener. Transm. Distrib., Vol. 143, No. 1, pp. 106-114, 1996.

[70]   Bakirtzis, A. G., Theocharis, J. B., Kiartzis, S. J., and Satsios, K. J. "Short Term Load Forecasting Using Fuzzy Neural Networks", IEEE Transaction on

Power Systems, Vol. 10, No. 3, pp. 1518-11524, 1995.

[71]   Mori, H., and Kobayashi, H., "A Fuzzy Neural Net for Short-Term Forecasting", Proc. ISAP, pp. 775-782, 1994.

[72]   Chang, H. C., and Wang, M. H. "Neural Network-Based Self-Organizing Fuzzy Controller for Transient Stability of Multimachine Power Systems", IEEE Transaction on Energy Conversion, Vol. 10, No. 2, pp. 339-346, 1995.

[73]   Ichihashi, H., "Learning in Hierarchical Fuzzy Models by Conjugate gradient Method using Backpropagation Errors" , Proc. of Intelligent System Symp., pp. 235-240, 1991.

[74]   DADiSP Version 1.05b, DSP Development Corporation, 1 Kendal Square, Cambridge MA 02139.

[75]   Neural Works Professional II Plus, Scientific Computing Ltd, Victoria Road, Burgess Hill, West Sussex RH15 9LH.

Related Publications

[1]   Joorabian, M., Aggarawal, R. K., "An Accurate Fault Location Technique For Transmission Line using Artificial Neural Network", Third Iranian Conference on Electrical Engineering, Iran University of Science and Technology, ICEE 1995.

[2]   Joorabian, M., Aggarawal, R. K., "An Accurate Fault Location Technique For Transmission Line using Artificial Neural Network", UPEC 1995.

[3]   Joorabian, M., Aggarawal, R. K., "Fuzzy Neural Network Approach to Accurate Fault Location on Transmission Lines", UPEC 1996.

[4]   Joorabian, M., Aggarawal, R. K., "A Fuzzy Neural Network Approach to Accurate Transmission Line Fault Location", Submitted to IEEE Transactions, 1996.

AN ACCURATE FAULT LOCATION TECHNIQUE FOR TRANSMISSION LINE USING ARTIFICIAL NEURAL NETWORK

M. Joorabian   R.K. Aggarawal

MIEE, SMIEEE

School of Electronic and Electrical Engineering, University of Bath, UK

ABSTRACT

The aim of this paper is to present an accurate fault location technique using artificial neural networks(ANNs). The feed-forward multi-layer neural network (NN) with the use of supervised learning and the common training rule of error back-propagation is chosen for this study. The instantaneous three phase voltages and currents derived at the fault locator point on the line which contain fault information at different frequencies are used to train and test the artificial neural network(ANN). In this paper, neural network architecture to distinguish between different types of faults is proposed and neural network topology for accurate fault location under different system conditions is discussed.

KEYWORDS

Neural network, Fault Location, Fault Classification, Transmission Line

Introduction

Electrical power systems are designed to ensure a reliable supply of energy with the highest possible continuity. Electrical faults can occur at any point in an electric power system and the most exposed parts are over head transmission lines. A transmission line is also one of the most difficult parts of the power system to maintain and inspect, simply because of its dimension and the environment it is built in [1].

Fast and accurate location of faults on an electrical power transmission line is vital for economic operation of power systems. This is more so in view of the fact that because of an increase in transmission requirements and environmental pressures, power authorities are being forced to maximize the transmission capabilities of existing transmission lines. This effectively means that in order to maintain system security and stability, there is a demand for minimizing damage by restoring the faulted line to normal as quickly as possible, hence the requirements for the development of an accurate fault locator. The degree of accuracy required is therefore increasing and is much higher than could be obtained using simple conventional techniques. Even a small measurement error may require detailed local examination over several kilometres of a typical line.

Artificial intelligence provides powerful techniques for processing symbolic or declarative knowledge and for automated reasoning. In this respect, the advent of artificial neural networks has provided power engineers with powerful tools which are promising for solving some long standing power system problems. Neural networks possess the ability to perform pattern recognition, prediction and optimisation in a fast and efficient manner. This is by virtue of the fact that they have the ability to map very complex and highly non-linear input/output patterns.

This paper presents the fault location technique, which uses NN for accurately locating all types of faults on transmission line. The results, in this paper, show that the trained NN is able to make correct decision under various system fault conditions.

Neural Networks

Neural networks constitute a new approach to computation based on modern neurophysiology; a simplified model of the human neuron is organized into networks similar to those found in the brain.These networks, having characteristics analogous to human intelligence, are solving problems that have proven difficult or impossible to solve using conventional computation [2]. Recently, researchers focusing their efforts on neural nets have produced impressive results.

The principal components of a neural network consists of a number of neurons which are the elementary processing units that are connected together according to some pattern of connectivity. this model of a neuron is illustrated in Figure 1.

Neuron j is characterized by the number of inputs x1 ....xn, the weights wj1,...,wjn connecting each input to the neuron, its activation function a and its output oj. The

inputs of a particular type are combined together to give a net input netj of the jth unit. Typically, the weighted contributions from all inputs are summed to determine an activation level for that unit:

$$net_j = \sum W_{jk} X_k \qquad (1)$$

The neuron uses this net input, together with information on its current activation state to determine its new state of activation. Therefore neuron j will have activation values of the form:

$$O_j = F(net_j) = F(\sum W_{jk} X_k) \qquad (2)$$

There are several activation functions. The most frequently used ones are the identity, the linear threshold function and the sigmoid function. The neurons are normally connected to each other in a specified fashion to form the neural network. These arrangements of interconnections could form a single layer or several layers. In a large number of neural network models, such as the Perceptron, Linear Association, Multi-layer feed-forward network and the ART model, the output from the units from one layer is only allowed to activate neurones in the next adjacent layer. However, in some models such as Kohonen nets, the signal is allowed to activate neurons in the same layer [3,4].

Lastly, the neural network must have a mechanism for learning. Learning (also called training) is done for a subset of the input vectors, called the training set, whose properties are known or representative. Learning alters the weights associated with the various interconnections and thus leads to a modification in the strength of interconnections.

A neural network is characterized by its architecture, its processing algorithm and its learning algorithm. The architecture specifies the way the neurons are connected. The processing algorithm specifies how the neural network with a given set of weights calculates the output vector o for any input vector x. The learning algorithm specifies how the neural network adapts its weights for all given training vectors x.

Power System Simulation

The simulation of the power system has been done using the well proven Electro-Magnetic Transients Program (EMTP). The overhead transmission line used in this work is based on a single circuit of the typical quad-conductor 400 kV vertical construction line currently used on the UK supergrid system [5]. The earth resistivity is taken to be 100 Ωm and the power system frequency of 50 Hz was used. Figure 2(a) and 2(b), show power system and line configurations. An X:R ratio of 30 and Zs0:Zs1 ratio of 1.0 were used for each source.

Neural Network Based Scheme

Neural networks have the ability to learn the desired inputs/outputs mapping based on training examples, without looking for an exact mathematical model. Once an

appropriate neural network has been trained, the interconnections or links of the NN will contain a representation of the nonlinearity of desired mapping between inputs and outputs. Feature extraction is the first step to any pattern recognition method to effectively reduce the size of the neural network and improve its performance. In order to catch the features in the accurate fault location technique, the instantaneous three phase voltages and currents, which contain fault information of different frequency components, are used to train the NN. Since the fault transients generated on transmission system contain a wide range of frequency components, it is impractical to use the time-domain waveforms as the input to a NN.

The method is based on utilising voltage and current waveforms at the fault locator end of the line. The signals for estimation of fault location are based on phase values. The effect of transducers (CTs and CVTs) and hardware errors such as anti-aliasing filters and quantisation are taken into account, so that the information processed throughout the fault locator algorithm is very close to real-life situation.

Feature Extraction

Transient behaviour of the overhead line has been accurately predicted using EMTP for simulation of the power system. Figure 3(a) and 3(b) show the primary voltage and current waveforms related to typical 400 kV transmission line as seen at the sending-end of the line.

Voltage and current waveforms are sampled at a regular interval and quantised for digital protection proposes [6]. Samples of data often require transformation and manipulation to render the inherent information into a form suitable for the neural network. Feature extraction process typically involves some reduction in the amount of data, which reduces the number of input nodes and thus the size of the neural network required [7]. Transforming the data and reducing the amount of data results in requiring a smaller neural network to perform the desired function, with a resulting reduction in the training and an increased ability to generalise.

Applying Discrete Fourier Transform (DFT) to the current and voltage waveforms, figure 4 (a) and (b) show the spectra of the a-phase voltage and current under an a-phase to ground fault occurring at the middle of the line and a-phase to b-phase fault at the remote end of the line respectively. It is important to note that different fault types occurring at different locations produce different frequency components. This also means that these signals vary with fault type, location and fault inception angle.

Input Data for NN

The inputs of NN are composed of V_a, V_b, V_c, i_a, i_b, i_c. Using spectrum analysis for each cycle at the sampling frequency of 4000 Hz certain frequency bands are used as the potential features. The four parameters for each phase current and voltage are:
1) DC Component ; 2) Fundamental Component
3) Components over 100 +...+350 Hz range
4) Components over 400 +...+1000 Hz range

Therefore the number of neurons in the input layer is reduced to 24 elements by taking four components of frequency bands for each waveform.

Neural Network Topology

As explained before different transient frequency components are caused by different fault type, fault location and fault inception angle. The fault type indicates in which phase there is a fault and whether the fault connects to ground or not, no matter where the fault position is. Hence, this is a rough detection problem. The precis fault location needs to be known after the fault is detected. This belongs to a fine detection problem. Thus, the two issues can not be solved in one neural network, since the NN would not converge. Thus the first step is to find a neural network topology best suited for locating a fault and recognizing the fault type, under all practically encountered different system and fault conditions, is to separate the NNs.

The feed-forward multi-layer neural network with the use of supervised learning and common training rule of error back-propagation is used for this study. Supervised learning requires an external "teacher" that evaluates the behaviour of the system and directs the modifications [8]. The training is accomplished by adjusting the weights. This is done by presenting a set of patterns at the input, each with a desirable output pattern. Weights are then adjusted to minimize the error between the desired and actual output patterns.

Fault Type Classification

The output of the NN are made up of A, B, C, and G which indicate a, b, c phase operation states and connection to ground information respectively. Each of the A, B and C which approaches a value 1 means that phase is faulty. The G which approaches 1 indicates the fault is connected to ground. Table 1 shows fault type identification for output of NN1.

Using a 3-layer feed-forward NN as shown on figure 5 and taking back-propagation Learning Rule, a hidden layer with 14 neurons was selected for NN1.

Analysis of Test Results

Table 2 shows the test results which are used for testing NN1. The left four items indicate the desired outputs, and the right four items indicate the actual outputs. The results show faults under various fault conditions. Although the NN1 is trained under fixed fault points, it can detect faults for every point under various conditions.

A	B	C	G	TYPE OF FAULT
0	0	0	0	no fault
1	0	0	1	a phase to ground fault
0	1	0	1	b phase to ground fault
0	0	1	1	c phase to ground fault
1	1	0	0	a phase to b phase fault
0	1	1	0	b phase to c phase fault
1	0	1	0	a phase to c phase fault
1	1	0	1	a - b phase to ground fault
0	1	1	1	b - c phase to ground fault
1	0	1	1	a - c phase to ground fault
1	1	1	0	three phases fault
1	1	1	1	three phases to ground fault

Table 1. Fault type classification for Neural Network output

Network Architecture for Fault Location

In order to find NN topology for accurate fault location and to have a good generalization, a number of different NN topology were tried. From this experience, Separate NNs are designed to locate all eleven types of faults on transmission lines. They will all be driven from NN1 and the input data was generated the same way as input data for NN1.

The feed-forward multi-layer NN with 24 neurons in the input layer and 1 in the output layer were chosen, where the output shows the location of the fault. To consider complexity of the problem and the amount of the data available, different combinations of the following network training methods were chosen and tested: (1)different number of hidden layers; (2)different hidden neurons in each layer; (3)different transfer functions; (4)different learning set data (sequential or random) in training the networks; (5)different error back-propagation schemes.

Throughout a series of tests and modification separate network were designed for each type of fault. Due to page limitation, only the NN for performing of a-phase to ground fault is shown on figure 6. The network is a four-layer preceptron, with 24 inputs, 1 output, and 18 neurons in the first hidden layer and 6 neurons in the second hidden layer.

The trained network was then tested by a number of test data, which are generated in the same way as training data. Table 3 shows the test results for a-phase to ground fault which are tested by the NN.

Conclusions

This paper presents a novel fault location technique by using artificial neural networks for transmission line, which has better performance than the conventional techniques. The technique shows NNs can solve the problem where the traditional schemes have difficulty.

The paper places emphasis on the feature extraction of NNs and designing of NNs. the test results show the trained NNs can very accurately classify fault type and locate fault position under various system and fault conditions such as different fault types, system source capacity, fault resistance and position of the fault.

References:

[1]   Saha, M.M. and Erikson, L., "Microcomputer Based Accurate Fault Locator with Remote-End Infeed Compensation", IEE Conference Publication, N o . 249, pp. 193-198, April 1985.

[2]   Wasserman, P.D. and T. Schwartz, "Neural Networks, Part 1", IEEE Expert, Vol. 2, No. 4, pp. 10-12, 1987.

[3]   Hertz, J. , Krogh, A. and Palmer, R.G. , "Introduction to the Theory of Neural Computing", Addison Wesley, Reading, Ma, 1991.

[4]   Pao, Y.H. , "Adaptive Pattern Recognition and Neural Networks", Addison Wesley, Reading, Ma, 1989.

[5]   Johns, A.T. , Aggarwal, R.K. ,"Digital Simulation of faulted e.h.v. transmission lines with particular reference to very-high-speed protection", Proc. IEE, Vol. 123, No. 4, April 1976.

[6]   Lewis Blacburn, J. , "IEEE Tutorial Course, Microprocessor Relays and Protection System" , IEEE Publication 88EH0269-1-PWR, 1988.

[7]   Song, Y.H. , Aggarwal, R.K, Johns, A.T. , Dunn, R. , Fitton, D. , "Adaptive autoreclosure Technique for Long-distance Compensated Transmission System Using Neural Network Approach", UPEC 1993.

[8]   Kandil, N. , Sood, V.K. , Khorasani, K. and Patel, R.V. , "Fault Identification in AC-DC Transmission System Using Neural Networks", Transaction on Power System, Vol. 7. No. 2, May 1992.

Figure 2(a) Power System Configuration.
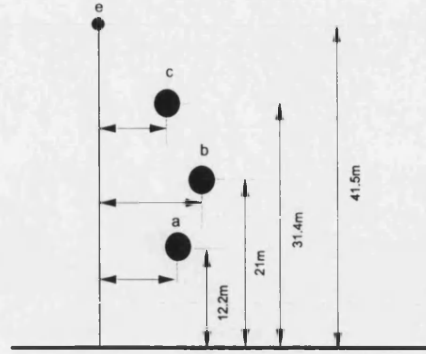
Figure 2(b) Transmission Line Configuration.
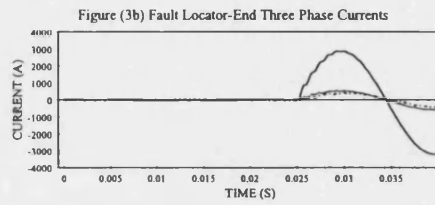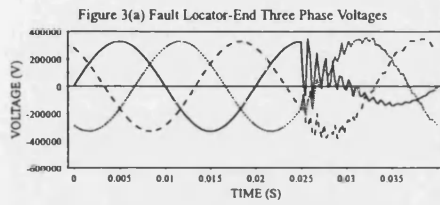
a-phase to ground fault at the middle of the line, S1 = 2.5GVA , S2 = 20GVA
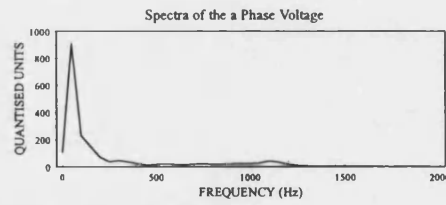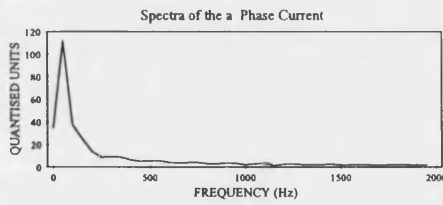
Figure (4a) Spectrum analysis, a-phase to ground fault at the middel of the line.
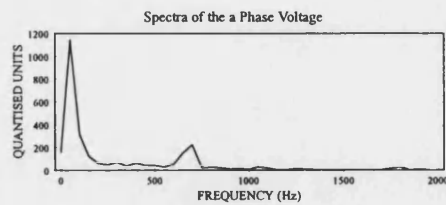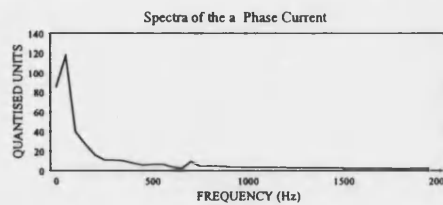
Figure (4b) Spectrum analysis, a-phase to b-phase fault at the end of the line.
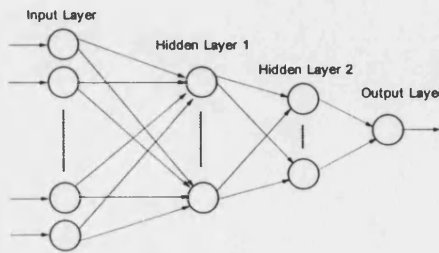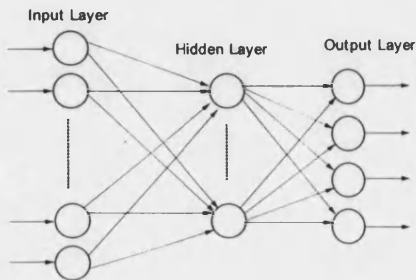
Figure 5, Feed-forward NN for Fault Type classification. Figure 6, Feed-forward NN for Fault Location.

AN ACCURATE FAULT LOCATION TECHNIQUE FOR TRANSMISSION LINE USING ARTIFICIAL NEURAL NETWORK

M. Joorabian, R. K. Aggarawal
MIEE, SMIEEE

School of Electronic and Electrical Engineering, University of Bath, UK

ABSTRACT

The aim of this paper is to present an accurate fault location technique using artificial neural networks(ANNs). The feed-forward multi-layer neural network (NN) with the use of supervised learning and the common training rule of error back-propagation is chosen for this study. The instantaneous three phase voltages and currents derived at the fault locator point on the line which contain fault information at different frequencies are used to train and test the artificial neural network(ANN). In this paper, a neural network architecture to distinguish between different types of faults is proposed and neural network topology for accurate fault location under different system conditions is discussed.

1. INTRODUCTION

Fast and accurate location of faults on an electrical power transmission line is vital for economic operation of power systems. This is more so in view of the fact that because of an increase in transmission requirements and environmental pressures, power authorities are being forced to maximize the transmission capabilities of existing transmission lines. This effectively means that in order to maintain system security and stability, there is a demand for minimizing damage by restoring the faulted line to normal as quickly as possible, hence the requirements for the development of an accurate fault locator. The degree of accuracy required is therefore increasing and is much higher than could be obtained using conventional techniques. Even a small measurement error may require detailed local examination over several kilometres of a typical line.

Artificial intelligence provides powerful techniques for processing symbolic or declarative knowledge and for automated reasoning. In this respect, the advent of artificial neural networks has provided power engineers with powerful tools which are promising for solving some long standing power system problems. In this respect, neural networks possess the ability to perform pattern recognition, prediction and optimisation in a fast and efficient manner. This is by virtue of the fact that they have the ability to map very complex and highly non-linear input/output patterns.

With the recent advances in learning techniques of artificial neural networks(ANNs), ANNs are being applied to many areas of power systems. ANNs show a high potential as an alternative to algorithmic and expert system methods. ANNs have been used to preform electric load forecasting[1], detection of faults on power distribution feeders[2], autoreclosure for EHV transmission systems, real-time and off-line fault analysis, fault identification in an AC-DC transmission system and high speed protective relaying.

This paper presents a fault location technique, which uses NN for accurately locating faults on transmission line under all types of faults encountered in practice. The results, in this paper, show that the trained NN is able to make correct decision under various system fault conditions.

1.1 Neural Networks Terminology

Neural networks constitute a new approach to computation based on modern neurophysiology; a simplified model of the human neuron is organized into networks similar to those found in the brain. These networks, having characteristics analogous to human intelligence, are solving problems that have proven difficult or impossible to solve using conventional computation [3]. Recently, researchers focusing their efforts on neural nets have produced impressive results.

The ANNs considered in this paper consist of a large number of simple processing elements called nodes. Signals are passed between nodes along weighted connections, where the weights are the network's adjustable parameters. The arrangement of the network's nodes and connections defines its architecture and there are many possible variations. One popular arrangement is shown in Figure 1, where the nodes are arranged into layers and each node in one layer has connections only within the preceding layers.
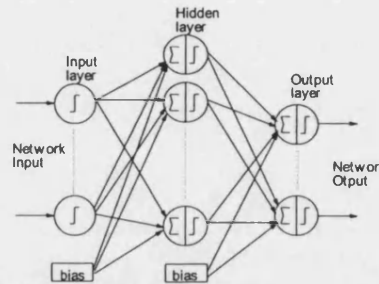
Figure 1: A feed-forward multi-layer network.

The network input is presented to the first layer and this information is propagated feed-forwards through the network such that the output signal of each node never forms part of its input signal. After the input has been propagated through the network, the signals at the output layer provide the network output.

2. POWER SYSTEM SIMULATION

The simulation of the power system has been carried out using the well proven Electro-Magnetic Transients Program (EMTP). The overhead transmission line used in this work is based on a single circuit of the typical quad-conductor 400 kV vertical construction line currently used on the UK supergrid system [4]. The earth resistivity is taken to be 100 Ωm and the power system frequency of 50 Hz was used. Figure 2(a) and 2(b), show power system and line configurations. An X:R ratio of 30 and Zs0:Zs1 ratio of 1.0 were used for each source.
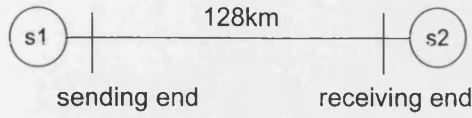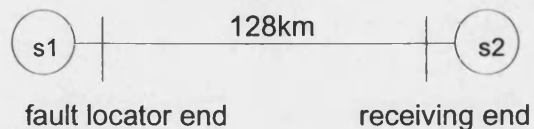

Figure 2(a): Power system configuration.
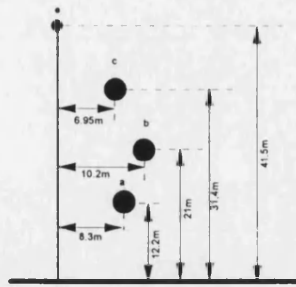
Figure 2(b): Transmission line configuration.

3. NEURAL NETWORK BASED SCHEME

Neural networks have the ability to learn the desired inputs/outputs mapping based on training examples, without looking for an exact mathematical model. Once an appropriate neural network has been trained, the interconnections or links of the NN will contain a representation of the non-linearity of desired mapping between inputs and outputs. Feature extraction is the first step to any pattern recognition method to effectively reduce the size of the neural network and improve its performance. In order to catch the features in the accurate fault location technique, the instantaneous three phase voltages and currents, which contain fault information at different frequencies, are used to train the NN. Since the fault transients generated on transmission system contain a wide range of frequency components, it is impractical to use the time-domain waveforms as the input to a NN.

The method is based on utilising voltage and current waveforms at the fault locator end of the line. The signals for estimation of fault location are based on phase values. The effect of transducers (CTs and CVTs) and hardware errors such as anti-aliasing filters and quantisation are taken into account, so that the information processed throughout the fault locator algorithm is very close to real-life situation.

4. FEATURE EXTRACTION

Transient behaviour of the overhead line has been accurately predicted using EMTP for simulation of the power system. Figure 3(a) and 3(b) show the primary voltage and current waveforms related to typical 400 kV transmission line as seen at the sending-end of the line.
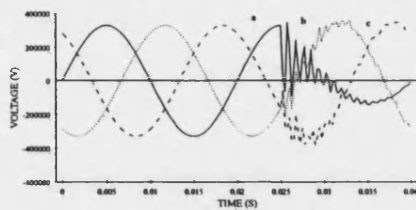
Figure 3(a): Fault locator-end three phase voltages.
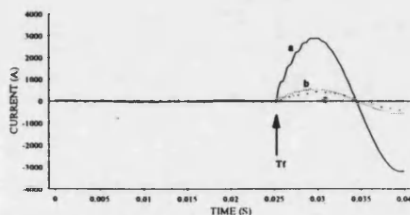
Figure 3(b): fault locator-end three phase currents.

Voltage and current waveforms are sampled at a regular interval and quantised for digital protection proposes [5]. Samples of data often require transformation and manipulation to render the inherent information into a form suitable for the neural network. Feature extraction process typically involves some reduction in the amount of data, which reduces the number of input nodes and thus the size of the neural network required [6]. Transforming the data and reducing the amount of data results in requiring a smaller neural network to perform the desired function, with a resulting reduction in the training and an increased ability to generalise.

Applying Discrete Fourier Transform (DFT) to the current and voltage waveforms, figure 4 (a) and (b) show the spectra of the 'a'-phase voltage and current under an 'a'-phase to ground fault occurring at the middle of the line and 'a'-phase to 'b'-phase fault at the remote end of the line respectively. It is important to note that different fault types occurring at different locations produce different frequency components. This also means that these signals vary with fault type, location and fault inception angle.

Figure 4(a): Spectrum analysis; a phase to ground fault at the middle of the line.
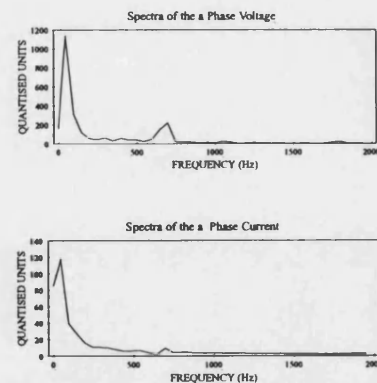
Figure 4(b): Spectrum analysis; a phase to b phase fault at the end of the line.

5. INPUT DATA FOR NN

The inputs of NN are composed of V_a, V_b, V_c, i_a, i_b, i_c. Using spectrum analysis for each cycle at the sampling frequency of 4000 Hz, certain frequency bands are used as the potential features. The four parameters for each phase current and voltage are:

1) DC Component.
2) Fundamental Component.
3) Components over 100 +...+350 Hz range.
4) Components over 400 +...+1000 Hz range.

Therefore the number of neurons in the input layer is reduced to 24 elements by taking four components of frequency bands for each waveform.

6. NEURAL NETWORK TOPOLOGY

As explained before, different transient frequency components are generated by different fault types, fault location and fault inception angle. The fault type indicates in which phase there is a fault and whether the fault connects to ground or not, no matter where the fault position is. Hence, this is a rough detection problem. The precise fault location needs to be known after the fault type has been detected. This entails a fine detection problem. Thus, the two issues can not be solved in one neural network, since the NN would not converge. Thus the first step is to find a neural network topology best suited for locating a fault and recognizing the fault type, under all practically encountered different system and fault conditions, is.

The feed-forward multi-layer neural network with the use of supervised learning and common training rule of error back-propagation is used for this study. Supervised learning requires an external "teacher" that evaluates the behaviour of the system and directs the modifications [7]. The training is accomplished by adjusting the weights. This is done by presenting a set of patterns at the input, each with a desirable output pattern. Weights are then adjusted to minimize the error between the desired and actual output patterns.

8. FAULT TYPE CLASSIFICATION

The outputs of the NN are made up of A, B, C, and G which indicate a, b, c phase operation states and connection to ground information respectively. Each of the A, B and C which approaches a value 1 means that phase is faulty. The G which approaches 1 indicates the fault is connected to ground.

| Example:	A	B	C	G	
	0	0	0	0	...................no fault
	1	0	0	1	.... a phase fault
	1	1	0	0	.... a-b phase fault
	1	1	1	1	.... 3-phase fault

A 3-layer feed-forward NN with back-propagation Learning Rule and 14 neurons in the hidden layer was selected for fault type classification.

8.1 Analysis of Test Results

Table 1 shows the test results which are used for testing NN1. The left four items indicate the desired outputs, and the right four items indicate the actual outputs. The results show faults under various fault conditions. Although the NN1 is trained under fixed fault points, it can detect faults for every point under various conditions.

9. NETWORK ARCHITECTURE FOR FAULT LOCATION

In order to find NN topology for accurate fault location and to have a good generalization, a number of different NN topologies were tried. From this experience, Separate NNs are designed to locate all eleven types of faults on transmission lines. They are all driven from NN1 and the input data is generated the same way as input data for NN1.

The feed-forward multi-layer NN with 24 neurons in the input layer and 1 in the output layer was chosen, where the output shows the location of the fault. Bearing in mind the complexity of the problem and the amount of the data available, different combinations of the following network training methods were chosen and tested:

(1)different number of hidden layers; (2)different hidden neurons in each layer; (3)different transfer functions; (4)different learning set data (sequential or random) in training the networks; (5)different error back-propagation schemes.

Throughout a series of tests and modifications, a separate network were designed for each type of fault. Due to page limitation, only the NN concerned with an 'a'-phase to ground fault is considered. The network is a four-layer perceptron, with 24 inputs, 1 output, and 18 neurons in the first hidden layer and 6 neurons in the second hidden layer.

The trained network was then tested by a number of test data, which are generated in the same way as training data. Table 2 shows the test results for an 'a'-phase to ground fault which are tested by the NN. It is clearly evident that the NN gives a very high accuracy in fault location for this type of fault. Although not shown here, this is also the case for other types of faults.

10. CONCLUSIONS

This paper presents a novel fault location technique by using artificial neural networks for transmission line, which has a vastly improved performance in terms of accuracy compared with the conventional techniques. The technique shows NNs can solve the problem where the traditional schemes have difficulty.

The paper places emphasis on the feature extraction of NNs and designing of NNs. The test results show the trained NNs can very accurately classify fault type and locate fault position under various system and fault conditions such as different fault types, system source capacity, fault resistance and position of the fault.

References:

[1] Moharari, N. S. and Debs, A. S., "A Rule-Based Artificial Neural Networks Approach for Electric Load Forecasting", Proceeding of the 1993 North American Power Symposium, pp. 145-150, 1993.

[2] Ebron, s., Lubkeman, D. L. and White, M., "A Neural Network Approach to the Detection of Incipient Faults on Power Distribution Feeders", IEEE Trans., Vol. 5, No. 2, pp. 905-914, 1990.

[3] Wasserman, P.D. and T. Schwartz, "Neural Networks, Part 1", IEEE Expert, Vol. 2, No. 4, pp. 10-12, 1987.

[4] Johns, A.T. , Aggarwal, R.K. ,"Digital Simulation of faulted e.h.v. transmission lines with particular reference to very-high-speed protection", Proc. IEE, Vol. 123, No. 4, April 1976.

[5] Lewis Blacburn, J. , "IEEE Tutorial Course, Microprocessor Relays and Protection System" , IEEE Publication 88EH0269-1-PWR, 1988.

[6] Song, Y.H. , Aggarwal, R.K, Johns, A.T. , Dunn, R. , Fitton, D. , "Adaptive autoreclosure Technique for Long-distance Compensated Transmission System Using Neural Network Approach" , UPEC 1993.

[7] Kandil, N. , Sood, V.K. , Khorasani, K. and Patel, R.V. , "Fault Identification in AC-DC Transmission System Using Neural Networks", Transaction on Power System, Vol. 7. No. 2, May 1992.

Table 1. Test Cases for Fault Type Classification

	Desired Output A	B	C	G	Actual Output A	B	C	G
case1	source capacity at S1 = 2.5GVA , S2 = 20GVA , Rf = 1Ω							
	1.000000	0.000000	0.000000	1.000000	1.011094	-0.005564	0.002189	0.997017
	1.000000	0.000000	0.000000	1.000000	1.009681	-0.003867	0.009098	0.992361
	1.000000	0.000000	0.000000	1.000000	1.002198	-0.008918	0.056867	0.980379
	1.000000	0.000000	0.000000	1.000000	1.032604	-0.025302	0.012839	0.991368
case2	source capacity at S1 = 2.5GVA , S2 = 20GVA , Rf = 25Ω							
	1.000000	0.000000	0.000000	1.000000	1.004467	-0.013390	-0.008907	1.065959
	1.000000	0.000000	0.000000	1.000000	0.878603	-0.013466	0.001625	0.958465
	1.000000	0.000000	0.000000	1.000000	1.020388	-0.012546	0.017788	0.994778
case3	source capacity at S1 = 2.5GVA , S2 = 20GVA , Rf = 50Ω							
	1.000000	0.000000	0.000000	1.000000	1.006127	-0.000088	-0.004785	0.999904
	1.000000	0.000000	0.000000	1.000000	0.998842	-0.000370	0.027632	0.997932
	1.000000	0.000000	0.000000	1.000000	1.008211	-0.000587	-0.005221	1.001869
case4	source capacity at S1 = 2.5GVA , S2 = 20GVA , Rf = 75Ω							
	1.000000	0.000000	0.000000	1.000000	0.998658	0.001370	-0.004710	1.003653
	1.000000	0.000000	0.000000	1.000000	0.992289	0.008573	0.020636	1.008668
	1.000000	0.000000	0.000000	1.000000	1.003691	0.001675	-0.005093	1.004690
case5	source capacity at S1 = 2.5GVA , S2 = 20GVA , Rf = 100Ω							
	1.000000	0.000000	0.000000	1.000000	0.976371	0.004585	-0.004212	1.005741
	1.000000	0.000000	0.000000	1.000000	0.976109	0.016361	0.016260	1.018738
	1.000000	0.000000	0.000000	1.000000	0.995934	0.004722	-0.005080	1.009168
	1.000000	0.000000	0.000000	1.000000	0.933369	0.006688	-0.003461	0.994014
	1.000000	0.000000	0.000000	1.000000	0.946971	0.021203	0.013316	1.021569
case6	source capacity at S1 = 2.5GVA , S2 = 20GVA , Rf = 1Ω							
	1.000000	1.000000	0.000000	0.000000	1.017133	1.010564	-0.071688	0.154254
	1.000000	1.000000	0.000000	0.000000	1.034088	1.004155	-0.082066	0.092595
	1.000000	1.000000	0.000000	0.000000	1.007674	0.998853	0.005622	-0.000511
	1.000000	1.000000	0.000000	0.000000	0.924853	1.021994	0.180527	0.155483
	1.000000	1.000000	0.000000	0.000000	0.956661	1.017044	0.150242	0.034190
case7	source capacity at S1 = 2.5GVA , S2 = 20GVA , Rf = 1Ω							
	1.000000	1.000000	1.000000	1.000000	1.020454	1.016629	1.007422	0.968767
	1.000000	1.000000	1.000000	1.000000	1.030693	1.022364	0.982367	0.944676
	1.000000	1.000000	1.000000	1.000000	1.037847	1.036369	1.000222	1.116488

Table 2. Test cases for fault location, a-phase to ground fault

	Desired Output (Km)	Actual Output (Km)
case 1	source capacity at S1=2.5GVA, at S2=20GVA, Rf = 1Ω	
	62.0000	63.0745
	120.0000	119.8063
	8.0000	7.6481
case 2	source capacity at S1=20GVA, at S2=2.5GVA, Rf = 1Ω	
	1.0000	0.8007
	128.0000	127.3414
case 3	source capacity at S1=2.5GVA, at S2=20GVA, Rf = 25Ω	
	60.0000	59.9401
	120.0000	120.2625
case 4	source capacity at S1=2.5GVA, at S2=20GVA, Rf = 50Ω	
	18.0000	20.0167
	60.0000	59.6146
	120.0000	120.8432
case 5	source capacity at S1=2.5GVA, at S2=20GVA, Rf = 75Ω	
	18.0000	20.0354
	60.0000	58.7553
	120.0000	119.9437
case 6	source capacity at S1=2.5GVA, at S2=20GVA, Rf = 100Ω	
	60.0000	58.5333
	120.0000	118.3701

FUZZY NEURAL NETWORK APPROACH TO ACCURATE FAULT LOCATION ON TRANSMISSION LINES

M. Joorabian, R. K. Aggarawal
MIEE, SMIEEE

School of Electronic and Electrical Engineering, University of Bath, UK

ABSTRACT
A new technique for accurate fault location on transmission lines is discussed. The technique is based on a hybrid intelligent model that integrates artificial neural networks (ANN) and fuzzy logic system (FLS). The frequency components of the instantaneous three phase voltages and currents derived at the fault locator-end of the line are used to train an ANN to classify the fault type, and a separate FNN is used to accurately locate all types of fault on transmission lines.

1. INTRODUCTION
Accurate location of transmission line faults has been a subject of interest for several years. The major reason for this activity is that an accurate location of fault can reduce the time required for restoring service to customers. A very high degree of accuracy is thus required that cannot be obtained using conventional techniques; this is principally so because of the wide variations in both system and fault conditions that occur in practice and these in turn can have a significant influence on the degree of accuracy achievable with conventional fault location techniques.

Artificial neural network (ANN)-based techniques have the advantage over conventional techniques in significantly improving the accuracy. This is so by virtue of the fact that ANNs have the capability of non-linear mapping, parallel processing and learning; these attributes make them ideally suited for providing a high accuracy in fault location under a wide variety of different systems and fault conditions. However, These are still a number of contingencies under which an ANN-based fault location technique's performance can be adversely affected. This paper thus proposes the use of fuzzy logic to further improve the accuracy of an ANN-based fault location technique.

The fuzzy logic is characterized as an extension of binary Boolean Logic. It is a class in which the transition from membership to non-membership is gradual rather than abrupt. Both the ANN and the fuzzy logic have some drawbacks when used on their own. The ANN can produce mapping rules from empirical training data sets through learning, but the mapping rules in the network are not visible and are difficult to understand. On the other hand, since the fuzzy logic does not have learning capability, it is difficult to tune the rules. In order to solve these difficulties, in recent years the link between symbolic processing (fuzzy) and numerical processing (neural) has been investigated, and this has resulted in architectures in which an attempt has been made to integrate the representational ability of fuzzy systems, and it is often call fuzzy neural network (FNN).

The potential of the learning depends on back-propagation ANN, and triangular membership functions define the fuzziness of the system. The ANN acts as the operator of fuzzy inference for optimisation process, and automates the process of determining the membership function parameters.

The results, in this paper, from the performance of the technique confirm that the FNN approach can be used as an attractive and effective means for very accurately locating faults on transmission lines and the FNN improves the performance attainable from the technique based solely on an ANN architecture as described in reference [1].

2. FUZZY NEURAL NETWORK ARCHITECTURE
The basic configuration of the fuzzy logic system (FLS) used in this paper is shown in figure 1. There are four basic elements in a fuzzy system: fuzzification, fuzzy rule base, fuzzy inference engine, and defuzzification.

The *fuzzification* is a mapping from the crisp sets in the input universe U to a fuzzy set in U. Hence, the fuzzification interface provides a link between the non-fuzzy outside world and the FLS framework. A fuzzy set [2] defined in U is characterised by a membership function μ_A: $U \rightarrow [0, 1]$, and is labelled by a linguistic term A. Five linguistic values such as "small", "medium small", "medium", "medium large", "large" are used in this paper.

The *fuzzy rule base* is a set of linguistic rules or conditional statements in the form of: "IF a set of conditions is satisfied, THEN a set of consequences are inferred". In the *fuzzy inference engine* fuzzy logic principles are used to combine fuzzy IF-THEN rules from the fuzzy rule base into a mapping from fuzzy input sets to fuzzy output sets.

The *defuzzification* stage produces a non-fuzzy (crisp) output for FLS from the fuzzy set that is the output of the inference block. The centroid defuzzification, the most commonly used method, is used here.
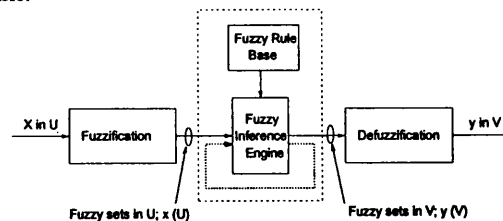
Figure 1. The basic configuration of the fuzzy logic system (FLS)

The fuzzy inference engine and the fuzzy rule base blocks in FLS are changed with an ANN to design the structure of the fuzzy neural network (FNN) used in this paper (figure 2). In this respect ANN automates the process of determining the membership function parameters and learns the best rules from the training set. After the training process, the resultant weights and biases are formed; the fuzzy rule base and the ANN structure will be the inference engine.
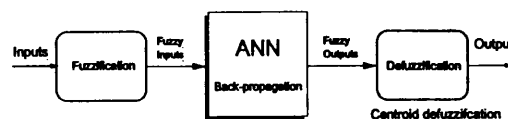
Figure 2. Fuzzy neural network structure (FNN)

4. FUZZY NN BASED FAULT LOCATION SCHEME
In order to find the best network topology for accurate fault location and recognizing the fault type under all practically encountered different system and fault conditions, first, an ANN is trained to indicate in which phase there is a fault and whether the fault

connects to ground or not, no matter where the fault position is, and secondly to have a good generalization, separate FNNs are designed to accurately locate all eleven types of faults on EHV transmission lines.They are all driven from ANN and the input data is generated the same way as input data for ANN. The method is based on utilising voltage and current waveforms at the fault locator end of the line. The signals for estimation of fault location are based on phase values. The effect of transducers (CTs and CVTs) and hardware errors such as anti-aliasing filters and quantisation are taken into account, so that the information processed throughout the fault locator algorithm is very close to real-life situation.

4.1 Fault Type Classification

Fault type classification technique is described in the previous work in reference [1]. The technique is based on training a three-layer perceptron by the Delta-Bar-Delta learning algorithm[3]. The outputs of the ANN are made up of A, B, C, and G which indicate a, b, c phase operation states and connection to ground information respectively. Each of the A, B and C which approaches a value 1 means that phase is faulty. The G which approaches 1 indicates the fault is connected to ground.

| Example:	A	B	C	G	
	0	0	0	0	.....................no fault
	1	0	0	1	..... a phase earth fault
	1	1	0	0	.... a-b phase fault
	1	1	1	1	..... 3-phase earth fault

The ANN consists of 24 inputs 4 outputs and 14 neurons in the hidden layer.

4.2 Fault Location

The structure of FNN is determined by the functions used to represent the linguistic fuzzy variables, the fuzzy logic operators, fuzzification, ANN learning and defuzzification strategies have been employed. The centre of gravity defuzzification algorithm is used to produce crisp output and obtain accurate fault location on EHV lines. As shown in figure 2, a crisp input (a single value rather than a fuzzy or possibility distribution) is presented to the network, and the memberships of the multivariate fuzzy input linguistic variables (represented by multivariate fuzzy sets) are calculated. The confidence in each of the fuzzy output linguistic variables are then determined, and the network output is obtained by defuzzifying the information.

Defuzzifier produces a crisp output for our FNN from the fuzzy set that is the output of the ANN learning block. The output of the ANN is defuzzified where each membership function is weighted by the state of the corresponding output neuron. The location of the fault is then obtained using centroid defuzzification:

$$Fault\ Location = \frac{\sum_{i=1}^{n} y_i \mu_A(y_i)}{\sum_{i=1}^{n} \mu_A(y_i)}$$

where:
  n is the number of quantization level of the output,
  y_i is the output value at the quantization level i,
  $\mu_A(y_i)$ is the value of membership function of the output fuzzy set at y_i.

5. TRAINING DATA FOR FNN

5.1 POWER SYSTEM SIMULATION

The simulation of the power system has been carried out using the well proven Electro-Magnetic Transients Program (EMTP). The overhead transmission line used in this work is based on a single circuit of the typical quad-conductor 400 kV vertical construction

line currently used on the UK supergrid system [4]. The earth resistivity is taken to be 100 Ωm and the power system frequency of 50 Hz was used. Figure 3(a) and 3(b), show power system and line configurations. An X:R ratio of 30 and $Zs_0:Zs_1$ ratio of 1.0 were used for each source.
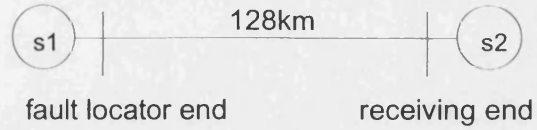
Figure 3(a): Power system configuration.
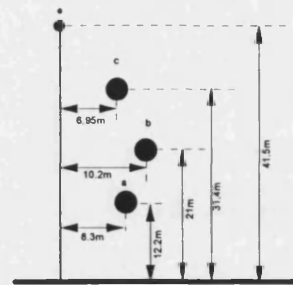
Figure 3(b): Transmission line configuration.

5.2 Feature Extraction

Transient behaviour of the overhead line has been accurately predicted using EMTP for simulation of the power system. Figure 4(a) and 4(b) show the primary voltage and current waveforms related to typical 400 kV transmission line as seen at the sending-end of the line.
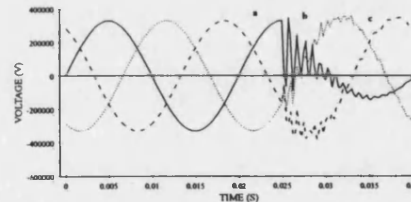
Figure 4(a): Fault locator-end three phase voltages.
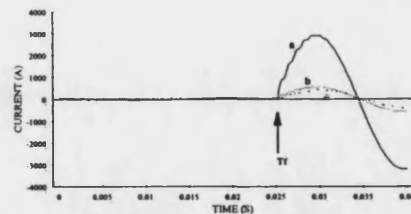
Figure 4(b): fault locator-end three phase currents.

Voltage and current waveforms are sampled at a regular interval and quantised for digital protection proposes [5]. Applying Discrete Fourier Transform (DFT) to the current and voltage waveforms, figure 5 and 6 show the spectra of the 'a'-phase voltage and current under an 'a'-phase to ground fault occurring at the middle of the line and 'a'-phase to 'b'-phase fault at the remote end of the line respectively. It is important to note that different fault types occurring at different locations produce different frequency components. This also means that these signals vary with fault type, location and fault inception angle.

Spectra of a phase voltage

Spectra of a phase current
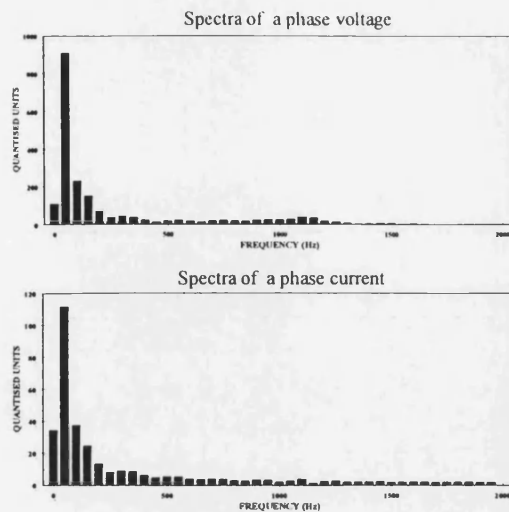
Figure 5.   Spectrum analysis; a phase to ground fault at the middle of the line.

Spectra of a phase voltage

Spectra of a phase current
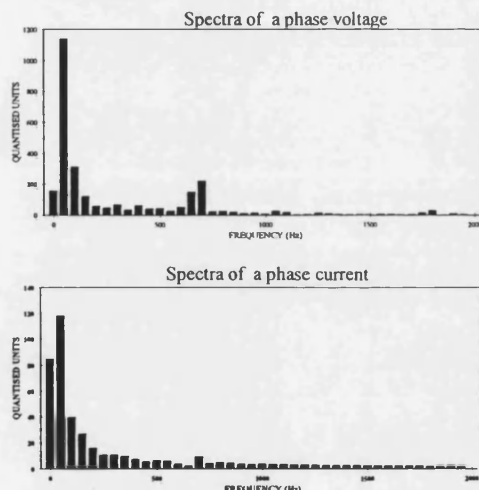
Figure 6.   Spectrum analysis; a phase to b phase fault at the remote end of the line.

The crisp inputs of FNN are composed of V_a, V_b, V_c, i_a, i_b, i_c. Using spectrum analysis for each cycle at the sampling frequency of 4000 Hz, certain frequency bands are used as the potential features. The two parameters for each phase current and voltage are:

1) DC Component.
2) Fundamental Component.

The training pattern vectors are selected from a set of data files representing different faults. The training set has to be carefully chosen so that all the different fault and system conditions are included.

5.3 Fuzzification of crisp data
As shown in figure 2 the FNN described in this paper contains three components: fuzzifier, ANN learning and defuzzifier. Using triangular membership functions and with respect to the linguistic terms we have defined the fuzziness of system. Extracted features from the spectrum analysis are converted to fuzzy sets. Therefore the inputs to ANN are fuzzy sets $(S_1, S_2, ..., S_n)$ in the universe of discourse $(X_1, X_2, ..., X_n)$ respectively. These fuzzy sets are

obtained by converting the DC and fundamental components from the spectrum analysis.

Five linguistic terms as "small", "medium small", "medium", "medium large" and "large" are used to convert the crisp values to fuzzy inputs. In this respect, the structure of ANN consists of 60 neuron in the input layer and five neuron in the output layer. The ANN has been trained to yield desired fuzzy outputs. The location of the fault was then obtained by defuzzifing the fuzzy outputs.

As far as the ANN architecture was concerned, the feed-forward multi-layer neural network with the use of supervised learning and common training rule of error back-propagation is used for this study.

In order to find the best network topology for accurate fault location and to have a good generalization, separate FNNs are designed to locate all eleven types of faults on transmission lines.

6. Analysis of Test Results

6.1 Testing ANN for fault type classification
Test results indicate that the performance of the fault classification technique is very accurate. Table 1 shows the test results which are used for testing ANN for fault type classification. The left four items indicate the desired outputs, and the right four items indicate the actual outputs. The results show faults under various fault conditions and fault positions. Although the ANN is trained under fixed fault points, it can detect faults for every point under various conditions.

6.2 Testing FNN for fault location
The FNNs trained networks were then tested by a number of test data, which are generated in the same way as training data. Table 2 summarises some of the fault location results obtain from testing FNNs for fault location. The algorithm has been tested for a wide variety of simulated fault conditions. These simulation studies have shown the accuracy of FNN technique for all types of faults. As seen in table 2 the proposed technique is highly accurate and very robust.

10. CONCLUSIONS
A fuzzy neural network for accurate fault location has been developed. The technique is based on neural network and fuzzy logic technology. The test results in this paper clearly show that the trained ANN can accurately detect all types of faults, and FNNs are able to accurately locate faults under various system and fault conditions such as different fault types, system source capacity, fault resistance, fault inception and position of the fault. The results in this paper clearly show that with an integrated FNN approach, the accuracy in fault location is significantly improved over other techniques solely based on an ANN architecture.

References:
[1]   Joorabian, M., Aggarawal, R. K., "An Accurate Fault Location Technique For Transmission Line using Artificial Neural Network", UPEC 1995.
[2]   Zadeh, L. A., "Fuzzy sets", Information and control, Vol. 141, No. 2, March 1994.
[3]   Aggarwal, R.K., Johns, A.T., Song, Y.H., Dunn, R. , Fitton, D. , "Neural- Network Based Adaptive single-pole autoreclosure Technique for EHV Transmission System", IEE Proc.-Gener. Transm. Distrib., Vol. 141, No. 2, March 1994.
[4]   Johns, A.T. , Aggarwal, R.K. ,"Digital Simulation of faulted e.h.v. transmission lines with particular reference to very-high-speed protection", Proc. IEE, Vol. 123, No. 4, April 1976.
[5]   Song, Y.H. , Aggarwal, R.K, Johns, A.T. , Dunn, R. , Fitton, D. , "Adaptive autoreclosure Technique for Long-distance Compensated Transmission System Using Neural Network Approach" , UPEC 1993.

Test cases	Desired Output				Actual Output			
case 1 S1=2.5GVA S2=20GVA Rf=1Ω	1.0000	0.0000	0.0000	1.0000	1.0110	-0.0055	0.0021	0.9971
	1.0000	0.0000	0.0000	1.0000	1.0096	-0.0038	0.0090	0.9923
	1.0000	0.0000	0.0000	1.0000	1.0021	-0.0089	0.0568	0.9803
	1.0000	0.0000	0.0000	1.0000	1.0326	-0.0253	0.0128	0.9913
case 2 S1=2.5GVA S2=20GVA Rf=50Ω	1.0000	0.0000	0.0000	1.0000	1.0061	-0.0001	-0.0047	0.9999
	1.0000	0.0000	0.0000	1.0000	0.9988	-0.0003	0.0276	0.9979
	1.0000	0.0000	0.0000	1.0000	1.0082	-0.0005	-0.0052	1.0001
	1.0000	0.0000	0.0000	1.0000	0.9978	-0.0069	-0.0168	1.0642
case 3 S1=2.5GVA S2=20GVA Rf=100Ω	1.0000	0.0000	0.0000	1.0000	0.9763	0.0045	-0.0042	1.0057
	1.0000	0.0000	0.0000	1.0000	0.9761	0.0163	0.0162	1.0187
	1.0000	0.0000	0.0000	1.0000	0.9959	0.0047	-0.0050	1.0091
	1.0000	0.0000	0.0000	1.0000	0.9469	0.0212	0.0113	1.0215
case 4 S1=2.5GVA S2=20GVA Rf=1Ω	1.0000	1.0000	0.0000	0.0000	1.0171	1.0105	-0.0716	0.1542
	1.0000	1.0000	0.0000	0.0000	1.0340	1.0041	-0.0820	0.0092
	1.0000	1.0000	0.0000	0.0000	1.0076	0.9988	0.0056	-0.0005
	1.0000	1.0000	0.0000	0.0000	0.9566	1.0170	0.1502	0.0341
case 5 S1=2.5GVA S2=20GVA Rf=1Ω	1.0000	1.0000	1.0000	1.0000	1.0204	1.0166	1.0074	0.9687
	1.0000	1.0000	1.0000	1.0000	1.0306	1.0223	0.9823	0.9446
	1.0000	1.0000	1.0000	1.0000	1.0378	1.0363	1.0002	1.1146
	1.0000	1.0000	1.0000	1.0000	1.0126	1.0021	1.0698	1.0668

Table 1.   Test Cases for Fault Type Classification: each case represents different system and fault condition for different location on the line.

Fault Type	SCL at S1(GVA)	SCL at S2(GVA)	Rf (Ω)	Desired Output(km)	Actual Output(km)	% error
a-phase fault	2.5	5	1	18.0000	18.5701	0.44
a-phase fault	2.5	5	1	32.0000	31.1082	0.69
a-phase fault	2.5	5	1	48.0000	47.3402	0.51
a-phase fault	2.5	15	1	0.0000	1.18426	0.92
a-phase fault	2.5	15	1	5.0000	4.4394	0.43
a-phase fault	2.5	15	1	128.000	129.2763	0.99
a-phase fault	15	2.5	1	42.0000	41.0027	0.78
a-phase fault	15	2.5	1	82.0000	81.7920	0.16
a-phase fault	15	2.5	1	100.000	99.4633	0.42
a-phase fault	20	2.5	100	42.0000	42.0944	0.85
a-phase fault	20	2.5	100	82.0000	83.3833	1.0
a-phase fault	20	2.5	100	100.000	99.08389	0.72
a- b fault	5	20	20	62.0000	61.0615	0.73
a- b fault	20	5	50	62.0000	62.8382	0.65
a- b fault	10	20	100	8.0000	9.3341	1.04

Table 2. Fault location results obtained from testing FNNs under different fault conditions.

A Fuzzy Neural Network Approach to Accurate Transmission Line Fault Location

M. Joorabian R.K. Aggarwal (Senior M. IEEE) Y.H. Song (Senior M. IEEE)
School of Electronic & Electrical Engineering; University of Bath, Bath, United Kingdom

Abstract—This paper describes an accurate fault location technique using fuzzy neural networks(FNN). The technique, which utilises voltage and current fault data at one line end only, comprises of two stages: the first stage is based solely on an artificial neural network(ANN) in order to classify fault types and the second stage is based on a FNN whereby fuzzy logic is employed to process the information for a second ANN for the purposes of accurately locating a fault on the line. It is clearly shown that with this integrated approach, the accuracy in fault location is significantly improved over other techniques solely based on ANN architectures.

Keywords: Fault location, Transmission lines, Fuzzy logic, Neural networks.

1 INTRODUCTION

Fast and accurate location of faults on an electrical power transmission line is vital for economic operation of power systems. This is more so in view of the fact that because of an increase in transmission requirements and environmental pressures, power authorities are being forced to maximize the transmission capabilities of existing transmission lines. This effectively means that in order to maintain system security and stability, there is a demand for minimizing damage by restoring the faulted line to normal as quickly as possible, hence the requirements for the development of an accurate fault locator. The degree of accuracy required is therefore increasing and is much higher than would be possible using conventional techniques. Even a small measurement error may require detailed local examination over several kilometres of a typical line.

With the advent of microprocessor-based devices, better accuracy in locating faults in power systems has attracted much interest. Hitherto, considerable work has been done in developing digital techniques for locating faults on transmission lines. Sant and Paithnaker[1] have proposed a fault location technique that uses fundamental frequency voltages and currents measured at one of the line terminals. However, the technique assumes that the line is fed from one end only. The fault location estimates are, therefore, not accurate if fault current is contributed by sources connected to both terminals of the line and fault resistance is present.

Takagi et al[2], Winszniewski[3] and Eriksson et al[4] have used pre-fault currents, post-fault voltages and currents observed at one terminal of the line, and fault current distribution factors. However, impedances of equivalent sources connected to the line terminals are required for estimating current distribution factors and these are not readily available in all cases. Also, the system configuration changes from time to time modifying the distribution factors and these must be known at the time a fault occurs. There are some disadvantages to the algorithms developed in reference[5]; for example, the fault resistance is not taken into account and the effect of line shunt capacitance is neglected. Those developed in references[6-7] require a communication medium and fault recorded data at the two ends needs to be synchronised.

Artificial neural network(ANN)-based techniques have the potential advantage over conventional techniques in significantly improving the accuracy in fault location. This is so by virtue of the fact that ANNs have the capability of non-linear mapping, parallel processing and learning; these attributes make them ideally suited for providing a high accuracy in fault location under a wide variety of different systems and fault conditions. However, there are still a number of contingencies under which an ANN-based fault location technique's performance can be adversely affected. The technique presented herein thus proposes the use of fuzzy logic to further improve the accuracy of an ANN-based fault location technique.

This paper is concerned with outlining an integrated approach comprising fuzzy logic and ANNs for accurately locating faults on a transmission line. The technique is based on utilising voltages and currents at one end of the line and its performance is illustrated with respect to a typical 400kV transmission system of the type encountered on the British supergrid system. The results presented clearly show that an FNN gives a high accuracy in fault location under a whole variety of different system and fault conditions, and further improves on the accuracy attainable from fault location techniques based solely on ANN architectures[8].

2 FUZZY NN BASED FAULT LOCATION SCHEME

As mentioned before, the technique consists of two stages: (i) fault type classification based solely on ANN architecture and (ii) precise location of a fault on the line based on an integrated network comprising fuzzy logic and an ANN.
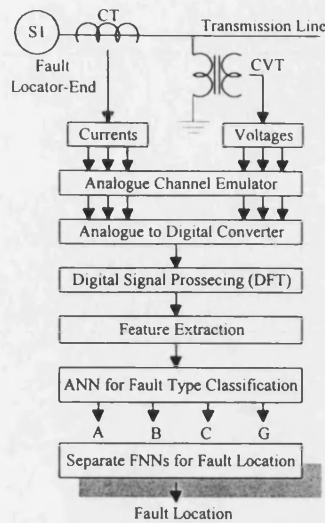
Fig. 1. A complete fault location scheme based on FNNs.

The complete fault locator scheme is shown in Fig. 1. The method is based on utilising voltage and current waveforms at the fault locator end of the line only and the signals employed are based on phase values. The effect of transducers - current transformers (CTs) and capacitor voltage transformers (CVTs), and hardware errors such as anti-aliasing filters and quantisation are taken into account, so that the information processed throughout the fault locator algorithm is very close to real-life situation; this is achieved through a data pre-processing stage whereby the primary system waveforms of voltages and currents are subjected to a full circuit emulation of the transducers/analogue interface modules via their practical frequency responses. The resultant data is then passed through a model of an analogue to digital (A/D) converter before being processed through the fault locator algorithm.

In order to find the best network topology for accurate fault location under all practically encountered different system and fault conditions, an extensive series of studies have revealed that it is not satisfactory to merely employ a single ANN and attempt to train it with a large amount of data. A much better approach is to separate the problem into two parts: firstly to employ and train a single ANN to indicate on which phase(s) the fault is and whether there is ground involved in a particular fault, irrespective of the actual fault position at this stage; secondly, in order to achieve a good generalisation, to use separately designed FNNs (one for each type of fault and each comprising fuzzy logic and an ANN) to accurately locate the actual fault position associated with all the commonly encountered types of fault on EHV transmission lines; these are of course all driven from the single ANN designed at the first stage and the input data for the FNNs is generated the same

way as that for the single ANN. Although this modular approach requires many networks, they are nonetheless quite simple in architecture, much easier to train and require significantly less training data than would otherwise be the case if simply one single ANN were to be employed; more importantly (as shown later), the accuracy achieved in fault location is significantly enhanced.

2.1 Fault Type Classification

The fault type classification technique is essentially the same as that described in reference[8]. It is based on training a three-layer perceptron by the Delta-Bar-Delta learning algorithm[9]. The outputs of the ANN comprise of four variables A, B, C and G; of these, a value close to unity for any of the first three variables corresponds to the appropriate a, b or c phases being faulty and a near unity value of G signifies that ground is involved in a fault. This ANN logic is depicted in the following example:

Example of ANN-logic for output representation				
A	B	C	G	TYPE OF FAULT
0	0	0	0	no fault
1	0	0	1	a-phase-earth fault
1	1	0	0	a-b fault
1	1	1	1	3-phase-earth fault

The ANN architecture is based on 24 inputs, 4 outputs and 14 neurons in the hidden layer.

2.2 Fault Location

The fuzzy logic is classified as an extension of binary Boolean Logic[10]. It is a class in which the transition from membership to non-membership is gradual rather than abrupt. Both the ANN and the fuzzy logic have some drawbacks when used on their own. The ANN can produce mapping rules from empirical training data sets through learning, but the mapping rules in the network are not visible and are difficult to understand. On the other hand, since the fuzzy logic does not have learning capability, it is difficult to tune the rules. In order to overcome these difficulties, the link between symbolic processing(fuzzy) and numerical processing(neural) has been investigated in recent years, and this has resulted in hybrid architectures based on integrating the representational ability of fuzzy systems[10,11], often referred to as a fuzzy neural network (FNN).

Fig. 2 illustrates the FNN considered herein. The FNN carries out fuzzy inference with ANN structure, and adjusts the fuzzy parameters using ANN learning. The ANN has been trained to extract the best rules and to learn membership functions from the training set.

The structure of the FNN is determined by the functions used to represent the linguistic fuzzy variables; these are employed

to set up fuzzification, ANN learning and defuzzification strategies. The centre of gravity defuzzification algorithm is used to produce a crisp output which indicates the actual fault location on the transmission line.

The information flow through a FNN can be clearly seen from Fig. 2. A crisp input (a single value rather than fuzzy or probability distribution) is presented to the network, and the memberships of the multivariate fuzzy input linguistic variables (represented by fuzzy sets) are calculated. The confidence in each of the fuzzy output linguistic variables is then determined, and the network output is obtained by defuzzifying the information.
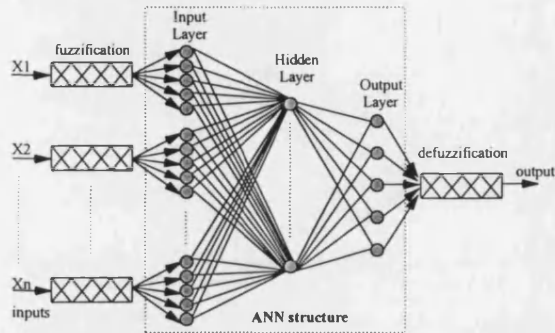

Fig. 2. Fuzzy neural network structure.

The FNN employed comprises of three components: fuzzifier, ANN learning and defuzzifier.

2.2.1 Fuzzification

A fuzzification operator has the effect of transforming crisp data into fuzzy sets; symbolically:

$$x = fuzzifier(x_o) \qquad (1)$$

where x_o is a crisp input value from a process; x is a fuzzy set and the fuzzifier represents a fuzzification operator[12]. The triangular membership functions are used to define the fuzziness of the system.

2.2.2 Acquisition of fuzzy knowledge and inference by neural networks

The operation of a FNN can best be understood by considering the basic configuration of a fuzzy logic system (FLS) with pre-processing (fuzzifier or encoder) and reformation (defuzzifier or decoder) as shown in Fig. 3. In such a system, a set of linguistic rules or conditional statements in the form of: "IF a set of conditions is satisfied, THEN a set of consequences are inferred" are employed; the fuzzifier maps the crisp sets in the input universe U to a fuzzy

set in U, and the defuzzifier maps the fuzzy sets in the output universe V of pure fuzzy logic system's output, to the crisp sets in V. However, it is virtually impossible to define these rules in a FLS on its own from the training set; this is so by virtue of the fact that the training data is highly complex in nature and is constituted by the interaction of many variables under different system and fault conditions. An integrated structure whereby the inference engine in Fig. 3 is replaced by an ANN (as shown in Fig. 2) is a much better alternative to deal with the problem and this is the approach adopted in the technique presented herein. The main attribute of such a structure is that the ANN automates the process of determining the membership function parameters and learns the best rules from the training set. After the training process, the resultant weights and biases become the principle base and the ANN takes over as the inference engine.
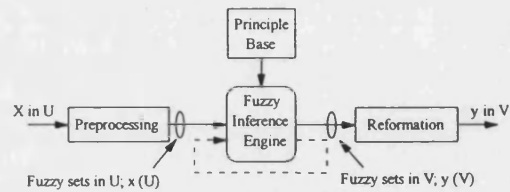

Fig. 3. Fuzzy Logic System (FLS).

The structure of the ANN employed within the FNN has one hidden layer and an output layer comprising of five nodes. It is a feedforward, fully connected network in which a hyperbolic tangent function is employed as the activation function. As mentioned before, once a fault has been classified to be of a particular type by the fault-classification ANN at the first stage, the appropriate FNN is then enabled for fault location identification at the second stage of the technique. In this respect, it should be noted that there are different FNNs employed (each with a slightly different architecture in terms of the number of hidden neurons and of course different training data) to cater for all types of commonly encountered faults.

Extracted features through spectrum analysis of the training data are converted into fuzzy sets; these are then used as inputs to train each ANN. The location of the fault is coded into a number of fuzzy membership functions determined by the desired resolution. In this study, five membership functions have been used. The number of output neurons of each ANN is the same as the number of the fuzzy membership functions.

2.2.3 Defuzzification

As shown in Fig. 2, the defuzzifier produces a crisp output from the fuzzy set which in turn is the output of the ANN learning block. In the defuzzification process, each membership

function is weighted by the state of the corresponding output neuron of the ANN. The location of the fault is then obtained using centroid defuzzification as given by:

$$Fault\ Location = \frac{\sum_{i=1}^{n} y_i \mu_B(y_i)}{\sum_{i=1}^{n} \mu_B(y_i)} \quad (2)$$

where: n is the number of quantization level of the output,
         y_i is the output value at the quantization level i,
         $\mu_B(y_i)$ is the value of membership function of the output fuzzy set at y_i .

3 PREPROCESSING OF THE FAULTED SYSTEM VOLTAGE AND CURRENTS

3.1 Power System Simulation

The simulation of the power system has been carried out using the well proven Electro-Magnetic Transients Program (EMTP). The overhead transmission line used in this work is based on a single circuit of the typical quad-conductor 400 kV vertical construction line currently used on the UK supergrid system [12]. The earth resistivity is taken to be 100 Ωm and the power system frequency as 50 Hz. Figs 4(a) and 4(b) show the power system and line configuration studied. An X:R ratio of 30 and $Zs_0:Zs_1$ ratio of 1.0 were used for each source terminating a busbar. The simulation is based on a sampling frequency of 4kHz and after convolving the primary system data with the unit impulse responses of the transducers and voltage/current interface modules, the digital data is quantised through a 12-bit ADC for subsequent processing in the fault location algorithm.
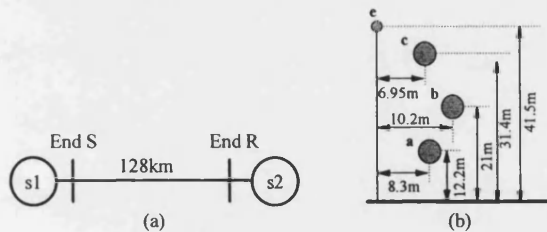

Fig. 4. The system studied.
(a) Power system configuration.
(b) Transmission line configuration.

3.2 Feature Extraction

Fig. 5 typifies the primary system voltage and current waveforms generated at end S of the line under an 'a'-phase-earth fault at the midpoint of the line.
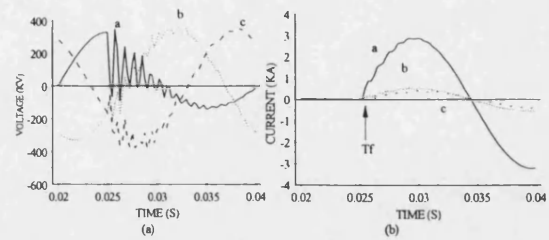

Fig. 5. Typical fault simulation waveforms at the fault locator end.
(a) The three phase voltage.
(b) The three phase currents.

As a first step in any pattern classification technique, feature extraction is used to reduce the dimension of the raw data and extract useful information in a concise form. For the ANN considered here, this process leads to a considerable reduction in the size of the network, thereby significantly improving the performance and speed of the training process.

The technique adopted here for feature extraction is the one based on time domain frequency decomposition of voltage and current waveforms using the Discrete Fourier Transform (DFT); a one cycle window is employed for this purpose. Fig 6 depicts the frequency spectra of the 'a'-phase voltage and current for the fault condition shown in Fig. 5; likewise, Fig. 7 shows the frequency spectra (again as observed at end S) for an 'a'-'b'-phase fault near end R. It is apparent from the foregoing that the frequency spectra are distinctly different for the two types of fault. In this respect, it is important to note that the frequency spectra attained vary quite significantly under different types of fault, fault location, fault inception angle, etc.
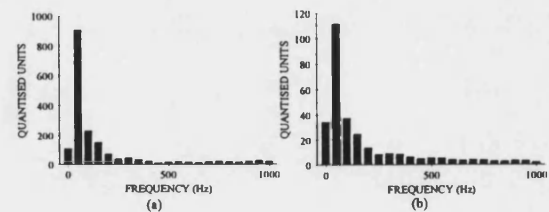

Fig. 6. Frequency spectra for an 'a'-phase-earth fault at the midpoint.
(a) Spectra of a phase voltage.
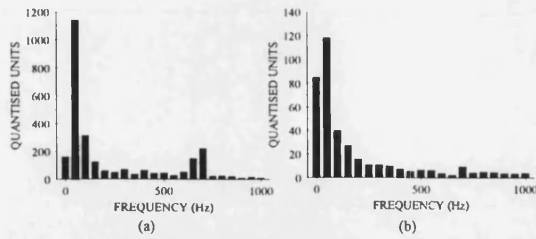(b) Spectra of a phase current.

Fig. 7. Frequency spectra for an 'a'-'b'-phase fault at the remote end.
(a) Spectra of a phase voltage.
(b) Spectra of a phase current.

3.3 Training data

In order to design a neural network, it is vitally important to train it correctly and then test it. The ANN involved in the first stage of the fault location technique is trained with the data obtained from the simulation of faults on a plain 400 kV transmission line shown in Fig. 4.

The inputs to the ANN comprise of a set of features based on the three-phase voltages V_a, V_b, V_c and three-phase currents I_a, I_b, I_c. With regard to the procedure for feature selection, an acceptable simple criterion used here is that a variable as a feature for the ANN input should provide more information for fault type classification than those not selected. In this respect, an extensive series of studies have revealed that the following frequency components (attained through the previously mentioned time-domain frequency decomposition of the fault waveforms) are representative of the vast majority of different system and fault conditions encountered in practice:
1) DC Component.
2) Fundamental Component.
3) Components over 100 - 350 Hz range.
4) Components over 400 - 1000 Hz range.

These are then converted into four features for each measured signal, those associated with (3) and (4) above comprising of the summated signal energy at all discrete frequencies within their appropriate range; with this approach, it becomes possible to confine the number of inputs into the ANN to 24 elements for the 6 signals.

The performance of the ANN is then tested using both patterns within and outside the training set. This is particularly so with reference to the speed of convergence and accuracy attained, essentially to ascertain if modification to the ANN structure or further training is necessary. The approach adopted here is based on the error-back-propagation training algorithm whereby an input pattern corresponding to a particular fault condition is fed to the ANN and the output of the network is compared with the desired output pattern corresponding to that fault condition.

3.4 Fuzzification of crisp information for the FNN

This section describes how triangular membership functions describing the fuzziness of the transmission system are used to convert the previously described extracted features into fuzzy sets for the FNN and these are shown in Fig. 8a. In order to facilitate this process, the overhead transmission line is divided into five sections as shown in Fig. 8b. Each output neuron corresponds to the value of the membership function. For a fault at 48 Km of the line, the membership function (and the ANN output) is [0 0.5 0.5 0 0].
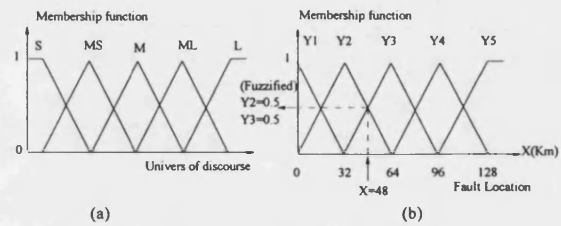

Fig. 8. Input/output membership functions.
(a)   Membership functions of linguistic values(S: small, MS: medium small, M: medium, ML: medium large, L: large).
(b)   Membership functions for the fuzzification mapping of the output neurons.

Frequency Component	Linguistic Values For Inputs						Fuzzy Outputs				
	I_a	I_b	I_c	V_a	V_b	V_c	Y1	Y2	Y3	Y4	Y5
DC	MS	ML	ML	M	ML	ML					
50 Hz	M	L	ML	MS	ML	M	0	0	1	0	0
100-350 Hz	MS	ML	M	S	MS	ML					
400-1000 Hz	MS	M	S	MS	M	L					

Table 1. Fuzzy input/output training data representation.

Inputs to ANN are fuzzy sets $(S_1, S_2, ..., S_n)$ in the universe of discourse $(X_1, X_2, ..., X_n)$ respectively. These fuzzy sets are obtained by converting the DC and other frequency components attained through the frequency decomposition of the time-domain waveforms. As shown in Fig. 8a, five linguistic terms as "small", "medium small", "medium", "medium large" and "large" are used to convert the crisp values to fuzzy inputs. In this respect, the structure of ANN consists of 60 neuron in the input layer and five neurons in the output layer. The FNN has been trained to yield desired fuzzy outputs. Table 1 illustrates the linguistic values of inputs and the fuzzy outputs for an 'a'-phase to ground fault occurring at the middle of the line; the frequency spectra associated with this fault is shown in Fig. 6. The training data for FNN consists of fuzzy inputs/outputs with respect to these linguistic terms and their membership functions. The location of the fault is then obtained using centroid defuzzification with respect to the membership functions shown in Fig. 8b.

4 ANALYSIS OF TEST RESULTS AND DISCUSSION

4.1 Performance of ANN for fault type classification

Following the training of the ANN, a separate set of test patterns were supplied as input to the ANN involved in the fault-type classification in order to evaluate its performance. Table 2 gives some examples of the test results. The left four columns are the desired outputs, ideally '1' or '0' (corresponding to the fault types as indicated by the logic shown in Section 2.1), and the right four columns are the actual outputs of the ANN; each test case comprises of four different fault positions at distances of 8, 62, 96 and 120 km, respectively from end S . It is evident from the results that although the ANN gives a high accuracy, there are small fluctuations in the actual ANN outputs around '1' and '0'; since in practice this cannot be avoided, small threshold levels have to be built into the ANN algorithm in order to minimise the degree of uncertainty. In this application, these levels were set such that if the output fell within the range <0.1 then it would be classed as '0' ie, a healthy phase indication, and if it fell within the range >0.9 then it was classed as unity ie, a faulted phase indication.

Test Cases	Desired Output				Actual Output			
Case 1	1.0000	0.0000	0.0000	1.0000	1.0110	-0.0055	0.0021	0.9971
S1=2.5GVA	1.0000	0.0000	0.0000	1.0000	1.0096	-0.0038	0.0090	0.9923
S2=20GVA	1.0000	0.0000	0.0000	1.0000	1.0021	-0.0089	0.0568	0.9803
Rf=1Ω	1.0000	0.0000	0.0000	1.0000	1.0326	-0.0253	0.0128	0.9913
Case 2	1.0000	0.0000	0.0000	1.0000	0.9763	0.0045	-0.0042	1.0057
S1=2.5GVA	1.0000	0.0000	0.0000	1.0000	0.9761	0.0163	0.0162	1.0187
S2=20GVA	1.0000	0.0000	0.0000	1.0000	0.9959	0.0047	-0.0050	1.0091
Rf=100Ω	1.0000	0.0000	0.0000	1.0000	0.9469	0.0212	0.0113	1.0215
Case 3	1.0000	1.0000	0.0000	1.0000	1.0104	1.0045	-0.0617	1.0055
S1=2.5GVA	1.0000	1.0000	0.0000	1.0000	1.0044	1.0087	-0.0280	1.0770
S2=20GVA	1.0000	1.0000	0.0000	1.0000	0.9899	1.0089	0.1032	0.9969
Rf=100Ω	1.0000	1.0000	0.0000	1.0000	1.0008	1.0210	-0.0054	1.0229
Case 4	1.0000	1.0000	1.0000	1.0000	1.0204	1.0166	1.0074	0.9687
S1=2.5GVA	1.0000	1.0000	1.0000	1.0000	1.0306	1.0223	0.9823	0.9446
S2=20GVA	1.0000	1.0000	1.0000	1.0000	1.0378	1.0363	1.0002	1.1146
Rf=1Ω	1.0000	1.0000	1.0000	1.0000	1.0126	1.0021	1.0698	1.0668

Table 2. Test cases for fault type classification.

In order to quantitatively evaluate the performance of the fault classification technique, three indices are proposed as follows:

Error index (EI)=No of error decisions / No of total tests
single confidence index (SCI)=Idesired - Iactual / desired
Average confidence index (ACI)=Sum of SCI / No of tests

Table 3 presents the overall performance of tests carried out over 200 system and fault conditions, which indicates that the overall confidence index is 99.66% with no single error decision.

		A	B	C	G
Single Confidence Index	Min	99.8%	99.98%	99.82%	99.2%
	Max	99.9%	99.9%	99.9%	99.9%
Average Confidence Index		99.8%	99.5%	99.85	99.55%
Overall Confidence Index	99.66%		Error Index		0%

Table 3. Performance evaluation of fault type classification.

4.2 Performance of FNN for fault location

Like in the previous case, the trained FNNs involved in the second stage of the fault location technique were tested with a separate set of test data *unseen* by the FNNs before. As mentioned before, this stage comprises of a number of FNNs (each corresponding to a different type of fault, the appropriate FNN being activated by the outputs from the ANN in the first stage. Table 4 gives some examples of the test results. The error for fault location is expressed as a percentage of the length of the line, and is given as:

$$\% \ error = \frac{actual \ location - desired \ location}{length \ of \ the \ line} \times 100$$

Fault Type	SCL at S1-GVA	SCL at S2-GVA	Rf (Ω)	Desired Output (Km)	Actual Output (Km)	% Error
a-earth fault	2.5	5	1	18.0000	18.5701	0.44
a-earth fault	2.5	5	1	48.0000	47.3402	0.51
a-earth fault	2.5	15	1	0.0000	1.118426	0.92
a-earth fault	2.5	15	50	5.0000	4.4394	0.43
a-earth fault	15	2.5	1	100.000	99.4633	0.42
a-earth fault	20	2.5	100	82.0000	83.3833	1.0
a-earth fault	20	2.5	100	100.000	99.0838	0.72
a-b fault	20	2.5	-	100.000	99.5221	0.37
a-b fault	5	20	-	62.0000	61.0615	0.73
a-b-earth fault	5	20	20	62.0000	61.0615	0.73
a-b-earth fault	20	5	50	62.0000	62.8382	.065
a-b-earth fault	10	20	100	8.0000	9.3341	1.04
3-phase-earth fault	20	2.5	100	42.0000	42.0944	0.85
3-phase-earth fault	20	2.5	100	82.0000	83.3833	1.0

Table 4. Fault location results obtained from testing FNNs under different fault condition.

It is clearly evident from the results that the accuracy achieved in fault location is very high, being <1% in the majority of cases. An extensive series of studies have shown that the fault location technique described herein maintains this high accuracy and robustness under a vast majority of different system and fault conditions; equally importantly, the improvement attained over the previous technique based solely on ANNs ie, without the integration of fuzzy logic and an ANN, is very significant, as indicated by the results shown in

Table 5. In practice, this improvement in accuracy is vitally important since it would considerably narrow the span of a line length which would be necessary to be scrutinised; this in turn would expedite the precise location of a fault thereby enabling the line to be restored to normal quickly.

Accurate fault location technique	ANN	FNN
Training patterns	105	105
Testing patterns	95	140
Maximum error in fault location	2.2%	1%

Table 5. Test results for a-phase-earth fault.

5 CONCLUSION

This paper presents a novel fault locator for EHV transmission systems, based on artificial intelligence techniques, and shows a vastly improved performance over conventional techniques. Furthermore, this technique, based on an integrated approach comprising fuzzy logic and ANNs, gives an accuracy of <1% under a vast majority of different system and fault conditions encountered in practice and is a considerable improvement over other artificial intelligence techniques solely based on ANN architectures; this is a major advantage in practice since it would expedite the exact location of a fault by significantly reducing the span of a line length that would have to be scrutinised.

The technique, although based on CAD, nonetheless takes into account the practical limitations associated with voltage / current transducers and hardware so that the performance attained is close to that which would be expected from a hardware model under service conditions.

6 REFERENCES

[1]   Sant, M.T. and Paithankar, Y.G., "On Line Digital Fault Locator For Overhead Transmission lines", IEE Proc., 127, No. 11, pp. 1181-1185, November 1979.

[2]   Takagi, T., Yamakoshi, Y., Yamaura, M. Kondow, R. and Matsushima, T., "Development of a New Type Fault Locator Using The One-Terminal Voltage and Current Data", IEEE Trans., PAS-101, No 8, pp. 2892-2898, August 1982.

[3]   Wiszniewski, A., "Accurate Fault Impedance Locating Algorithm", IEE Proc., 130, Part C, No. 6, pp. 311-314, 1983.

[4]   Eriksson, L., Saha, M.M., and Rockefeller, G.D., "An Accurate Fault Locator with Compensation for Appatent Reactance in the Fault Resistance from Remote-End Infeed", IEEE/PES 1984 Summer Meeting, Seattle, Washington, Paper No. 84 SM 624-3, 1-12.

[5]   Cook, V., "Fundamental Aspects of Fault Location Algorithms Used in Distance Protection", IEE Proc., 133, Part C, No. 6, pp. 359-368, September 1986.

[6]   Johns, A.T. and Jamali, S., "Accurate Fault Location Technique for Power Transmission Lines", IEE Proc. Vol 137, Part C, No. 6, pp. 395-402, September 1990.

[7]   Kezunovic, M., Mrkic, J. and Perunicic, B., "An Accurate Fault Location Algorithm Using Synchronized Sampling", EPSR, Vol. 29, No. 3, pp. 161-169, 1994.

[8]   Joorabian, M., Aggarwal, R. K., "An Accurate Fault Location Technique For Transmission Line using Artificial Neural Network", UPEC 1995.

[9]   Aggarwal, R.K., Johns, A.T., Song, Y.H., Dunn, R., Fitton, D., "Neural- Network Based Adaptive single-pole autoreclosure Technique for EHV Transmission System", IEE Proc.-Gener. Transm. Distrib., Vol. 141, No. 2, March 1994.

[10]   Ichihashi, H., "Learning in Hierarchical Fuzzy Models by Conjugate gradient Methode using Backpropagation Errors", Proc. of Intelligent System Symp., pp. 235-240, 1991.

[11]   Lee, C. C., "Fuzzy Logic in Control System: Fuzzy Logic Controller-Part I", IEEE Transaction on System, Man, and Cybernetics, Vol. 20, No. 2, 1 pp. 404-418, March/April 1990.

[12]   Johns, A.T., Aggarwal, R.K., "Digital Simulation of faulted e.h.v. transmission lines with particular reference to very-high-speed protection", Proc. IEE, Vol. 123, No. 4, April 1976.

Mahmood Joorabian received his MSc degree in Electric Power Engineering from Rensselaer Polytechnic Institute, Troy, NY, in 1985. He then joined Shahied Chamran University, Ahwaz, Iran as a lecturer in 1986. He is presently studying in the School of Electronic & Electrical Engineering, University of Bath for his PhD. His research interests are applications of intelligent techniques to power system analysis and protection.

Raj Aggarwal obtained his degrees of BEng and PhD from the University of Liverpool in 1970 and 1973 respectively. He then joined the University of Bath where he is a Reader in the Power and Energy Systems Group. His research interests are Power System Modelling, digital protection and application of AI to protection and control. He is a senior member of the IEEE, a member of the IEE and a Chartered Engineer in UK.

Yonghua Song received his degrees of BEng, MSc and PhD in 1984, 1986 and 1989 respectively. He is currently a lecturer at the University of Bath. His research interests are application of intelligent techniques to power system analysis, control and protection. He is a senior member of the IEEE, a member of the IEE and a Chartered Engineer in UK.